SCIENTIFIC NOTEBOOK
E590
Volume 1

by

Ronald Green

Southwest Research Institute
Center for Nuclear Waste Regulatory Analyses
San Antonio, Texas

May 21, 2003

Table of Contents

INITIAL ENTRIES

Scientific notebook: #590E Vol. 1
Issued to: R.T. Green
Issue Date: 21-May-2003

A series of MULTIFLO simulations are performed to examine data collected during the two lab-scale heater tests described in Scientific Notebook 209.

All simulations were performed with MULTIFLO Version 1.5.2 August 2002.

The objective of the analyses is to systematically vary different input parameters for numerical simulations of the lab-scale heater tests. The parameters in question include property values and conceptual model selections. Included are the AFM and the choice of gamma (either 0.2 or 0.4) when the AFM is invoked. If the AFM is not invoked, the effect of the areamodf is evaluated. Areamodf values assessed were 1.0, 0.1, and 0.001. Also assessed with the areadmodf was decoupling energy from mass. This decoupling is accomplished in the DCMPARAM input line.

```
DCMPARA
:     i1 i2 j1 j2 k1 k2   volf      areamodf   xlm    ylm     zlm
  1 24  1 14  1 30   0.050   1.0          .05     0.03   .05    -5 ! matrix
```

Note that the 1.0 entry under areamodf, before the xlm category is where values for areamodf are entered for coupled systems. When coupled, both energy (heat) and mass interaction between the continua are limited. For decoupled systems (i.e., energy communication is not decreased when mass is decreased), the 1.0 is maintained below the areamodf, but the –5 is replaced with a numerical value (i.e., 0.1) for the areamodf value. The –5 designation is for the AFM (active fracture model). The relative permeability for unit 5 is described in the Pckr section of the input file.

Also varied was the van Genuchten alpha value (equivalent to the inverse of t the air entry value). Values of 1e-3 and 1e-4 were considered.

Runs lst155 through lst172 were performed as part of this analysis. lst155 was assumed to be the basecase with on AFM, an alpha of 1e-4, and no reduction in areamodf. The 18 runs are described in Table 1.

Dec indicates whether heat transfer is decoupled from mass transfer.

Table 1. Summary of lst analyses: fracture

Run #	AFM	γ	α	A_{mod}	Dec	Sat	Flow	Pond	C Penet	Shed
lst155	Off	-	1e-4	1.0	No	0.179	Focused	No	Yes	Yes
lst156	On	0.4	1e-4	1.0	Yes	0.294	Focused	No	Yes	Yes
lst157	Off	-	1e-4	0.001	No	0.5796	Diffuse	No	Yes	No
lst158	Off	-	1e-3	1.0	No	0.1615	Focused	Yes	No	No
lst159	Off	-	1e-3	0.001	No	0.1709	Diffuse	No	No	No
lst160	On	0.4	1e-3	1.0	Yes	0.079	Focused	Yes	No	No
lst161	Off	-	1e-4	0.1	No	0.3133	Mix	No	Yes	N
lst162	Off	-	1e-3	0.1	No	0.1697	Smeared	Some	No	No
lst163	Off	-	1e-4	0.01	No	0.3213	Mix	No	Yes	No
lst164	Off	-	1e-3	0.01	No	0.1729	Mix	Some	No	No
lst165	On	0.2	1e-4	1.0	Yes	0.2399	Focused	No	No	Yes
lst166	On	0.2	1e-3	1.0	Yes	0.1213	Focused	Yes	No	No
lst167	Off	-	1e-4	0.001	Yes	0.3292	Focused	No	Yes	Yes
lst168	Off	-	1e-3	0.001	Yes	0.1695	Focused	Yes	No	No
lst169	Off	-	1e-4	0.1	Yes	0.3030	Focused	No	Yes	Yes
lst170	Off	-	1e-3	0.1	Yes	0.1635	Focused	Yes	No	No
lst171	Off	-	1e-4	0.01	Yes	0.3240	Focused	No	Yes	Yes
lst172	Off	-	1e-3	0.01	Yes	0.1685	Focused	Yes	No	No

Table 2. Summary of lst analyses: matrix

Run No	AFM	γ	α	A_{mod}	Dec	CPond	EPond	MTem	FTem
lst155	Off	-	1e-4	1.0	No	No	Some	185.1	184.6
lst156	On	0.4	1e-4	1.0	Yes	No	Some	185.3	184.8
lst157	Off	-	1e-4	0.001	No	Yes	No	187.9	143.7
lst158	Off	-	1e-3	1.0	No	No	Some	186.8	186.2
lst159	Off	-	1e-3	0.001	No	Yes	No	188.5	144.6
lst160	On	0.4	1e-3	1.0	Yes	No	Yes	186.8	186.3
lst161	Off	-	1e-4	0.1	No	Some	Some	185.1	180.6
lst162	Off	-	1e-3	0.1	No	Some	some	186.6	182.1
lst163	Off	-	1e-4	0.01	No	Yes	Yes	186.3	167.5
lst164	Off	-	1e-3	0.01	No	Yes	Yes	187.4	168.6
lst165	On	0.2	1e-4	1.0	Yes	No	Some	185.2	184.7
lst166	On	0.2	1e-3	1.0	Yes	No	Yes	186.8	186.3
lst167	Off	-	1e-4	0.001	Yes	No	Some	185.0	184.5
lst168	Off	-	1e-3	0.001	Yes	No	Some	186.7	186.2
lst169	Off	-	1e-4	0.1	Yes	No	Some	184.9	184.4
lst170	Off	-	1e-3	0.1	Yes	No	Yes	186.8	186.2
lst171	Off	-	1e-4	0.01	Yes	No	Some	185.0	184.4
lst172	Off	-	1e-3	0.01	Yes	no	Some	186.7	186.2

Discussion of analyses results.
There are several main classes of analyses:

1) AFM
2) reduced areamodf, heat and mass coupled
3) reduced areamodf, heat and mass uncoupled

Plus two sub-classes:

1) effect of alpha of 1e-3 versus 1e-4
2) effect of gamma=0.4 versus 0.2

Main observations:

Fracture continuum:

1) reduced areamodf and coupled heat and mass results is significant temperature differences between the fracture and matrix continua
2) reduced areamodf and uncoupled heat and mass maintain constant temperatures between the two continua
3) reduced areamodf and coupled heat and mass causes fracture flow to be diffuse
4) models which indicate penetration into the drift also indicate focused flow at point of shedding off the drifts
5) Coupled areamodf of 0.001 gives poorest estimate for focused fracture flow
6) Change of gamma from 0.2 to 0.4 has no appreciable effect

Matrix continuum:

1) AFM with γ=0.4 effectively indicates ponding at center plane of test cell, AFM is moderately effectively indicates ponding at test cell edge. Ponding as not nearly as prominent with γ=0.2.
2) Coupled areamodf of 0.001 gives poorest estimate for ponding at edge
3) Alpha of 1e-3 gives slightly better ponding than 1e-4, all else equal
4) Change of gamma from 0.2 to 0.4 has no appreciable effect
5) Matrix temperatures showed a maximum difference of 3.6 C. Even with significant differences in matrix saturations, matrix temperatures remain virtually unchanges

The basecase input file for MULTIFLO is lst155.dat. This data set is as follows:

```
+++++++++++++++++++++++++++++++++++++++++++++++++++++++++++++++++++++++++++++++
  Simulation of laboratory-scale dripping experiment - Bldg 51 CNWRA
  May 20, 2003
: lst155
: smaller model to fit in metra element dimension limitation
: This run statred with drip131 converted to DCM
: dcm-sm98 inc liq sat of matrix from 0.3 to 0.35
: lst112, areamodf=1e-2
: lst113, areamodf=1e-4
: lst115, repeat of lst113
: lst116, 115 matrix sat from 0.42 to 0.5 as in C3
: lst120, 116 with int sat from .35 to .20
: lst132, act fract model with ds103 properties
```

```
: lst133, corrected mflo 1.5.2
: lst134, initial sat from 0.2 to 0.3
: lst135, corrected fracture to matrix using TSW34
: lst137, afm with fm and ff new
: lst138, afm off
: lst139, modified liquid-gas capillary pressure, set ylm=0.3 not 0.03
: lst143, new rel perm with correct alpha, afm off with gamma=0.0
: lst145, new rel perm with correct alpha, afm off with gamma=0.0, areamodf=0.001
: lst146, new rel perm with correct alpha, alpha=1e-3, not 1.3e-1
: lst149, new rel perm with correct alpha, alpha=1e-4, not 1.e-3, afm on no areamodf
: lst152, same as 149, reduced from -50000 to -5000
: lst155, set ylm back to 0.03
:
RSTART  0
:
:     XYZ                    = 1 table look-up,; pref = ref. press.
:     RADIAL                   = 0 correlations;   tref = ref temp.
:     OTHER                      ^
:                           |
:grid  geometry  nx ny  nz ivplwr ipvtcal iout    pref tref  href
Grid   DCMXYZ    24 14  30    1      1     2     0       0    0     0
:
:      data taken from sandia report:Green et al. 1995, NUREG/CR-6348
Pckr                          :relative perm and pc
:   i  type-curv swirm  rpmm(lamda)  alpham  swext  sgc  iecm
    1  Van-Gen   0.05   .3717      6.36e-7    0     0.0  0    ! matrix block
:
:   i  type-curv swrim unused  unused     p@0-sat sgc   iecm
:   2  linear    0.00  0.000      0.00     1.0     0.0  0    ! emplacement drift
:   i  type-curv swrim unused  unused     p@0-sat sgc   iecm
    2  linear    0.01  0.800      1.0e-1   0.0     0.0  0    ! emplacement drift
:
:   i  type-curv swrim unused  unused     p@0-sat sgc   iecm
    3  linear    0.01  0.000      0.00     1.0     0.0  0    ! primary fracture
:
:   i  type-curv swirf  rpmf(lamda)  alphaf  swext  sgc  iecm
:   4  Van-Gen  0.01   0.800        1.3e-1    0.0    0.0   0   ! matrix fractures
:
: fracture to matrix cement
:SWT   FKRWT        FKRGT     PCWT
   5 TABular  .01   0.  0.  -130.0  0.  0
0      0            1.       0
0.01   0            1.       0
0.03   7.1183e-8     0.99999   0
0.05   9.5353e-7     0.99994   0
0.07   4.6026e-6     0.99981   0
0.09   0.00001435    0.99958   0
0.11   0.000035016   0.99923   0
0.13   0.000073023   0.99873   0
0.15   0.00013649    0.99806   0
0.17   0.00023537    0.99719   0
0.19   0.00038151    0.9961    0
0.21   0.00058884    0.99477   0
0.23   0.00087346    0.99316   0
0.25   0.0012538     0.99127   0
0.27   0.0017507     0.98905   0
```

```
0.29   0.0023876     0.98649   0
0.31   0.003191      0.98356   0
0.33   0.00419       0.98022   0
0.35   0.0054172     0.97645   0
0.37   0.0069085     0.97221   0
0.39   0.0087036     0.96748   0
0.41   0.010846      0.96221   0
0.43   0.013384      0.95638   0
0.45   0.01637       0.94993   0
0.47   0.019861      0.94284   0
0.49   0.023922      0.93506   0
0.51   0.028621      0.92653   0
0.53   0.034035      0.91722   0
0.55   0.040247      0.90706   0
0.57   0.047348      0.89599   0
0.59   0.055441      0.88395   0
0.61   0.064637      0.87087   0
0.63   0.075059      0.85667   0
0.65   0.086844      0.84127   0
0.67   0.10014       0.82456   0
0.69   0.11513       0.80644   0
0.71   0.132         0.78679   0
0.73   0.15096       0.76546   0
0.75   0.17227       0.74229   0
0.77   0.19622       0.71709   0
0.79   0.22313       0.68963   0
0.81   0.2534        0.65964   0
0.83   0.28752       0.62679   0
0.85   0.32606       0.59063   0
0.87   0.36977       0.55063   0
0.89   0.41962       0.50602   0
0.91   0.47695       0.45573   0
0.93   0.54373       0.39812   0
0.95   0.62321       0.33039   0
0.97   0.72179       0.24677   0
0.99   0.8587        0.12914   0
1.     1.            0         0
/
: fracture to fracture TSw34
   4 TABular  .01   0.  0.  -5000.0  0.  0 :cement
0      0             1.        50000.
0.01   0             1.        50000.
0.03   9.6473e-6     0.99999   47239.
0.05   0.000063208   0.99994   35503.
0.07   0.00019049    0.99981   29932.
0.09   0.00041774    0.99958   26447.
0.11   0.0007697     0.99923   23975.
0.13   0.0012704     0.99873   22087.
0.15   0.0019435     0.99806   20574.
0.17   0.0028126     0.99719   19319.
0.19   0.0039017     0.9961    18251.
0.21   0.0052347     0.99477   17324.
0.23   0.0068364     0.99316   16505.
0.25   0.0087318     0.99127   15774.
0.27   0.010947      0.98905   15113.
0.29   0.013509      0.98649   14509.
```

```
0.31   0.016444      0.98356   13954.
0.33   0.019783      0.98022   13439.
0.35   0.023555      0.97645   12959.
0.37   0.027791      0.97221   12509.
0.39   0.032524      0.96748   12084.
0.41   0.03779      0.96221   11682.
0.43   0.043624      0.95638   11299.
0.45   0.050067      0.94993   10934.
0.47   0.057158      0.94284   10583.
0.49   0.064942      0.93506   10245.
0.51   0.073466      0.92653   9919.5
0.53   0.082782      0.91722   9603.7
0.55   0.092944      0.90706   9296.7
0.57   0.10401       0.89599   8997.3
0.59   0.11605       0.88395   8704.5
0.61   0.12913       0.87087   8417.2
0.63   0.14333       0.85667   8134.4
0.65   0.15873       0.84127   7855.2
0.67   0.17544       0.82456   7578.6
0.69   0.19356       0.80644   7303.7
0.71   0.21321       0.78679   7029.4
0.73   0.23454       0.76546   6754.8
0.75   0.25771       0.74229   6478.6
0.77   0.28291       0.71709   6199.6
0.79   0.31037       0.68963   5916.3
0.81   0.34036       0.65964   5626.9
0.83   0.37321       0.62679   5329.1
0.85   0.40937       0.59063   5020.2
0.87   0.44937       0.55063   4696.5
0.89   0.49398       0.50602   4352.8
0.91   0.54427       0.45573   3981.1
0.93   0.60188       0.39812   3568.8
0.95   0.66961       0.33039   3092.7
0.97   0.75323       0.24677   2500.
0.99   0.87086       0.12914   1597.8
1.     1.            0         0
/
/
  Debug  1
  0
Thermal-prop
: no rho       cpr    ckdry  cksat    crp  crt   tau  cdiff   cexp  enbd
  1  1.600e+03 840.0   0.50   1.00     0     0    .5  2.13e-5  1.8  0. 0 !matrix
  2  1.600e+03 840.0   10.0   10.0     0     0    .5  2.13e-5  1.8  0. 0 !drift
skip
  3  1.600e+03 5.0e+7  0.50   1.00     0     0    .5  2.13e-5  1.8  0. 0 !side boundaries
  4  1.600e+03 1.0e+9  0.50   1.00     0     0    .5  2.13e-5  1.8  0. 0 !bottom boundary
  5  1.600e+03 5.0e+7  0.50   1.00     0     0    .5  2.13e-5  1.8  0. 0 !top boundary
  6  1.600e+03 5.0e+8  1.50   2.00     0     0    .5  2.13e-5  1.8  0. 0 !front bc near heater
: noskip
  3  1.600e+03 840.0   0.50   1.00     0     0    .5  2.13e-5  1.8  0. 0 !side boundaries
  4  1.600e+03 840.0   0.50   1.00     0     0    .5  2.13e-5  1.8  0. 0 !bottom boundary
  5  1.600e+03 840.0   0.50   1.00     0     0    .5  2.13e-5  1.8  0. 0 !top boundary
  6  1.600e+03 840.0   0.50   1.00     0     0    .5  2.13e-5  1.8  0. 0 !front bc near heater
noskip
: skip
```

```
  3  1.600e+03 1.0e3   0.50   1.00     0     0    .5  2.13e-5  1.8  0. 0 !side boundaries
  4  1.600e+03 1.0e3   0.50   1.00     0     0    .5  2.13e-5  1.8  0. 0 !bottom boundary
  5  1.600e+03 1.0e3   0.50   1.00     0     0    .5  2.13e-5  1.8  0. 0 !top boundary
  6  1.600e+03 1.0e3   0.50   1.00     0     0    .5  2.13e-5  1.8  0. 0 !front bc near heater
  7  1.600e+03 1.0e3   0.50   1.00     0     0    .5  2.13e-5  1.8  0. 0 !fractures
: noskip
0
:    igrid   rw      re
DXYZ   0
: (dx(i),i=1,nx)
0.004 .008 .015 .015 .015 .015 .015 .03 .03 .03 !total for line 0.177
0.03 .03 .03 .03 .03 .03 .03 .03 .03 .03  !total for line 0.3
0.03 .03 .03 .015  !total for line 0.105
:total in x-direction is 0.582 plus .019 beyond edge elements, 24 elements
: (dy(j),j=1,ny)
0.02 .02 .02 .02 .02 .02 .02 .02 .02 .02  !total for line 0.2
0.02 .02 .02 .01  !total for line .07
:total in y-direction is 0.27 plus .03 beyond edge elements, 14 elements
: (dz(k),k=1,nz)
: lowered heater by 0.1
0.03 .06 .06 .06 .06 .06 .06 .06 .04 .04  !total for line 0.53, and 0.56 from top
0.02 .02 .015 .015 .025 .03 .03 .025 .015 .015 !total for line 0.21
0.02 .02 .04 .04 .06 .06 .06 .06 .06 .03 !total for line 0.45 and 0.48 from bottom
:total z-direction is 1.19 plus .06 beyond end elements, 30 elements
:
PhiK
: i1 i2 j1 j2 k1 k2 ist ithrm vb  porf permxf permyf permzf pormm permm  istm ithrmm
  1  24  1 14  1  30 4   7   0.0  1.00 1.e-10 1.e-10 1.e-10 0.50  2.e-17 1     1 ! matrix
:
: skip
: following are new bc with more mass to have lower edge temps
  1  24 14 14   1 30 4   7 1.0e-2 1.00 1.e-10 1.e-10 1.e-10 0.12  2.e-17 1     3 ! front
 24  24  1 14   1 30 4   7 1.0e-2 1.00 1.e-10 1.e-10 1.e-10 0.12  2.e-17 1     3 ! side
  1   4 14 14  14 19 4   7 1.0e-2 1.00 1.e-10 1.e-10 1.e-10 0.12  2.e-17 1     6 ! front at heater
  1  24  1 14   1  1 4   7 1.0e-2 1.00 1.e-10 1.e-10 1.e-10 0.12  2.e-17 1     5 ! top
  1  24  1 14  30 30 4   7 5.0e-0 1.00 1.e-10 1.e-10 1.e-10 0.50  2.e-17 1     4 ! bottom
: noskip
  1   3  1 14  14 14 2   2     0. 1.00 1.e-10 1.e-10 1.e-10 0.99  1.e-12 4    2 ! drift
  1   5  1 14  15 15 2   2     0. 1.00 1.e-10 1.e-10 1.e-10 0.99  1.e-12 4    2 ! drift
  1   6  1 14  16 16 2   2     0. 1.00 1.e-10 1.e-10 1.e-10 0.99  1.e-12 4    2 ! drift
  1   6  1 14  17 17 2   2     0. 1.00 1.e-10 1.e-10 1.e-10 0.99  1.e-12 4    2 ! drift
  1   5  1 14  18 18 2   2     0. 1.00 1.e-10 1.e-10 1.e-10 0.99  1.e-12 4    2 ! drift
  1   3  1 14  19 19 2   2     0. 1.00 1.e-10 1.e-10 1.e-10 0.99  1.e-12 4    2 ! drift
: noskip
   0
:
Init
:  i1  i2  j1  j2  k1  k2  p        t     sg   xg2 pm        tm   sgm xgm
   1  24  1   14   1  30  1.0315e5 20.0  0.80 0.  1.0315e5 20.0 .70  0. ! matrix
   1  24  1   14  30  30  1.0315e5 20.0  0.90 0.  1.0315e5 20.0 .90  0. ! bottom
0
DCMPARA
: i1 i2 j1 j2 k1 k2   volf  areamodf  xlm   ylm   zlm
   1 24  1 14  1 30   0.050   1.0     .05   0.03   .05  -5 ! matrix
:  1 24  1 14  1 30   0.005   1.0    .005   .003  .005  1.0e-4 ! matrix
0
```

```
:
Recurrent
:       ns     fach        facm  (fach and facm are multipliers)
Source   2     1.00       1.
: this is for the heat source
:  is1 is2 js1 js2 ks1 ks2  istyp
   1   3   1  3   17  17   33
:0.0    0.0
1.e+4  3.51e+1
1.e+10 3.51e+1
0
: this for the water infiltration
:  is1 is2 js1 js2 ks1 ks2  istyp
   1   2   1  7    1   1   13
0.0    20.0   0.0
2.60e5 20.0   0.0
3.60e5 20.0  2.894e-6
1.486e7 20.0  2.894e-6
1.815e7 20.0  7.534e-7
1.e+10 20.0  7.534e-7
0
Output   C=-10 Q=-10   T=1   G=1   P=1
:
:    isolv  newtnmn  newtnmx  north  nitmax  level
Solve 4      2         12      4      100
:
:AUTO-step  DPMXE    DSMXE  DTMPMXE   DP2MXe TACCEL   IAUTODT  FAC1
AUTO-step   5.0E+4   0.03    5.0       1.e4  1.0e-3      0      0
:
:TOLR TOLP  TOLS  TOLT  TOLP2  TOLM  TOLA  TOLE rtwotol  rmxtol   smxtol
Tolr   1. 5.e-4  5.e-3  1.    1.e-3 1.e-3 1.e-3  1.e-12  1.e-12   1.e-12
:
:Limit dpmx    dsmx dtmpmx dp2mx dtmn dtmx icutmx
LIMIT  1.e5    .08    10.   1.e5 1.e-9 .8
:
:     target  dt    dpmx   dsmx   dp2mx   dtmpmx
:
:      print all at every target time
PLOTS 1 0 4
1 10 451 541
Time[d] 5.
Time[d] 10.
Time[d] 50.
Time[d] 110.
Time[d] 172.
Time[d] 210.
Ends
```

++

Calculation of relative permeability for the AFM (active fracture model)

A mathematica notebook was used to calculate the relative permeability values for the AFM (active fracture model). The notebook was originally written by Scott Painter and

later modified by R.T. Green. A copy of the notebook is attached as Appendix A for reference.
++

Matrix saturation

Matrix saturations measured at the conclusion of Test 2. The figure on the left is for saturation at the mid-plane of the test cell. The right figure is for saturation at the edge of the test. Saturation goes from 0 (white) to 1 (dark).

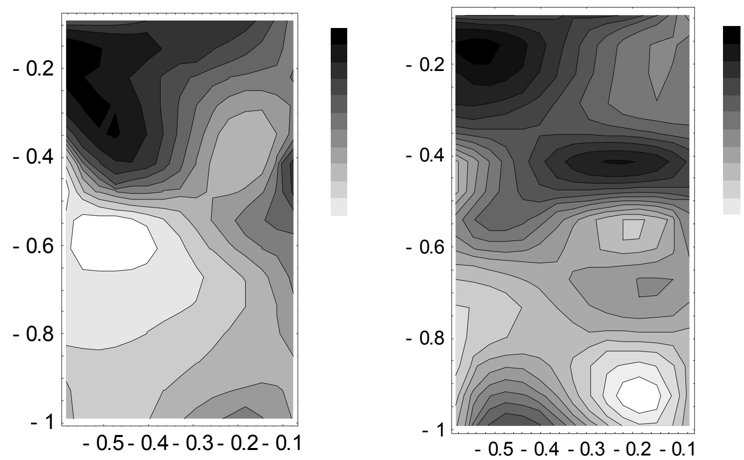

Results from simulations lst155 through lst172.

Following are graphs of

1) **matrix saturation**
2) **matrix temperature**
3) **fracture saturation**

Lst155

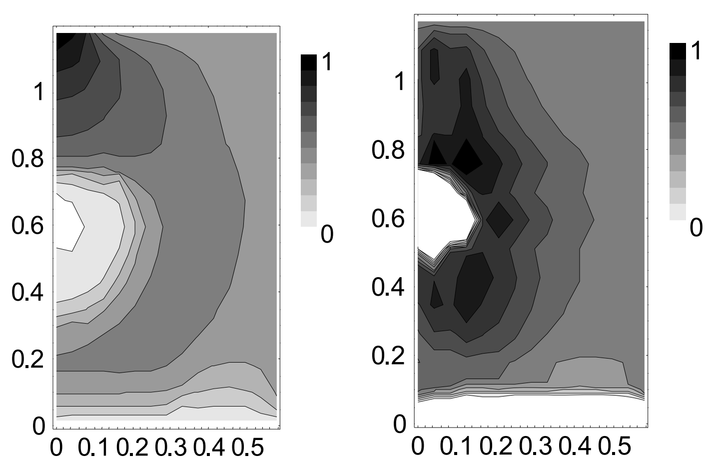

Lst156

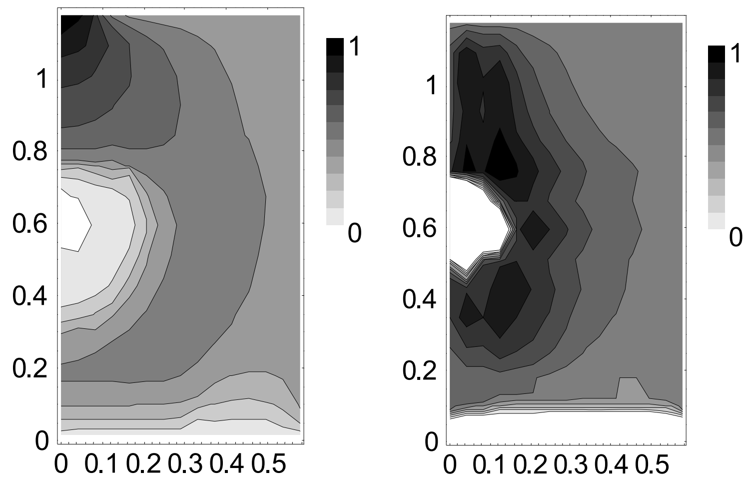

Lst157

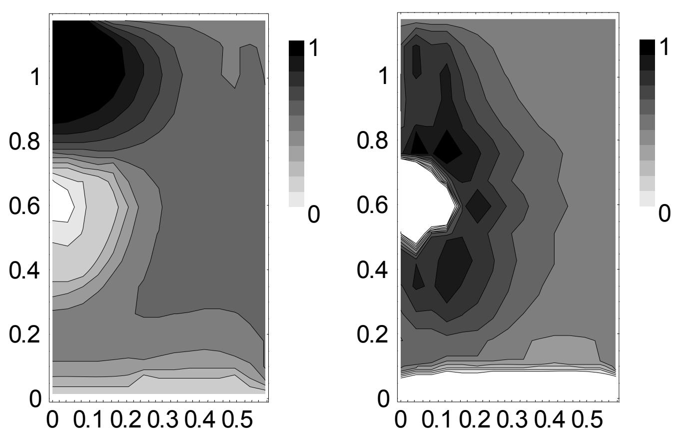

Lst158

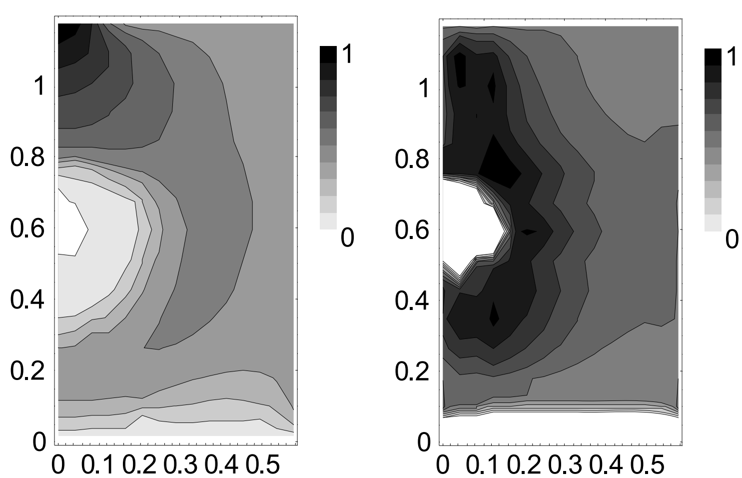

Lst159

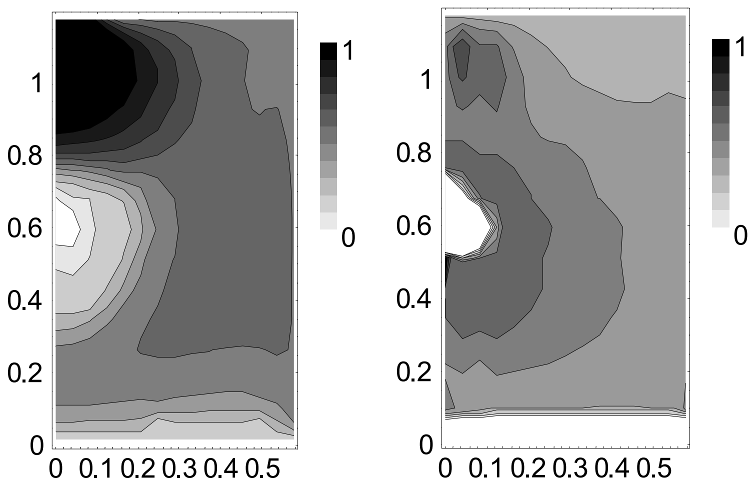

Lst160

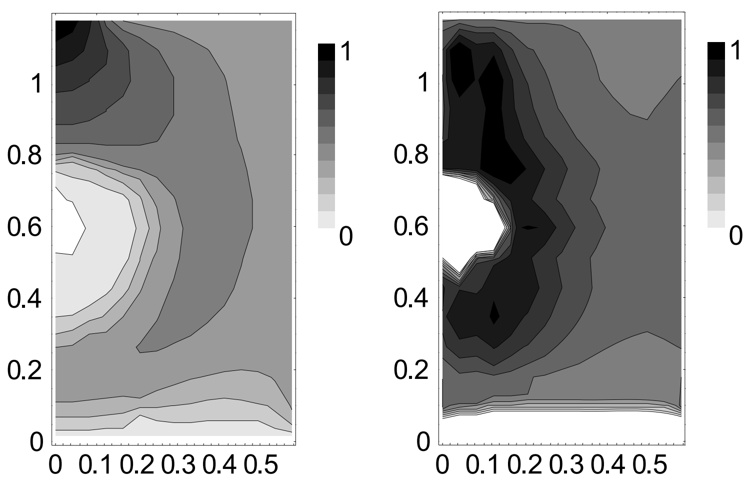

Lst161

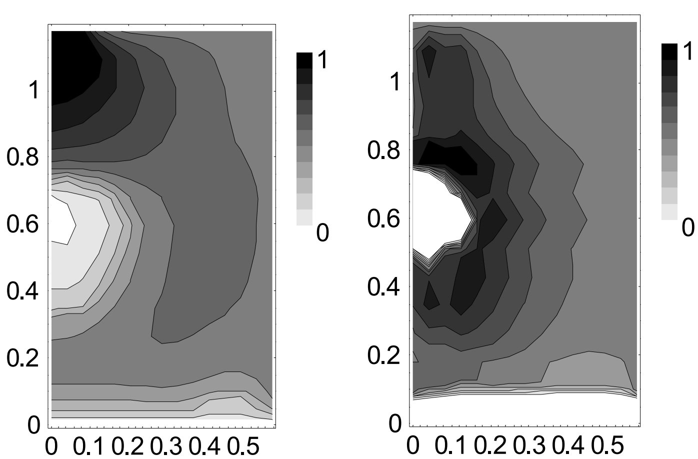

Lst162

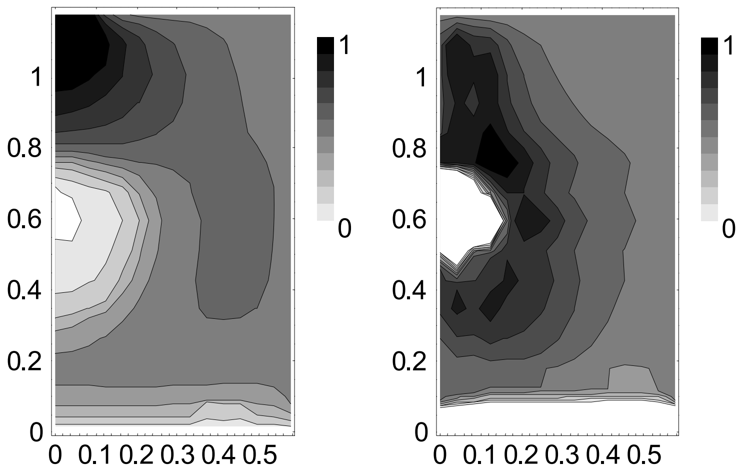

Lst163

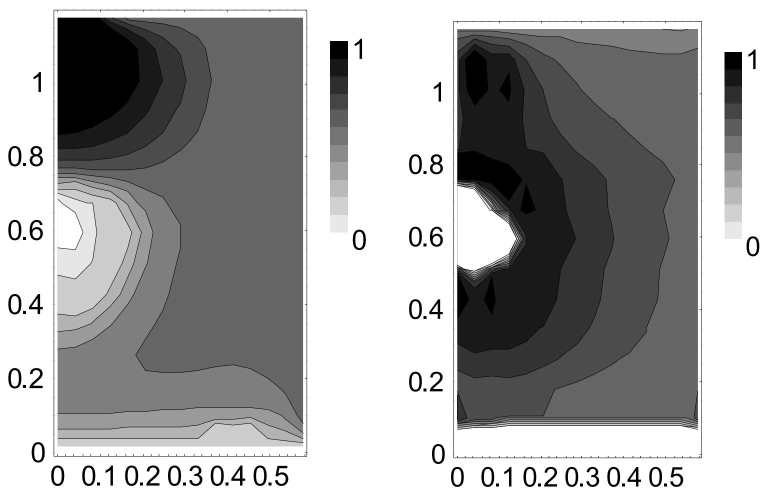

Lst164

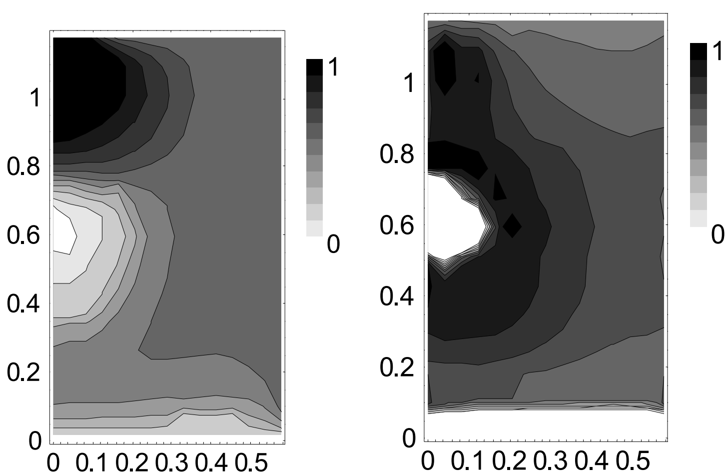

Lst165

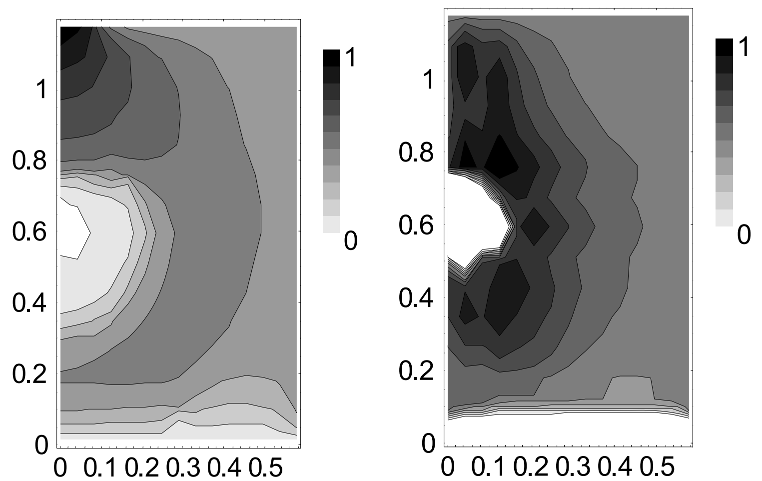

Lst166

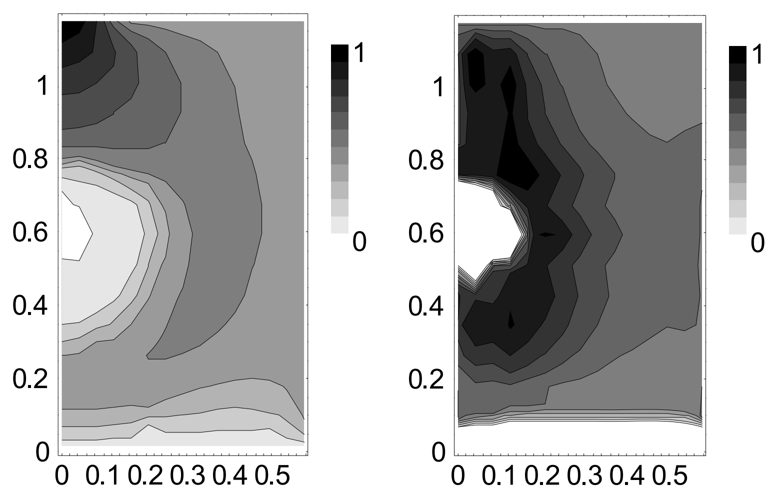

Lst167

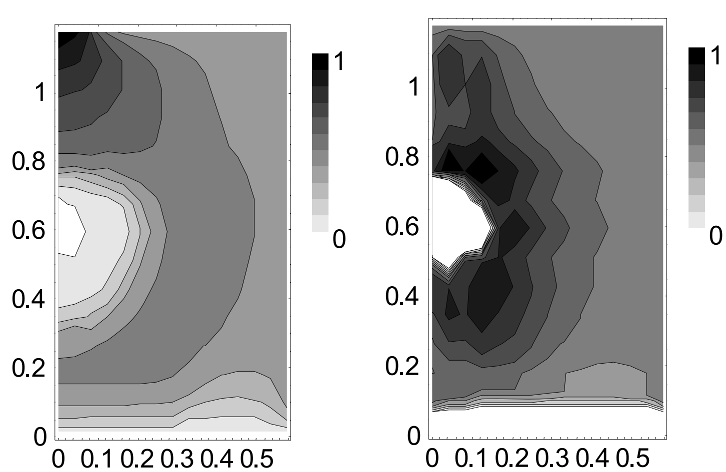

Lst168

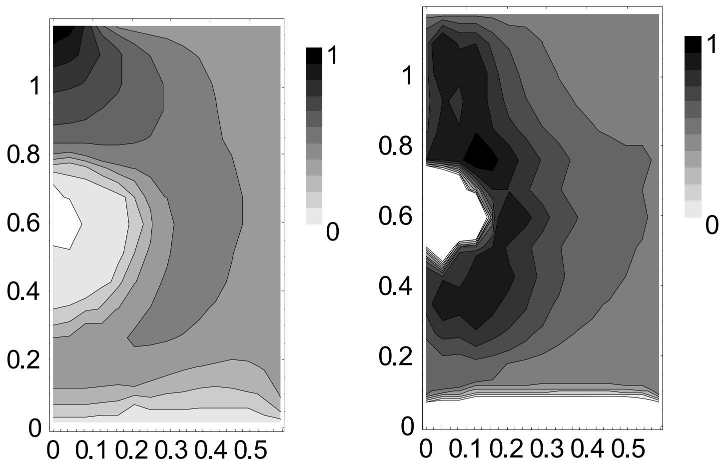

Lst169

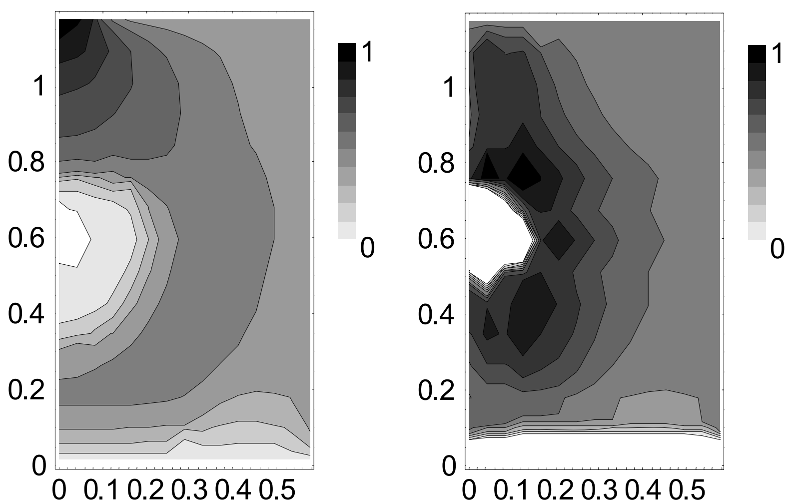

Lst170

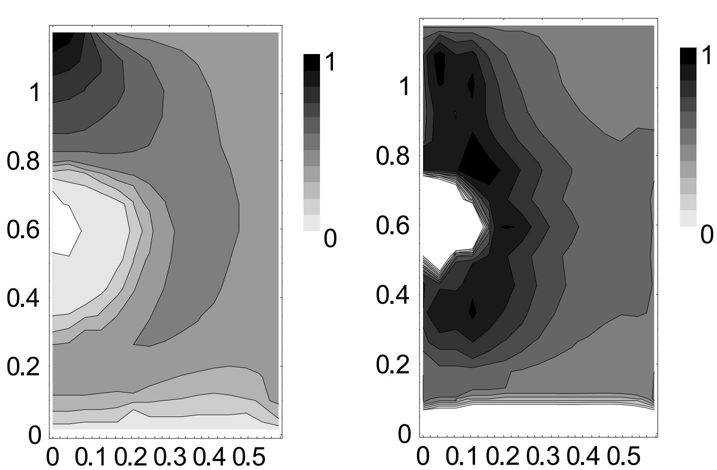

Lst171

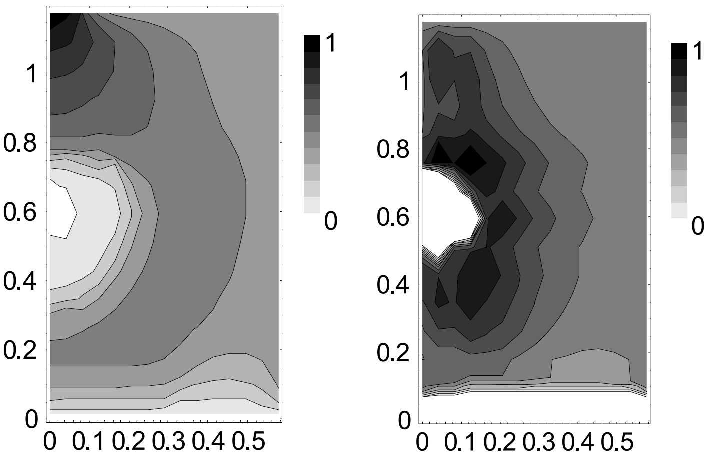

Lst172

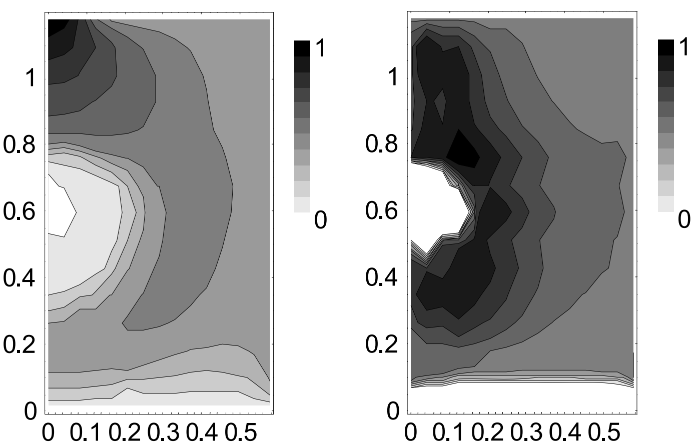

Matrix Temperatures

Temperatures range from 22 C (white) to the maximum (dark), as listed in Table 2 in this notebook. The left image is the xz plane. The right image is the yz plane.

Lst155

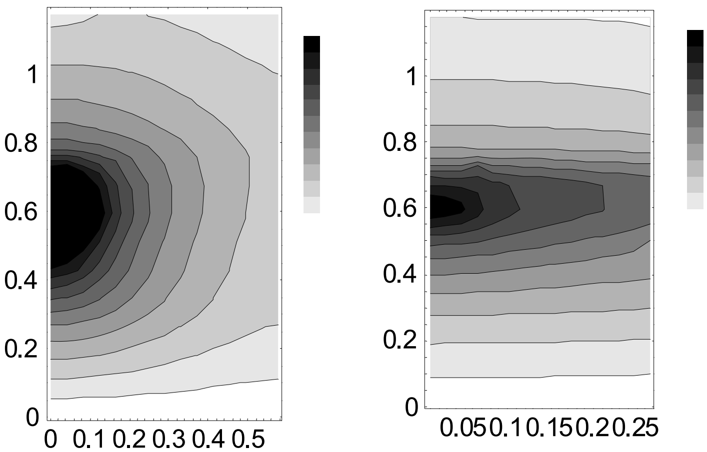

Lst156

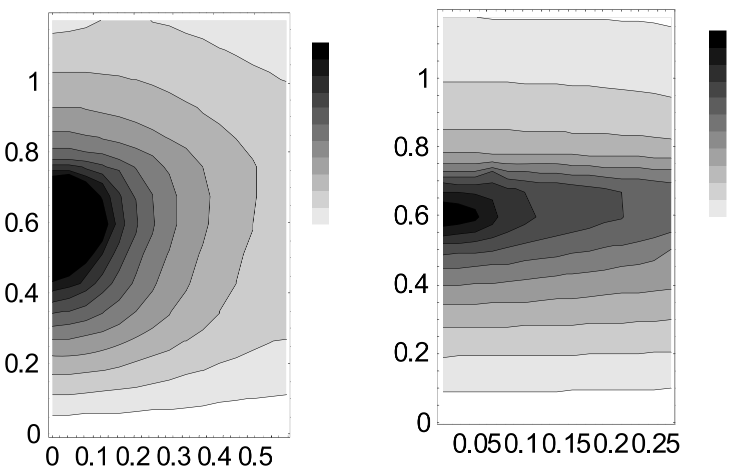

Lst157

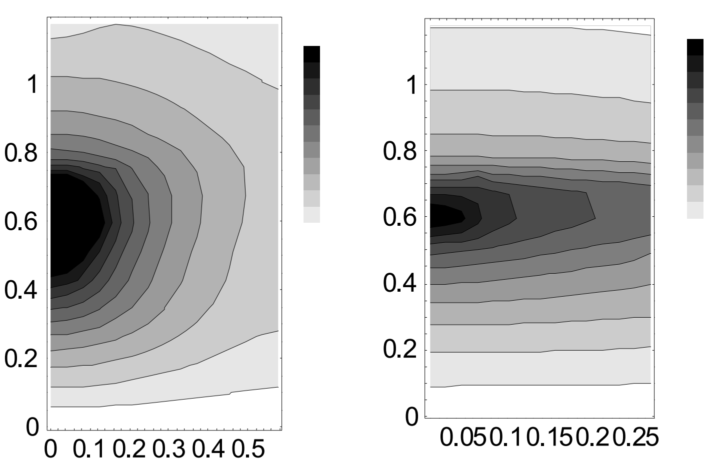

Lst158

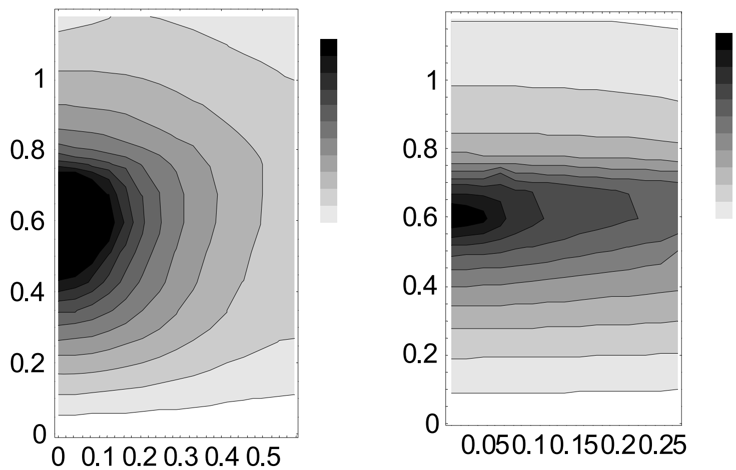

Lst159

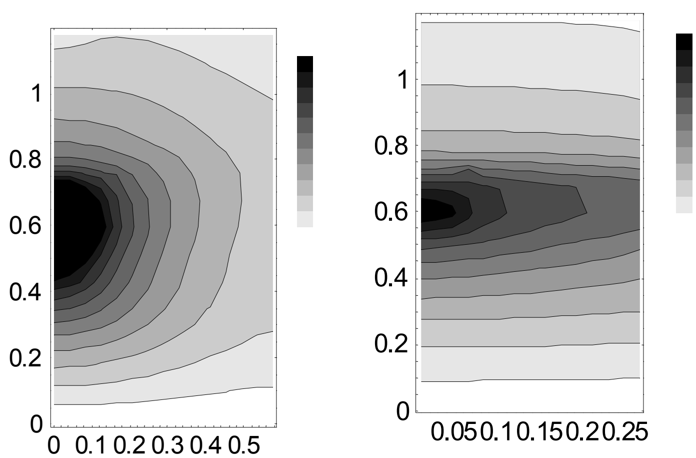

Lst160

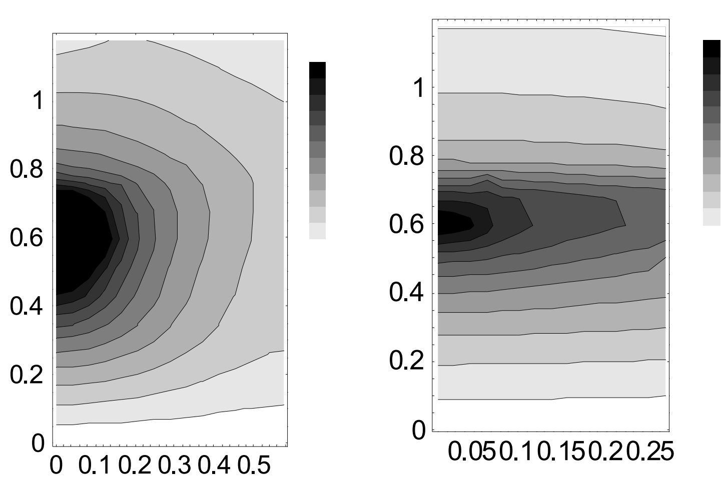

Lst161

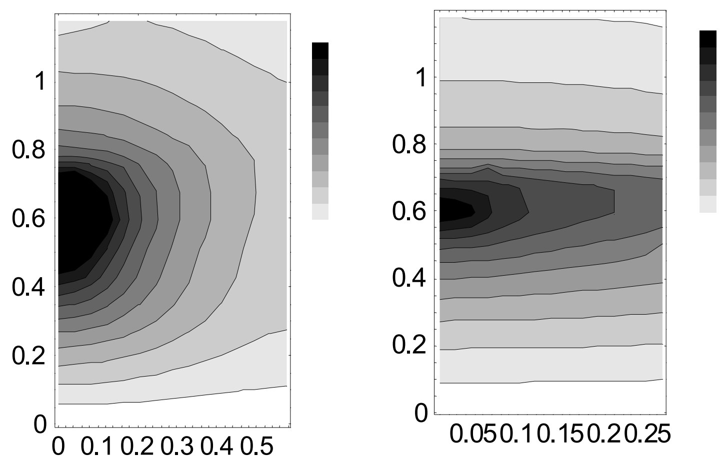

lst162

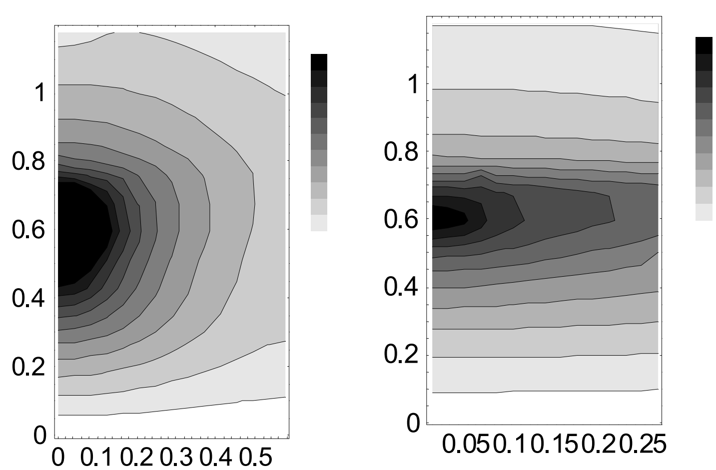

Lst163

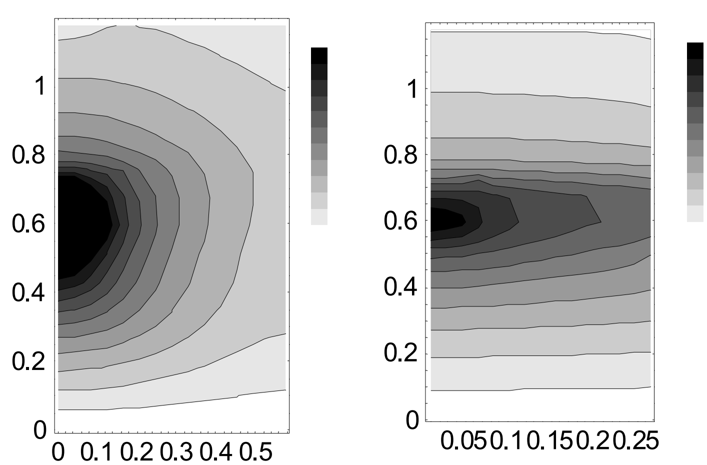

Lst164

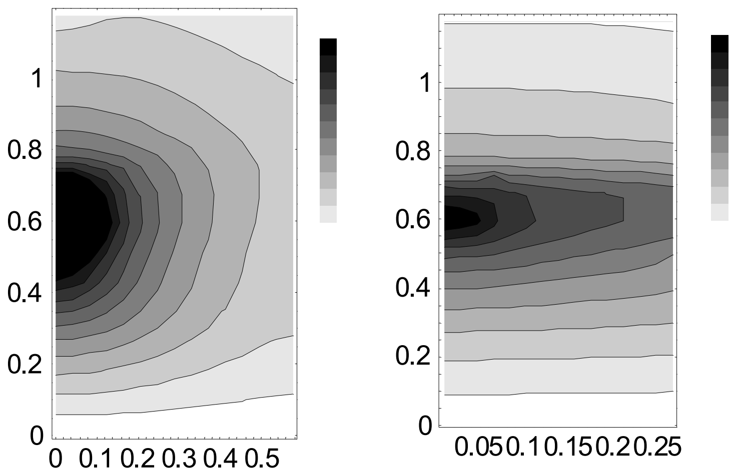

lst165

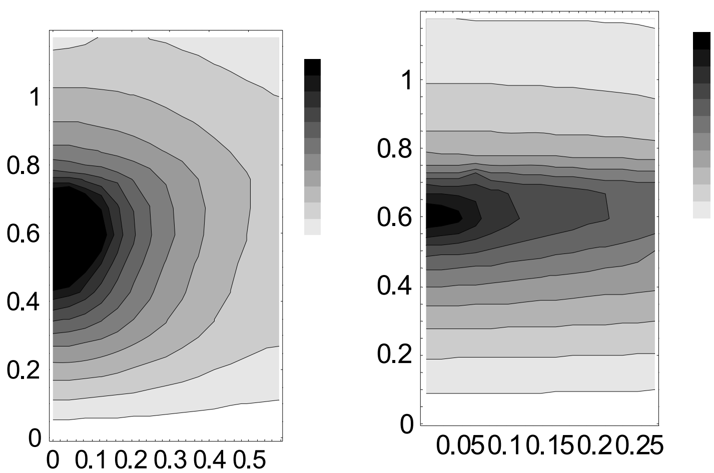

lst166

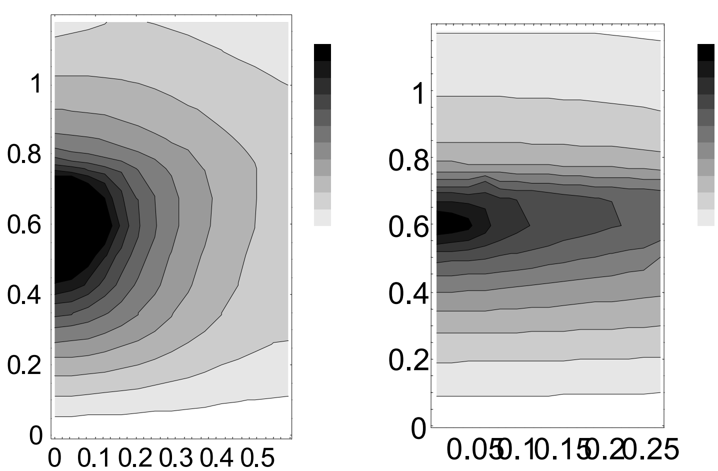

lst167

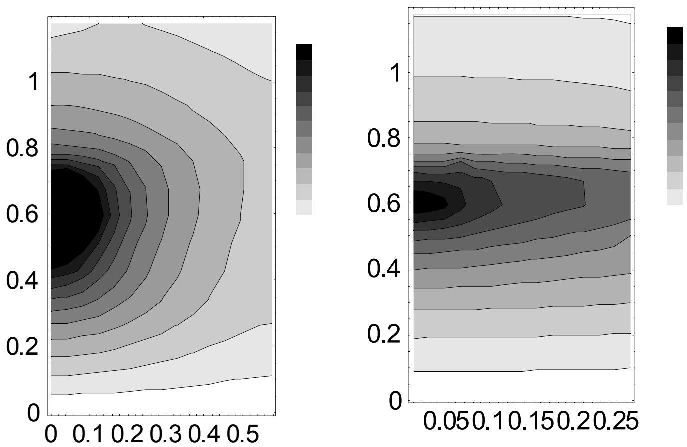

lst168

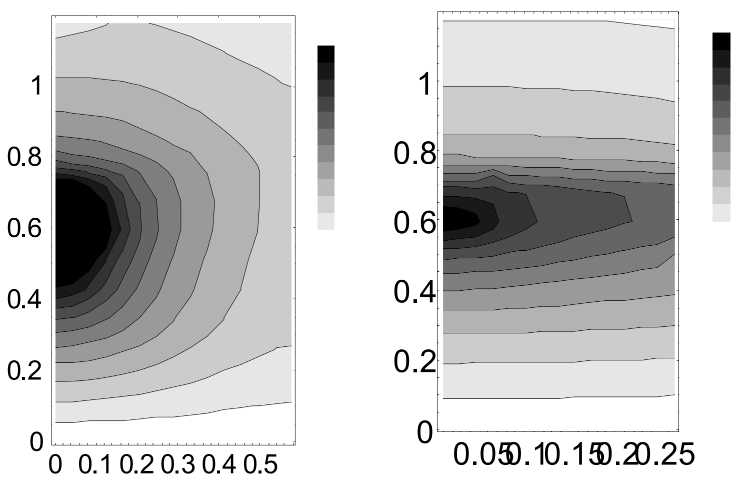

lst169

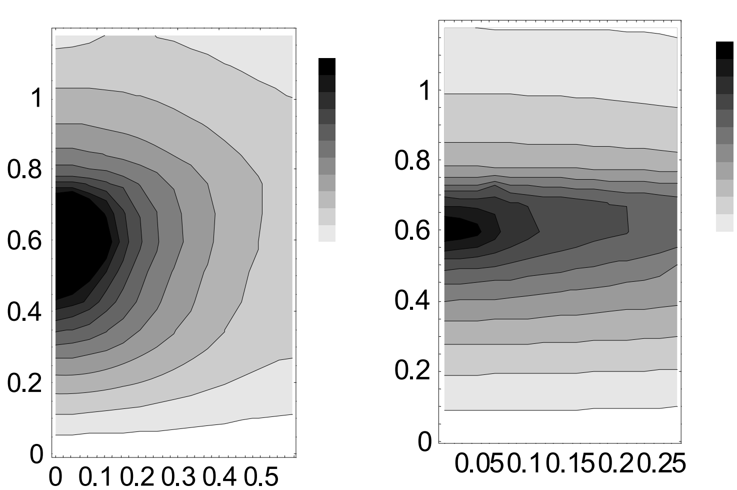

lst170

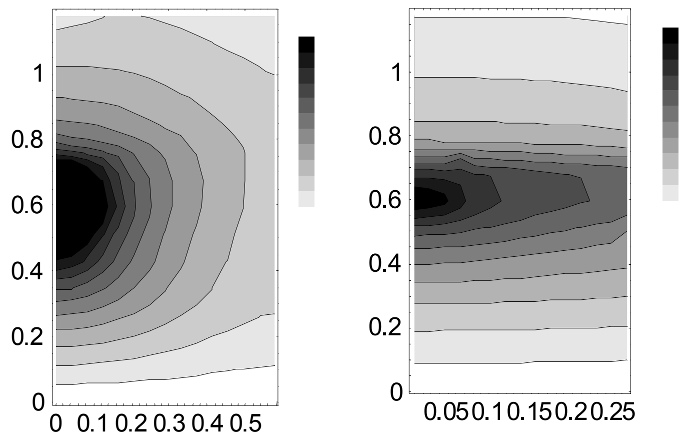

lst171

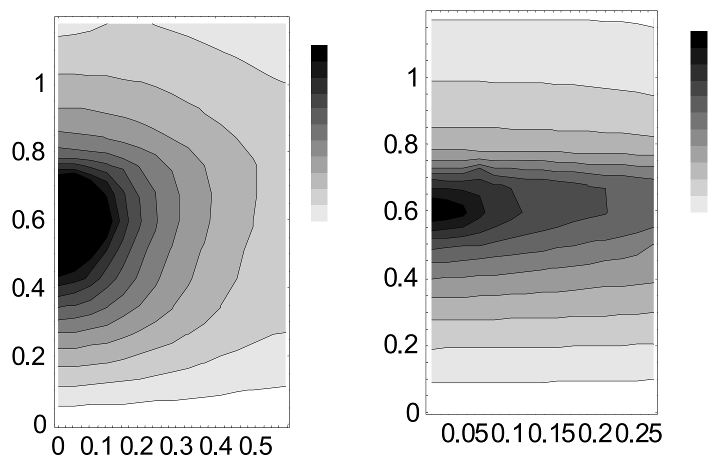

lst172

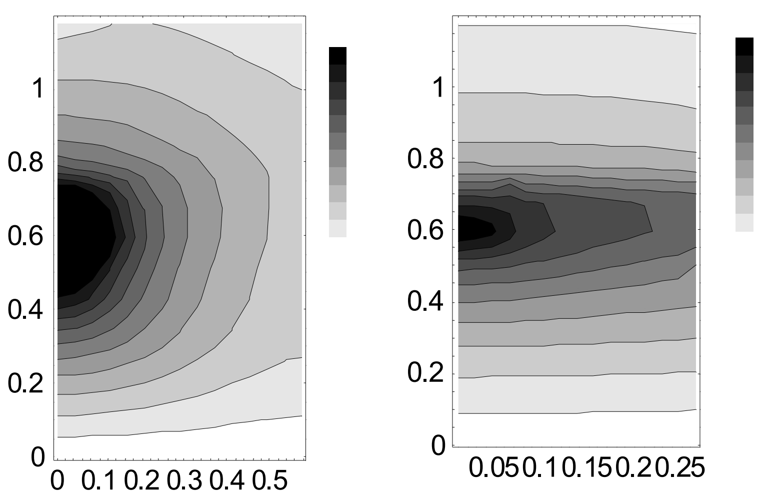

Fracture Saturations

Saturations range for 0 (white) to the maximum (see Table 1 in this notebook). There are four slices taken from each simulation. Of the ten slices provided in each mathematica notebook, slices 1, 5, 9, and 10 are copied to this scientific notebook.

Lst155

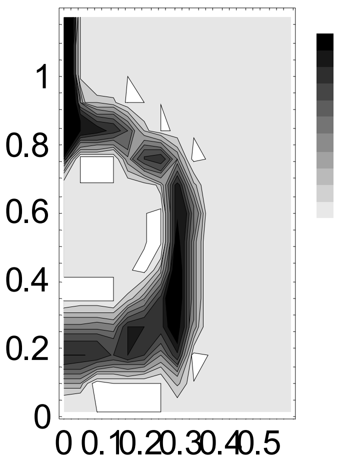

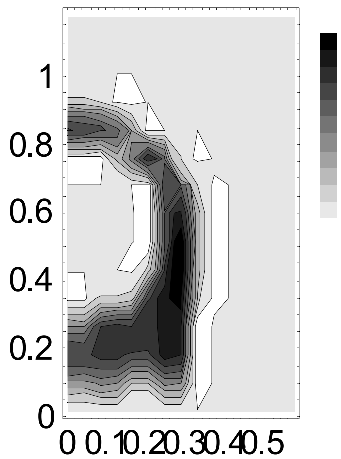

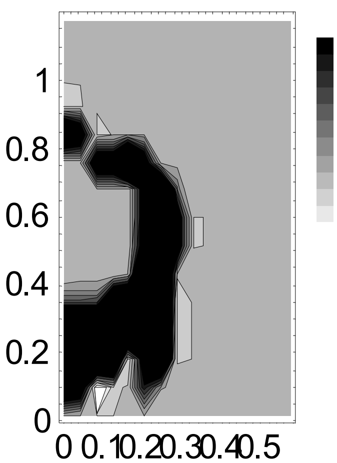

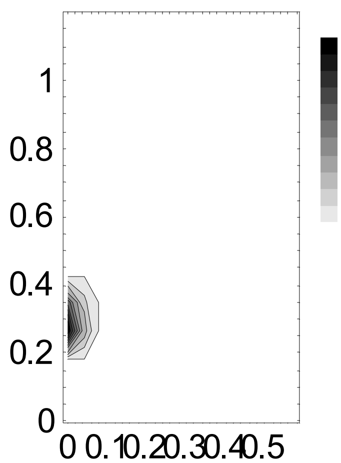

Lst156

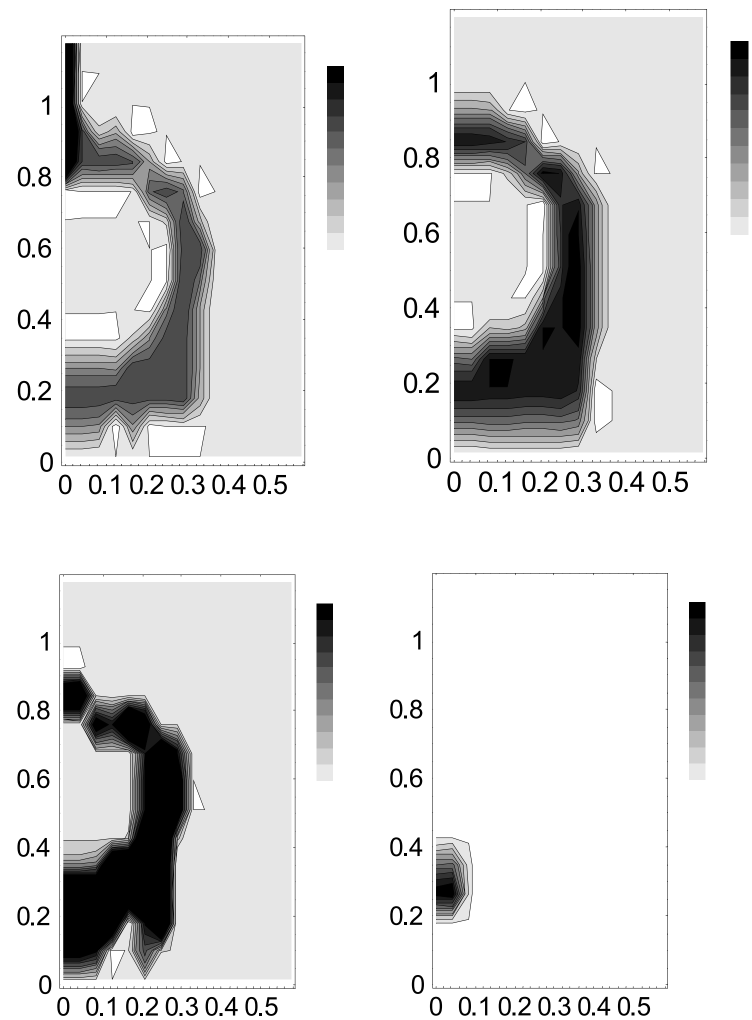
0 0.2 0.4 0.6 0.8 1
0 0.1 0.2 0.3 0.4 0.5
0 0.2 0.4 0.6 0.8 1
0 0.1 0.2 0.3 0.4 0.5
0 0.2 0.4 0.6 0.8 1
0 0.1 0.2 0.3 0.4 0.5
0 0.2 0.4 0.6 0.8 1
0 0.1 0.2 0.3 0.4 0.5

lst157

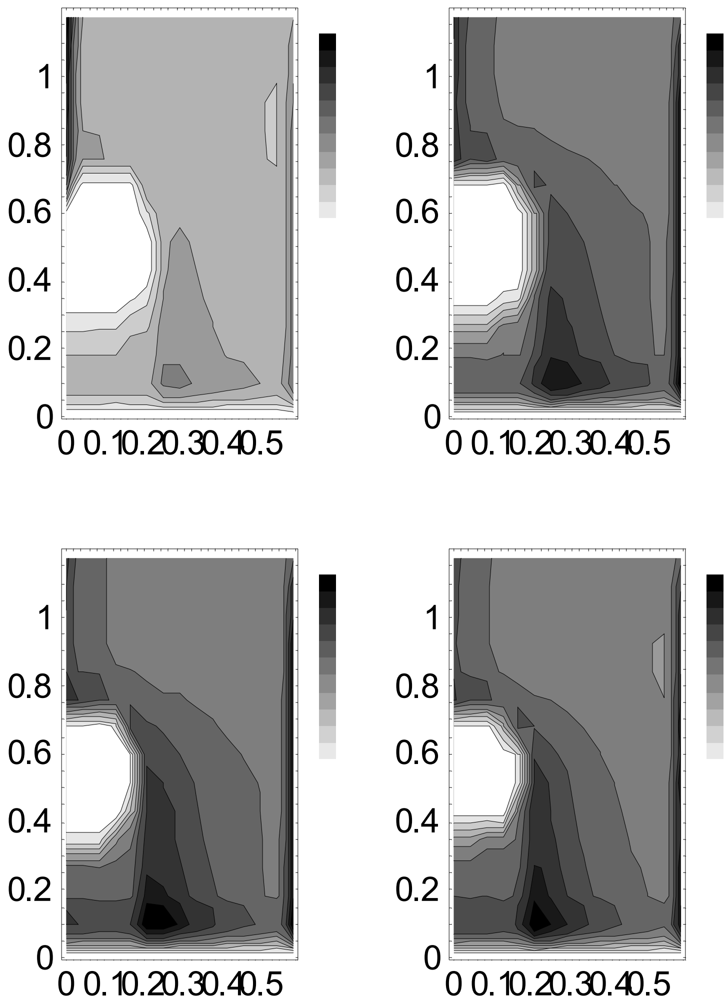

lst158

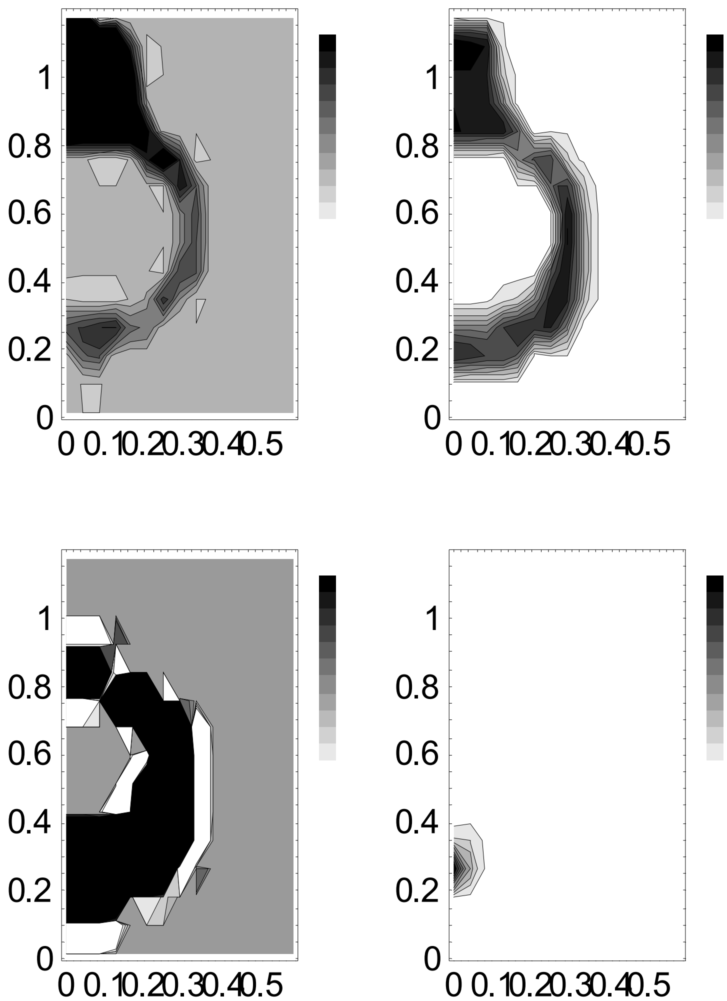
1
0.8
0.6
0.4
0.2
0
0 0.10.20.30.40.5
1
0.8
0.6
0.4
0.2
0
0 0.10.20.30.40.5
1
0.8
0.6
0.4
0.2
0
0 0.10.20.30.40.5
1
0.8
0.6
0.4
0.2
0
0 0.10.20.30.40.5

lst159

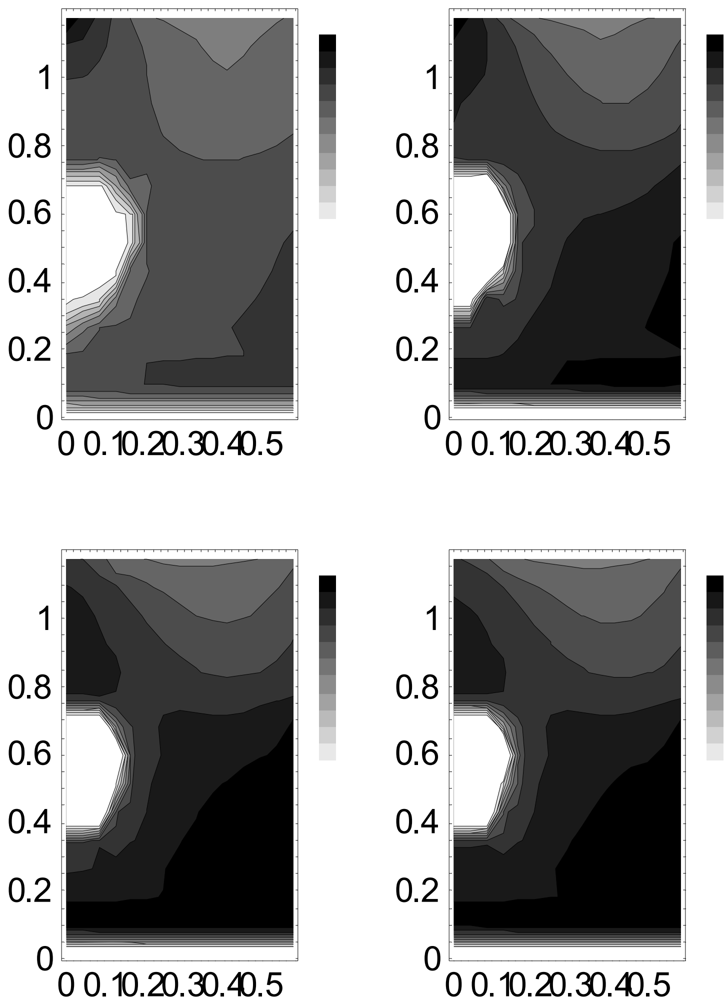
1
0.8
0.6
0.4
0.2
0
0 0.10.20.30.40.5
1
0.8
0.6
0.4
0.2
0
0 0.10.20.30.40.5
1
0.8
0.6
0.4
0.2
0
0 0.10.20.30.40.5
1
0.8
0.6
0.4
0.2
0
0 0.10.20.30.40.5

lst160

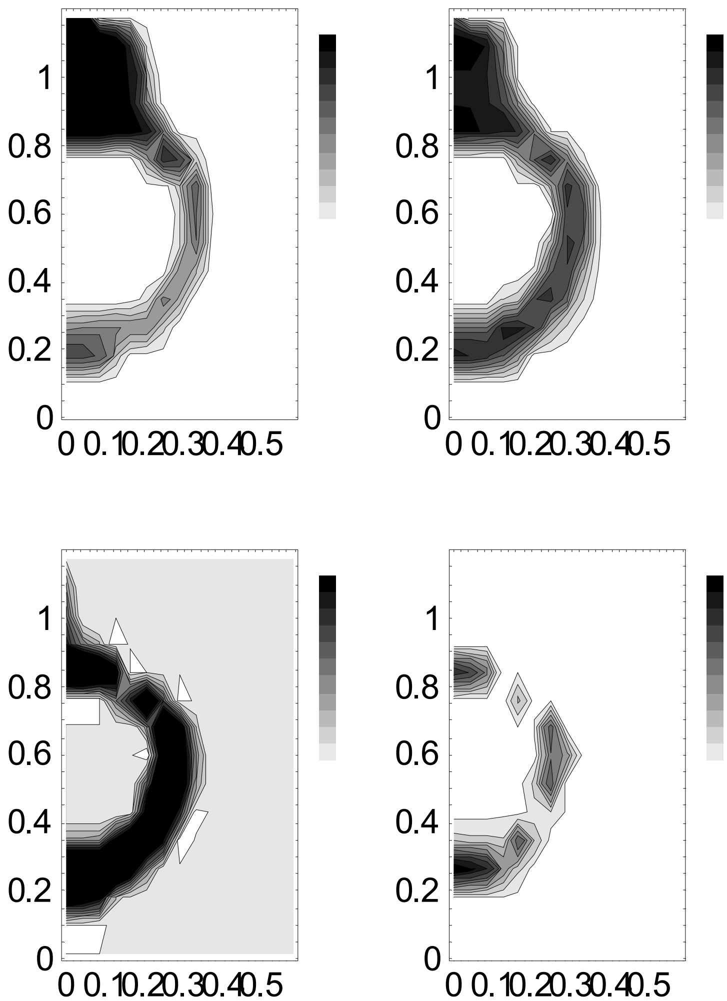

lst161

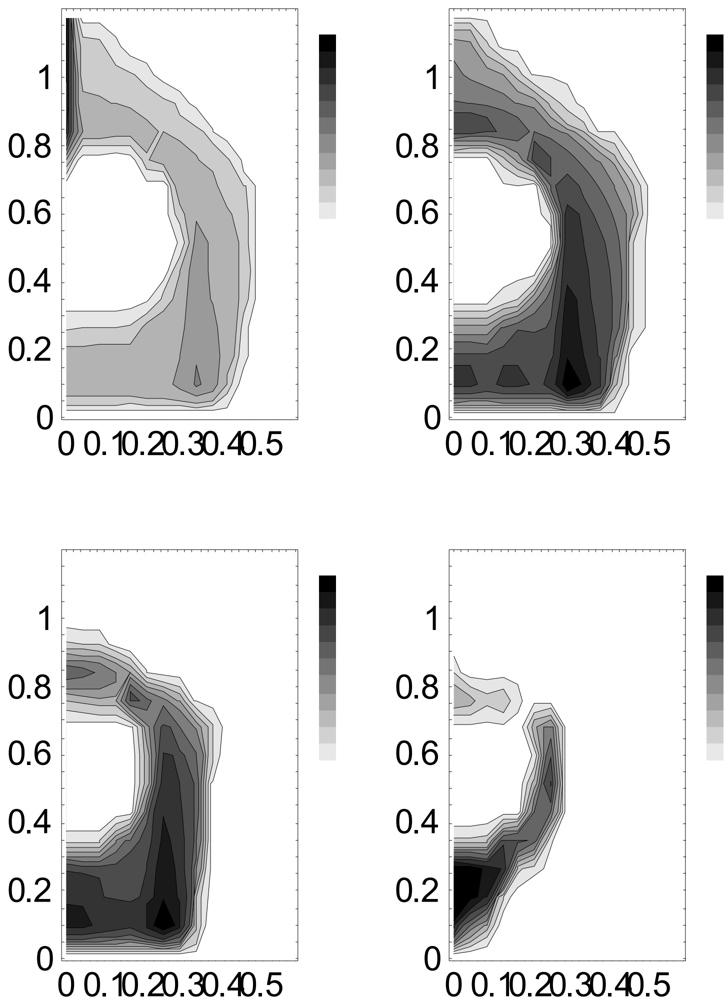

lst162

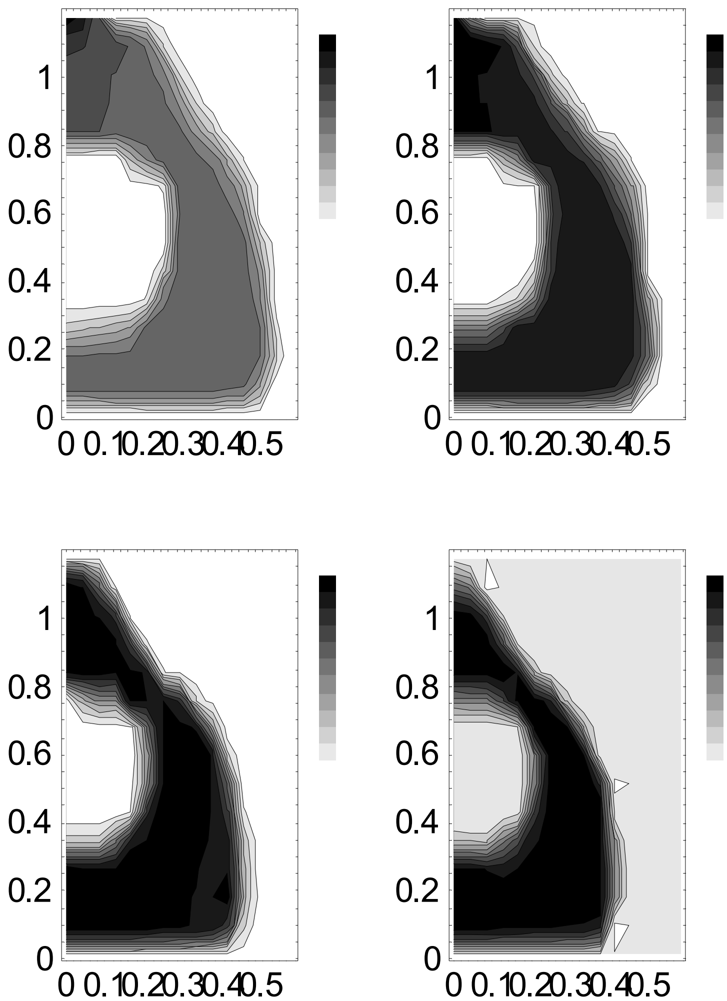
1
0.8
0.6
0.4
0.2
0
0 0.10.20.30.40.5
1
0.8
0.6
0.4
0.2
0
0 0.10.20.30.40.5
1
0.8
0.6
0.4
0.2
0
0 0.10.20.30.40.5
1
0.8
0.6
0.4
0.2
0
0 0.10.20.30.40.5

lst163

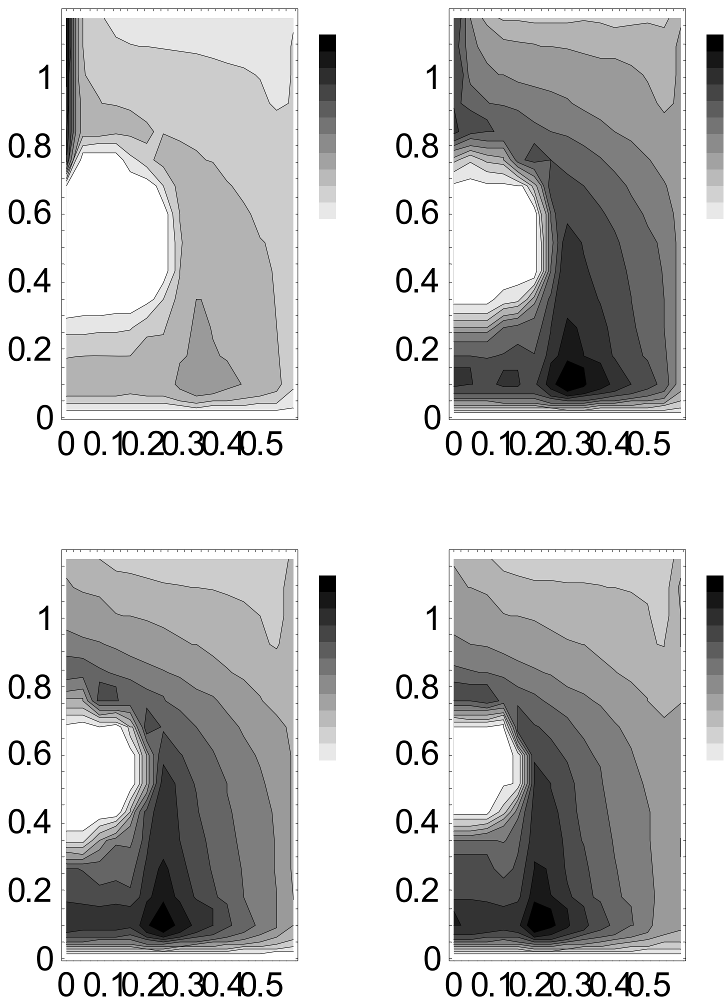

lst164

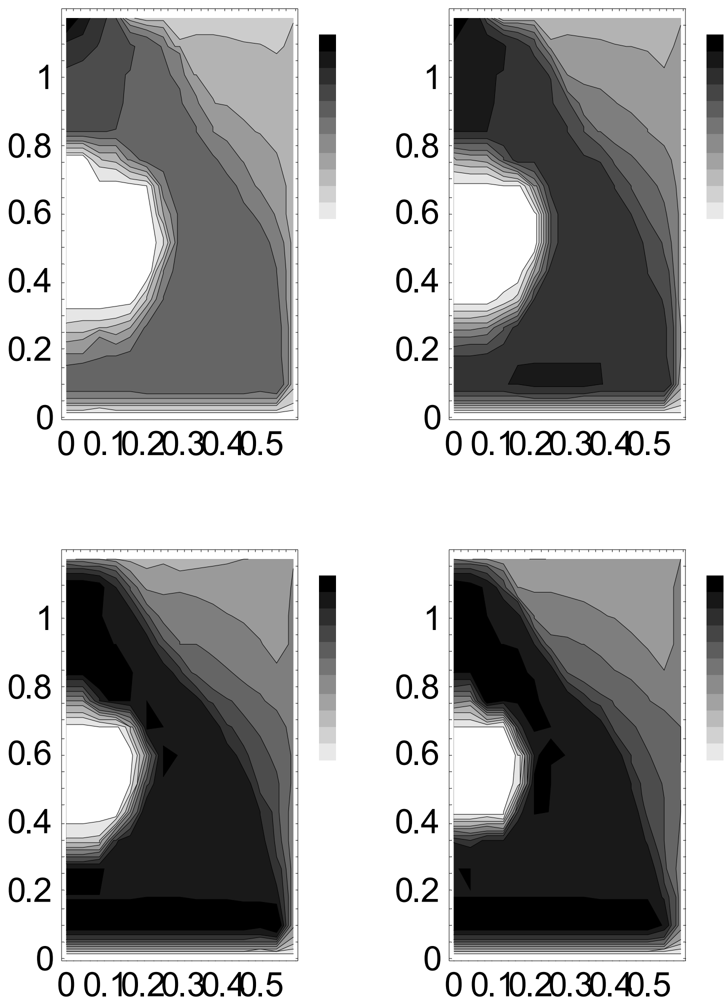
0 0.2 0.4 0.6 0.8 1
0 0.1 0.2 0.3 0.4 0.5
0 0.2 0.4 0.6 0.8 1
0 0.1 0.2 0.3 0.4 0.5
0 0.2 0.4 0.6 0.8 1
0 0.1 0.2 0.3 0.4 0.5
0 0.2 0.4 0.6 0.8 1
0 0.1 0.2 0.3 0.4 0.5

lst165

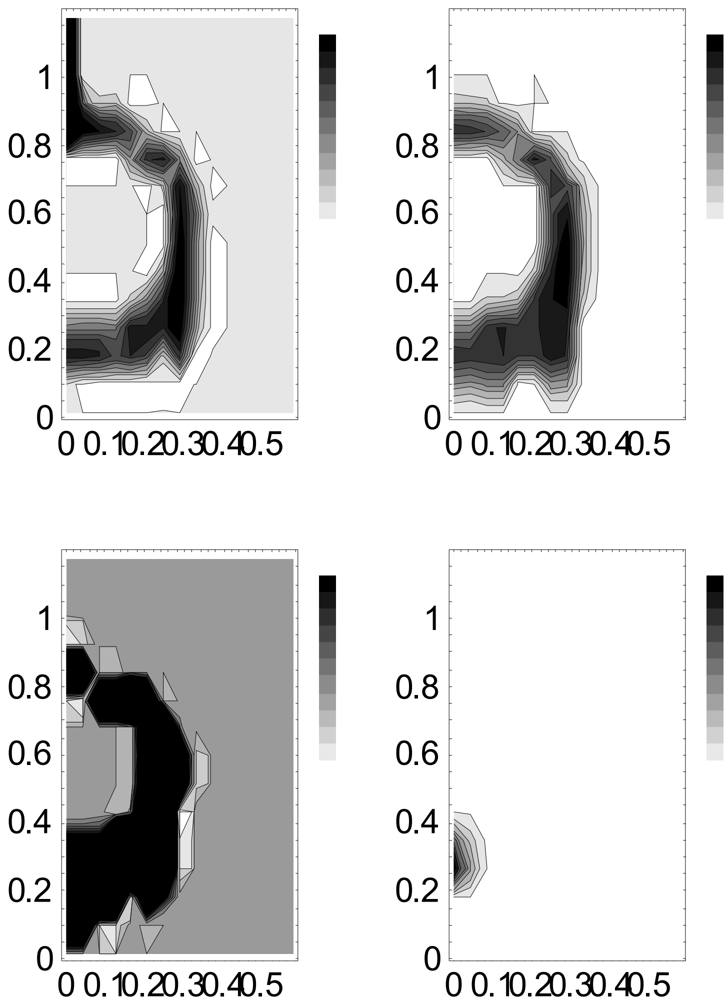
1
0.8
0.6
0.4
0.2
0
0 0.10.20.30.40.5
1
0.8
0.6
0.4
0.2
0
0 0.10.20.30.40.5
1
0.8
0.6
0.4
0.2
0
0 0.10.20.30.40.5
1
0.8
0.6
0.4
0.2
0
0 0.10.20.30.40.5

lst166

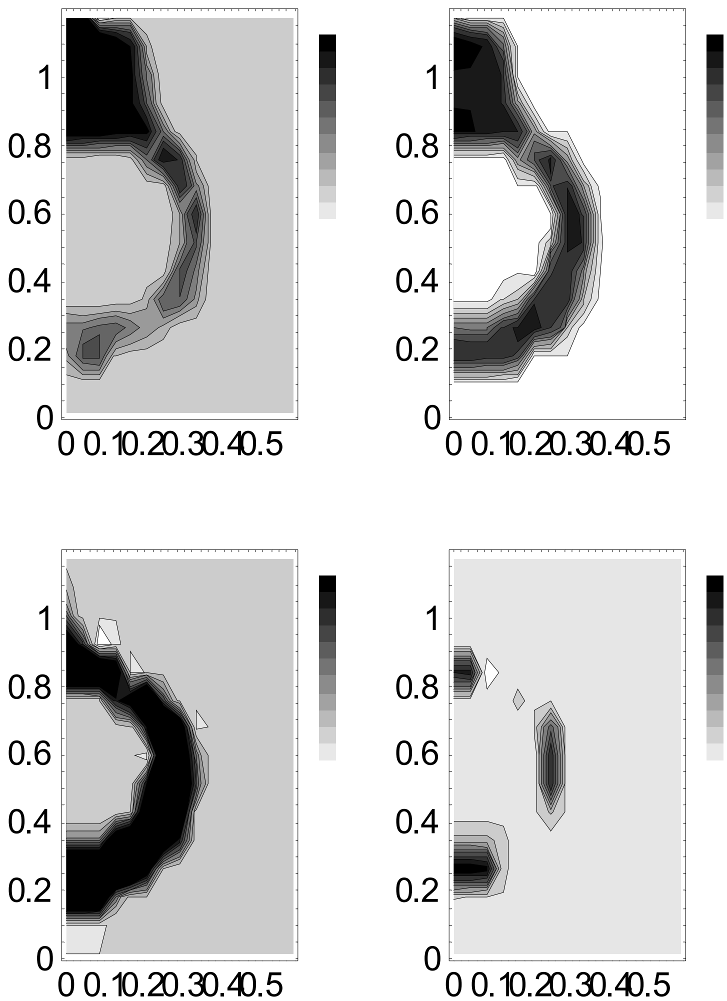
1
0.8
0.6
0.4
0.2
0
0 0.10.20.30.40.5
1
0.8
0.6
0.4
0.2
0
0 0.10.20.30.40.5
1
0.8
0.6
0.4
0.2
0
0 0.10.20.30.40.5
1
0.8
0.6
0.4
0.2
0
0 0.10.20.30.40.5

lst167

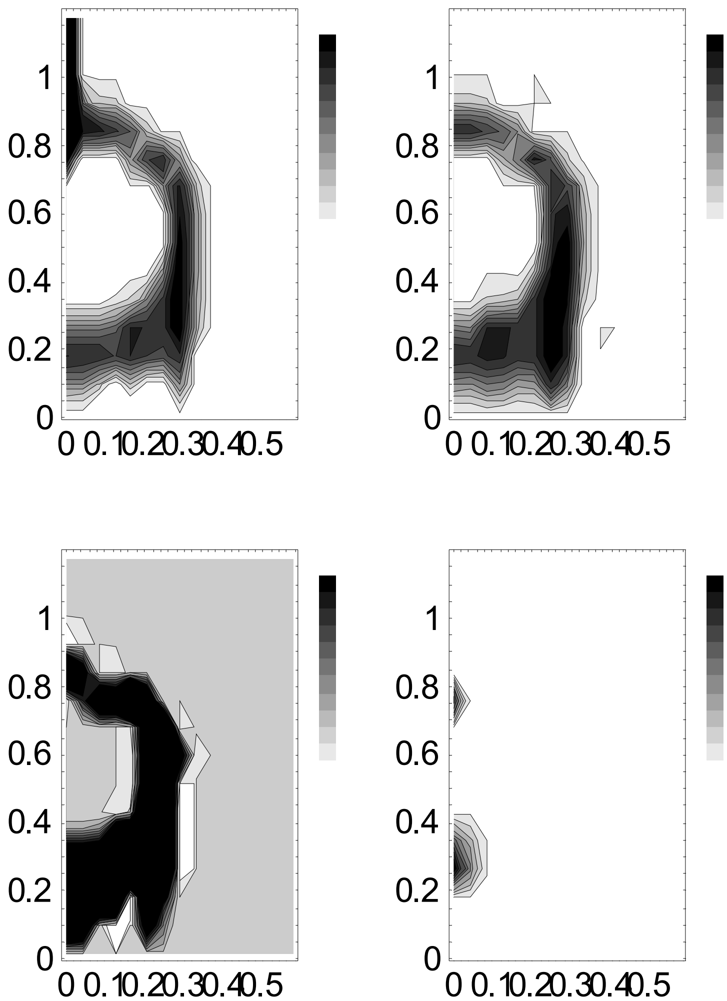

lst168

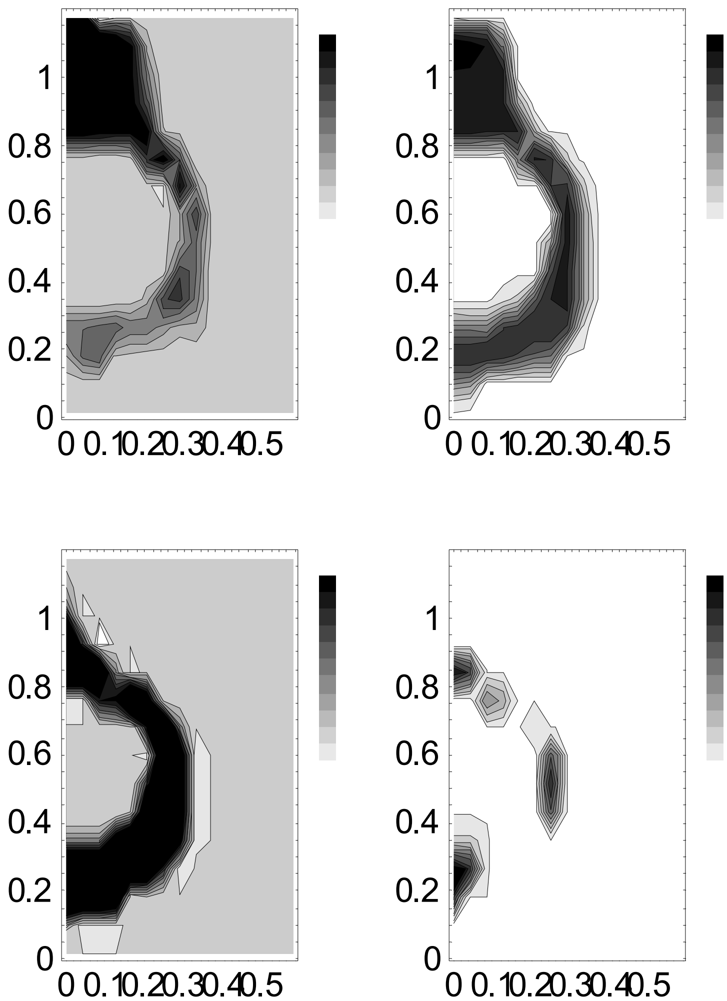

lst169

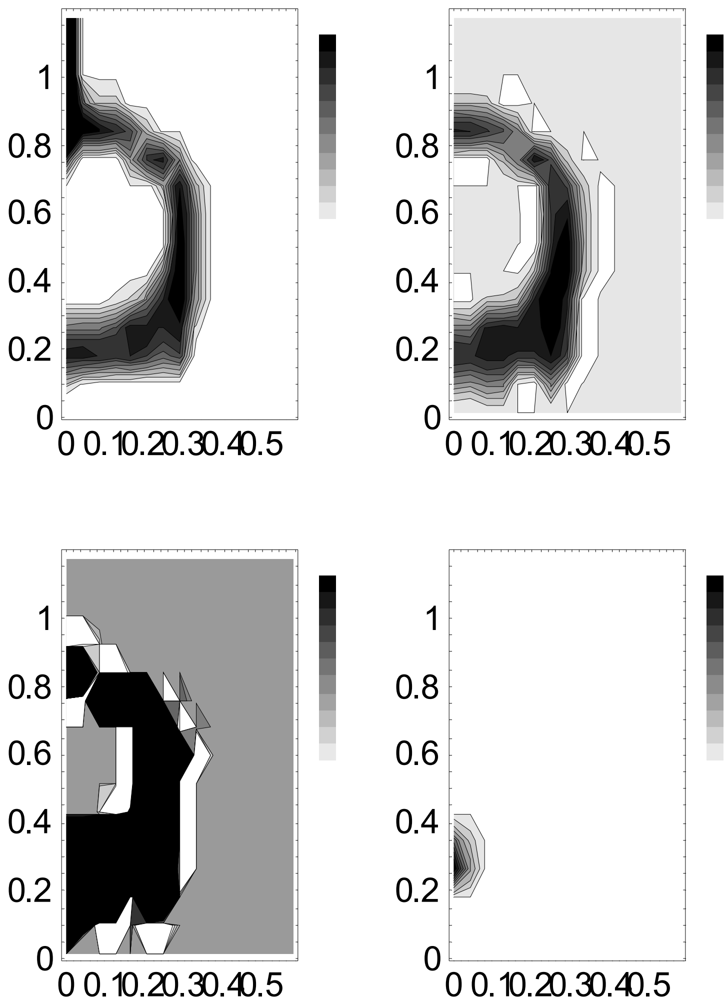

lst170

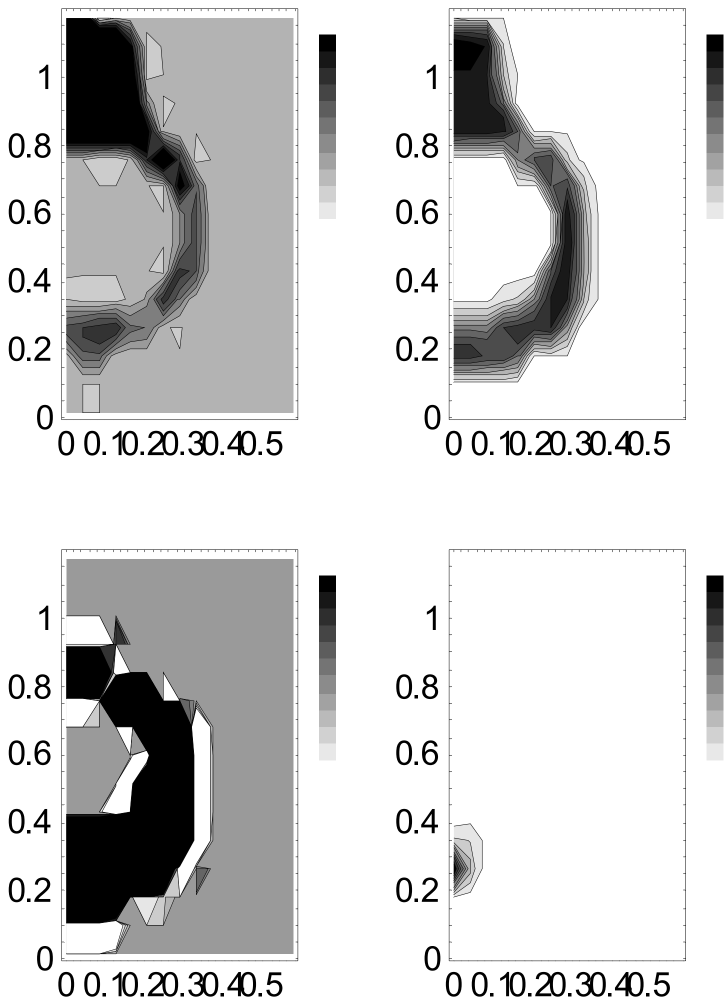

lst171

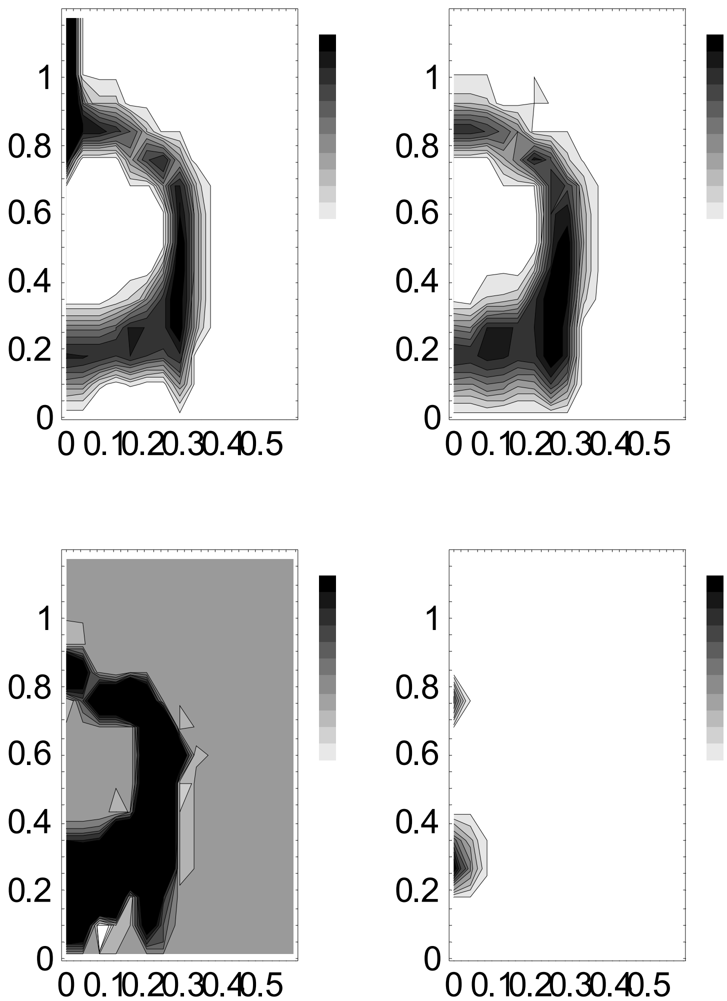

Lst172

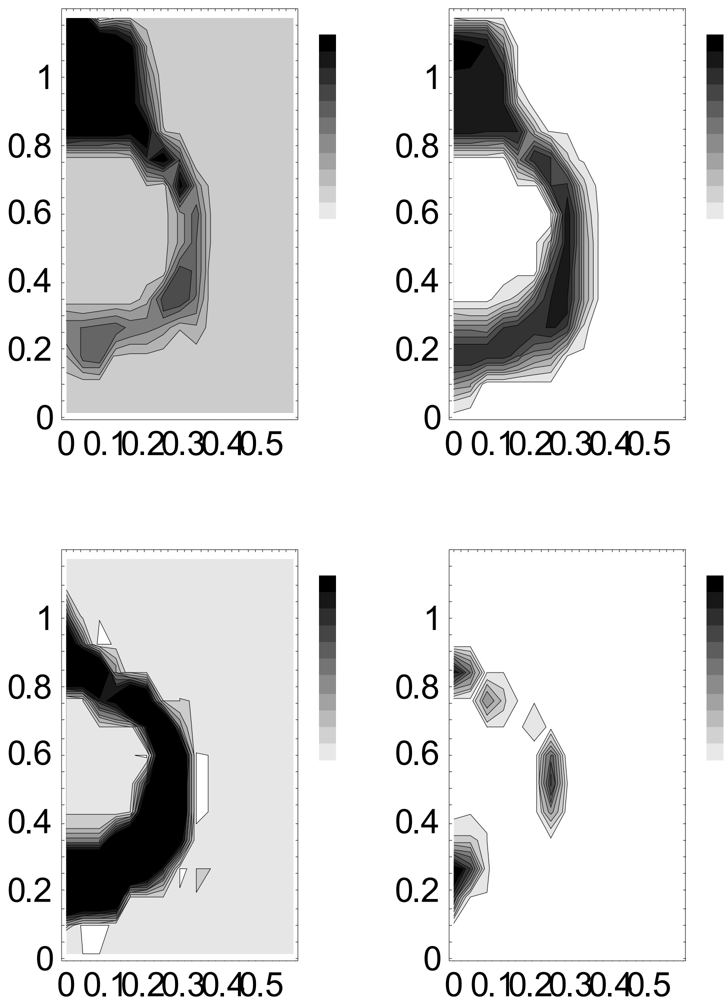

Sensitivity analysis of the effect of matrix/fracture permeability changes

Additional analyses are performed to evaluate the effect of changes in matrix and fracture permeability. Two sets of analyses are performed: one set varying matrix and fracture permeability for the lst155 basecase (simulations lst173-lst179). And one set (simulatons lst180-lst185) varying matrix and fracture permeability for the best match from the first set of analyses (lst160): AFM with 1.0×10^{-3} and $\gamma = 0.4$, 0.6, and 0.8. N/c denotes no convergence in simulation. Dec denotes that heat and mass transfer between the matrix and fracture continua are decoupled. Perm indicates whether the subject permeability is changed from the stated basecase. Flow denotes the presence of liquid flow features at the edge of the drift (i.e., shedding). Shed denotes whether there appears to be free (gravity-driven) flowing water at the edge of the drift. Pond denotes whether water is ponded above the drift. C Penet denotes whether there is evidence of downward flow penetrating into the drift (i.e., to what extent in the fracture below that to the side).

Table 3. Summary of lst analyses: fracture

Run No	AFM	γ	α	Perm	Shed	Sat	Flow	Pond	C Penet
lst173	Off	-	1e-4	1.0	Yes	0.3054	Diffuse		Yes
lst174	Off	-	1e-4	1.0	No	0.0460	Focused	No	No
lst175	Off	-	1e-4	-100x	No	0.8505	Focused	No	No
lst176	Off	-	1e-4	+100x	Yes	0.0260	Focused	N/c	No
lst177	Off	-	1e-4	1.0	No	0.0449	Focused	No	No
lst178	Off	-	1e-4	+10x	Yes	0.0702	Focused	N/c	Some
lst179	Off	-	1e-5	1.0	Yes	0.2942	Focused	No	No
lst180	On	0.4	1e-3	1.0	No	0.1457	Diffuse		No
lst181	On	0.4	1e-3	1.0	No	0.0000	None	No	No
lst182	On	0.4	1e-3	-100x	No	0.5571	Focused	Some	No
lst183	On	0.4	1e-5	1.0	Yes	0.1792	Focused	No	Yes
lst184	On	0.6	1e-4	1.0	Yes	0.1129	Focused		Yes
lst185	On	0.8	1e-4	1.0	Yes	0.0448	Focused		No
lst187	On	0.4	1e-3	1.0	No	0.0795	Focused		No
lst188	On	0.4	1e-3	1.0	No	0.0799	Focused		No

Table 4. Summary of lst analyses: matrix

Run No	AFM	γ	α	Perm	Sat	CPond	EPond	MTem	FTem
lst173	Off	-	1e-4	-10x	1.0000	Yes		179.8	179.3
lst174	Off	-	1e-4	+10x	0.9183	No	Some	187.5	187.0
lst175	Off	-	1e-4	1.0	1.0000	No	Some	187.4	186.9
lst176	Off	-	1e-4	1.0	0.9945	No	N/c	184.7	184.2
lst177	Off	-	1e-4	1.0	0.4653	No	Spme	188.3	187.8
lst178	Off	-	1e-4	1.0	0.9954	No	N/c	185.0	184.5
lst179	Off	-	1e-5	1.0	0.9992	No	Some	185.3	184.8
lst180	On	0.4	1e-3	-10x	1.0000	No		187.0	186.5
lst181	On	0.4	1e-3	+10x	0.8340	No	Some	183.6	183.1
lst182	On	0.4	1e-3	1.0	1.0000	No	Some	187.4	186.8

lst183	On	0.4	1e-5	1.0	0.9982	No	Some	185.1	184.6
lst184	On	0.6	1e-4	1.0	0.9969	No		185.0	184.5
lst185	On	0.8	1e-4	1.0	0.9956	No		185.0	184.5
lst187	On	0.4	1e-3	1.0	0.9978	No		186.8	186.3
lst188	On	0.4	1e-3	1.0	0.9979	No		184.2	183.7

Discussion of analyses results.
There are several main classes of analyses:

4) AFM
5) reduced areamodf, heat and mass coupled
6) reduced areamodf, heat and mass uncoupled

Plus two sub-classes:

3) effect of alpha of 1e-3 versus 1e-4
4) effect of gamma=0.4 versus 0.6 and 0.8.

Main observations:

Inc matrix perm to 2e-16 (from 2e-17) in lst181 reduces fracture saturation to 0 for entire simulation. Inc matrix perm in non-AFM (lst174) does not have this profound effect, although fracture sat is relatively low.

Lst173 and lst180 have shedding in fracture continua beyond end of drift. Both have reduced matrix perm from 2e-17 to 2e-18. Greatest smearing in fracture continuum occurred in lst173 and lst180, more in lst180.

Fracture ponding above drift observed.

No ponding (i.e., full saturation) observed in the matrix above the drift in all simulations. Higher than desirable saturation observed below the drift in all simulations.
Lst 174, lst175, and lst181 have minimal flow in fracture continuum above middle of cell.

Results from simulations lst173 through lst185, lst188

Following are graphs of

1) **matrix saturation**
2) **matrix temperature**
3) **fracture saturation**

Matrix saturation – at center plane and at edge plane

lst173

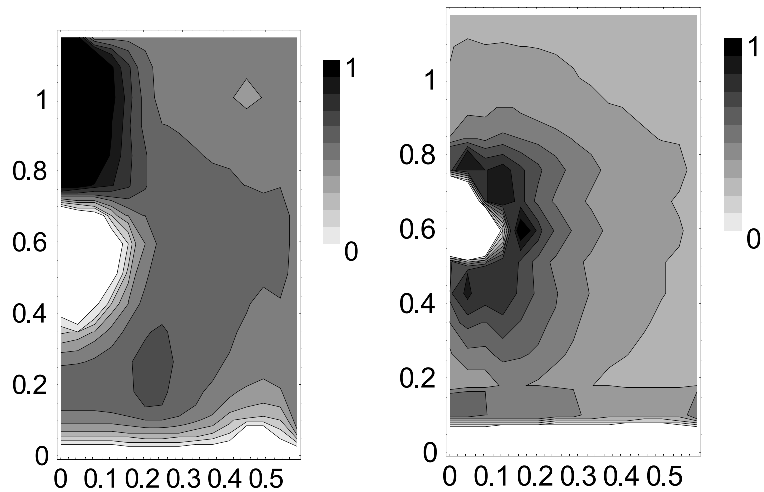

lst174

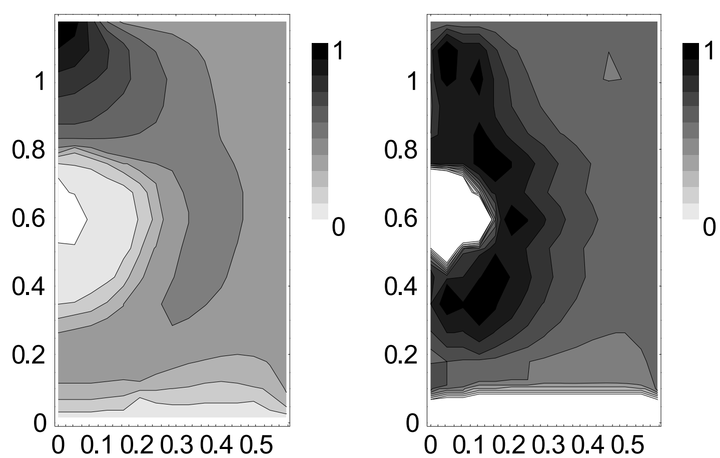

lst175

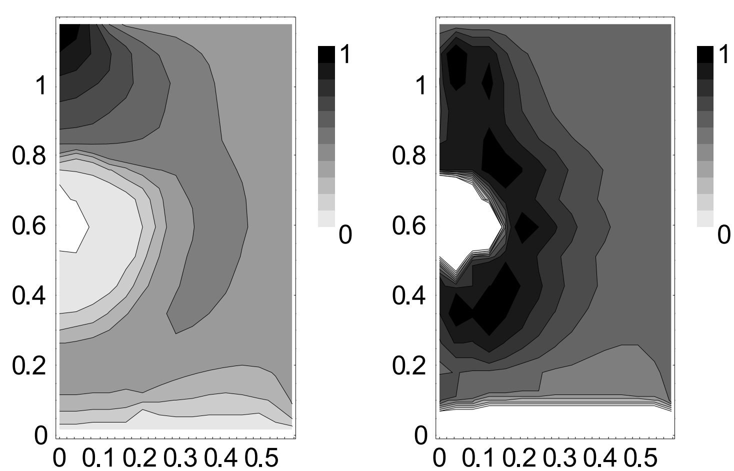

lst176

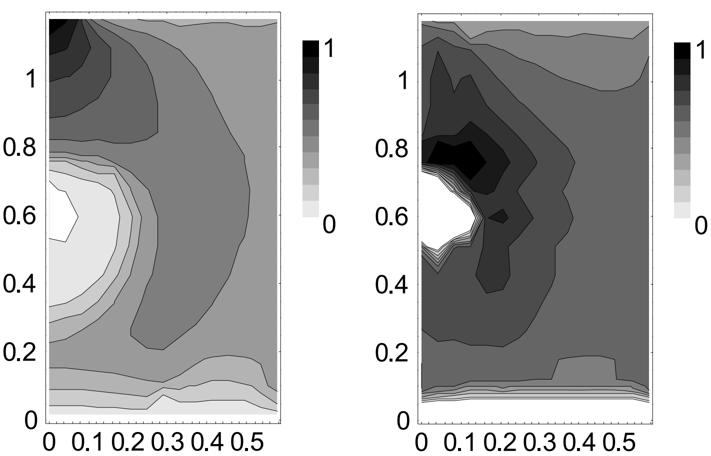

lst177

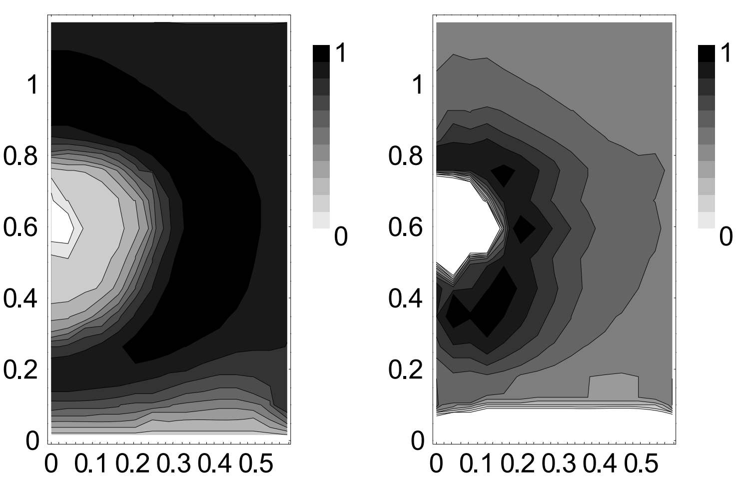

lst178

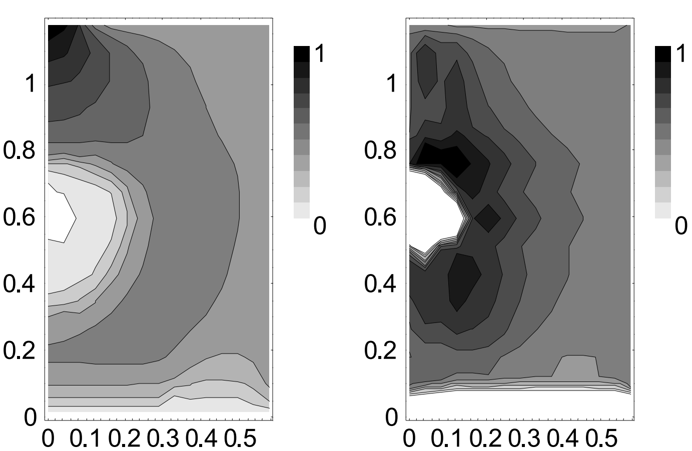

lst179

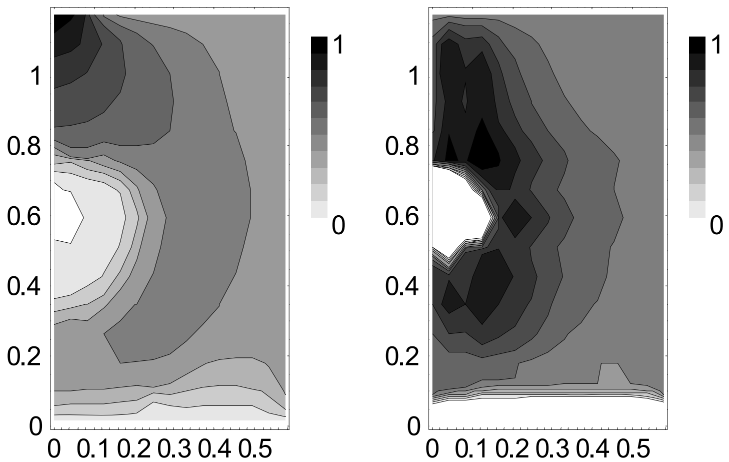

lst180

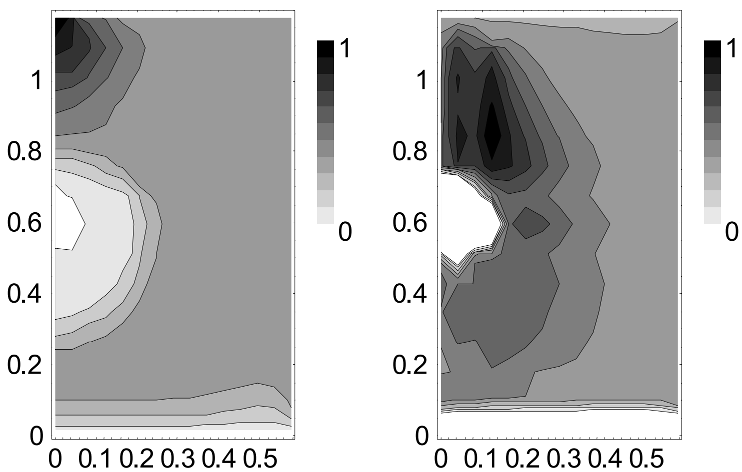

lst181

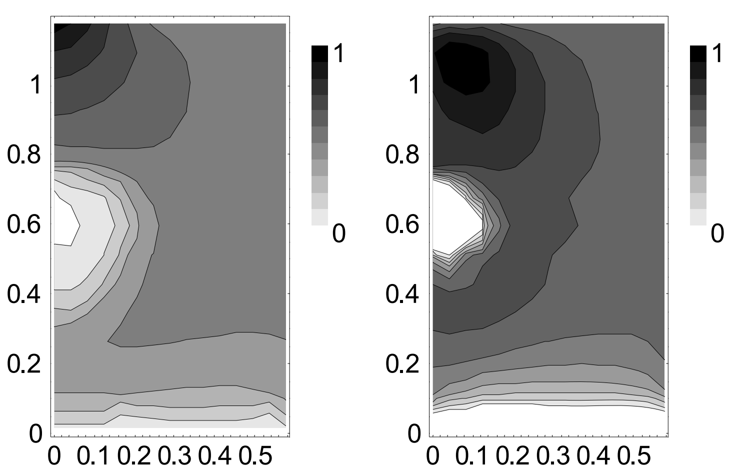

lst182

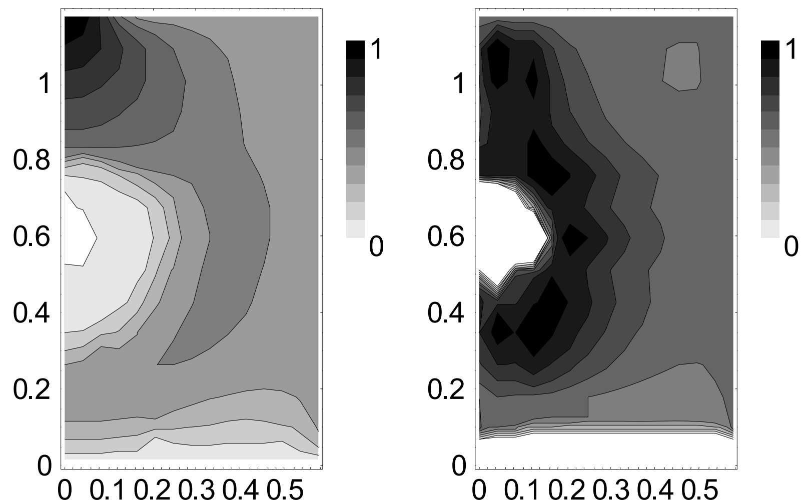

lst183

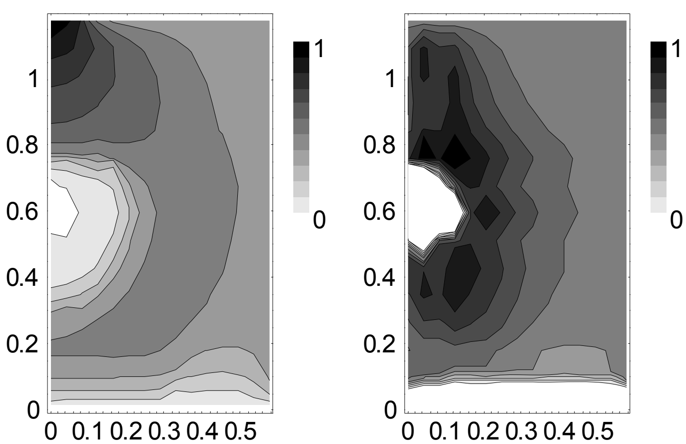

lst184

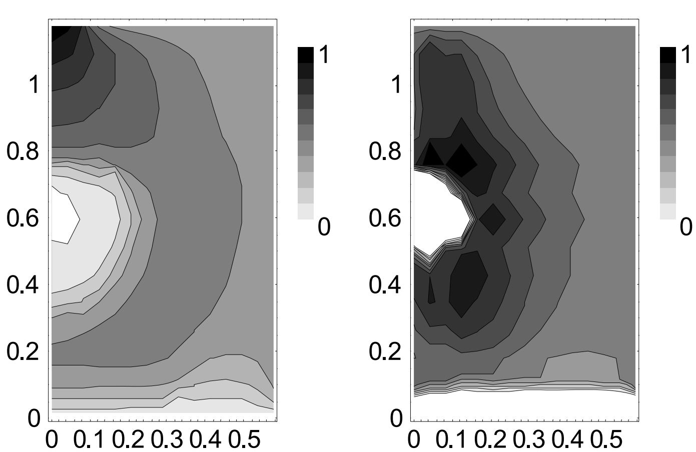

lst185

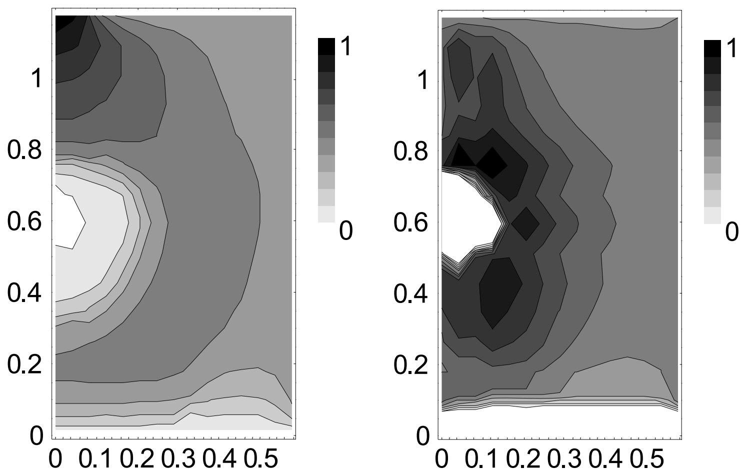

lst187

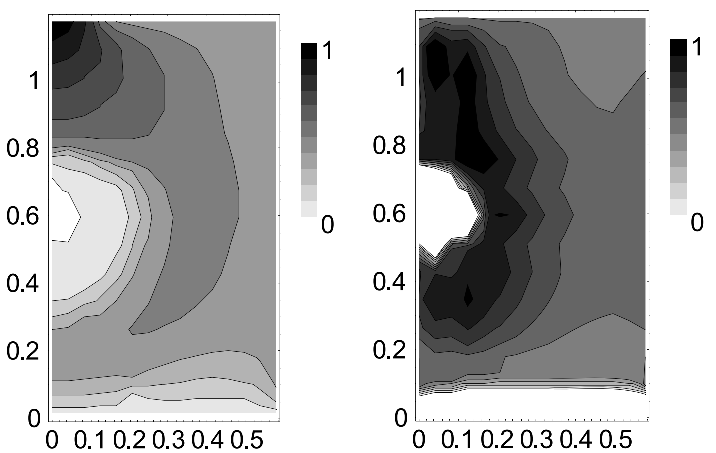

lst188

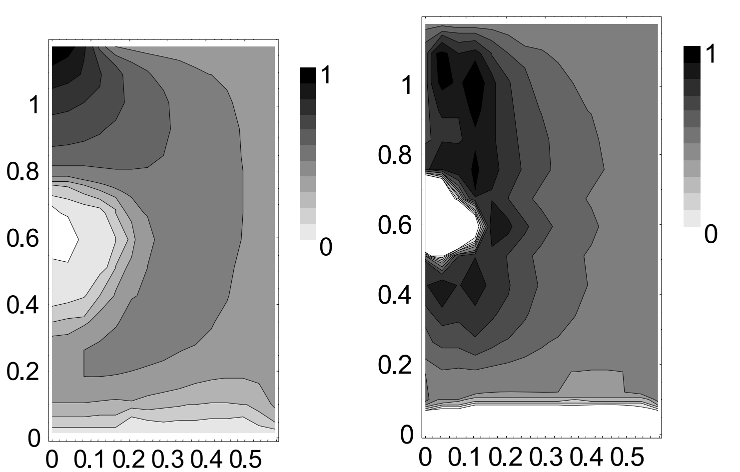

Matrix temperature

Temperatures range from 22 C (white) to the maximum (dark), as listed in Table 2 in this notebook. The left image is the xz plane. The right image is the yz plane.

lst173

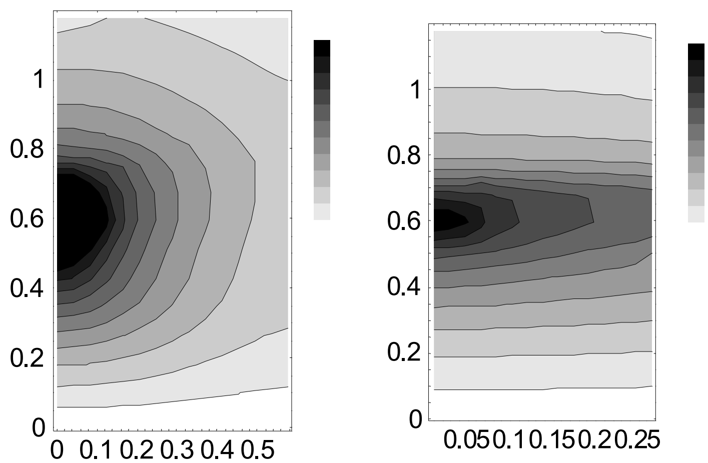

lst174

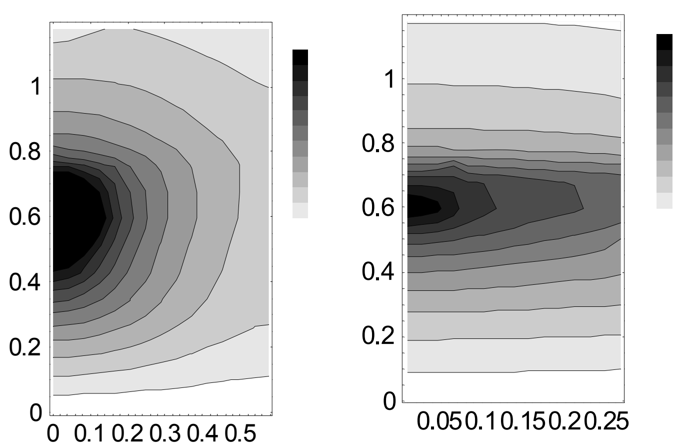

lst175

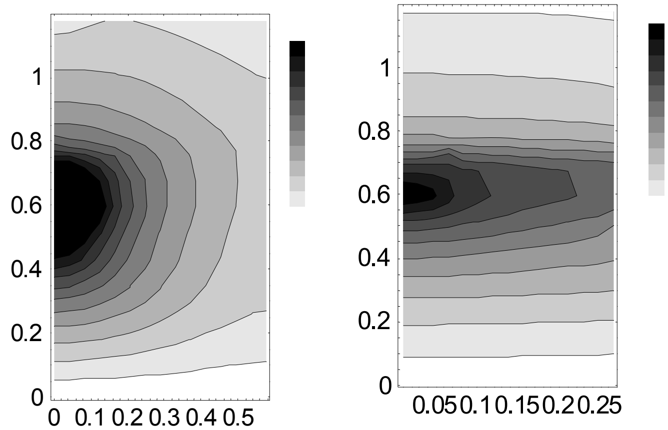

lst176

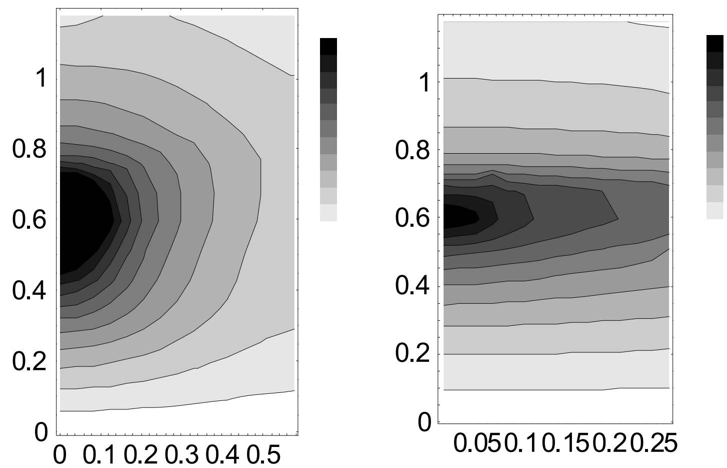

lst177

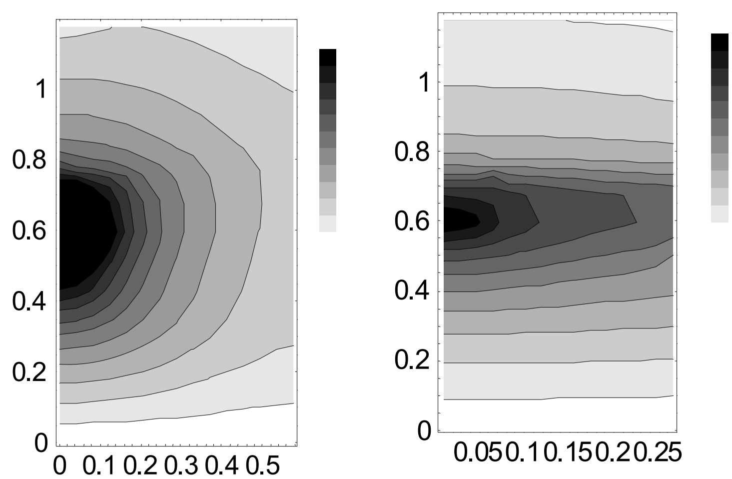

lst178

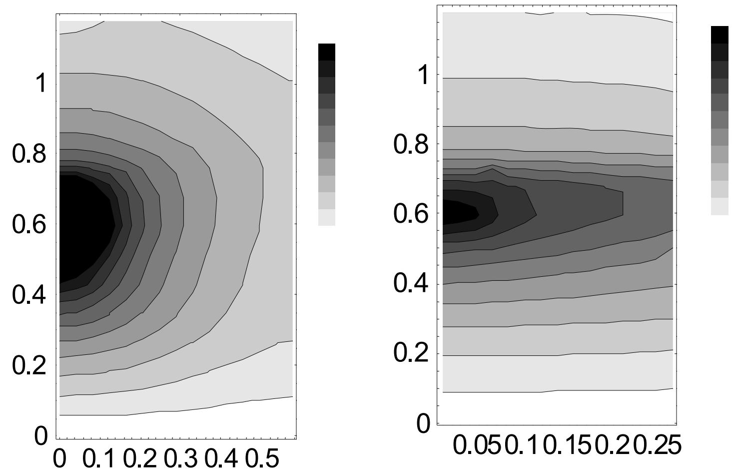

lst179

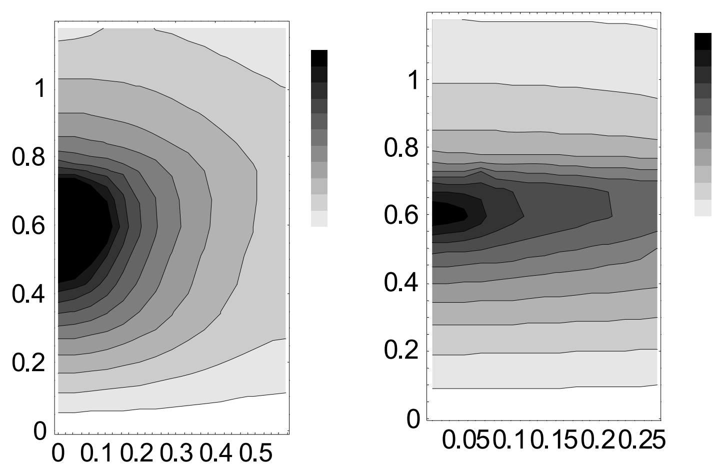

lst180

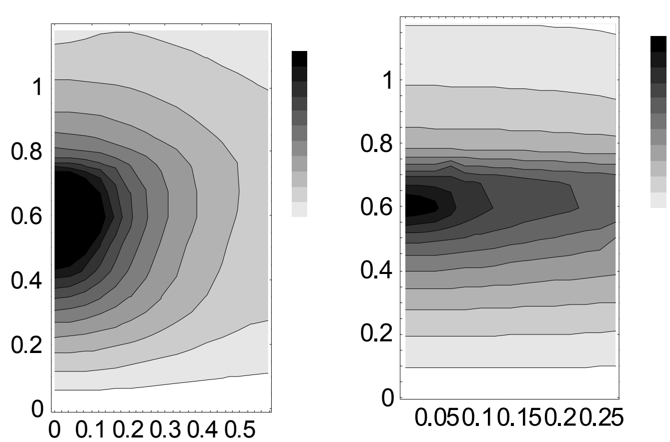

lst181

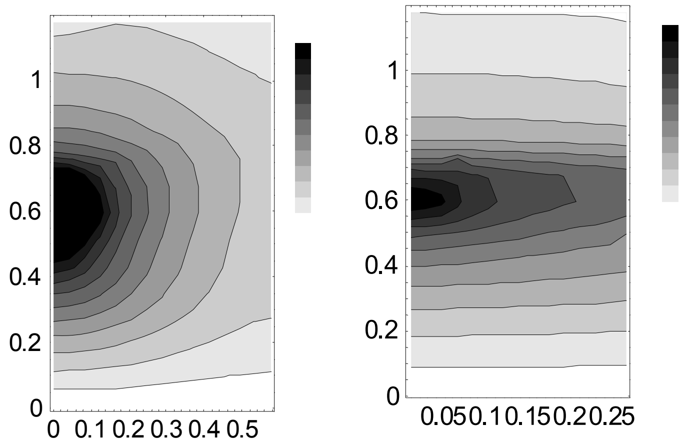

lst182

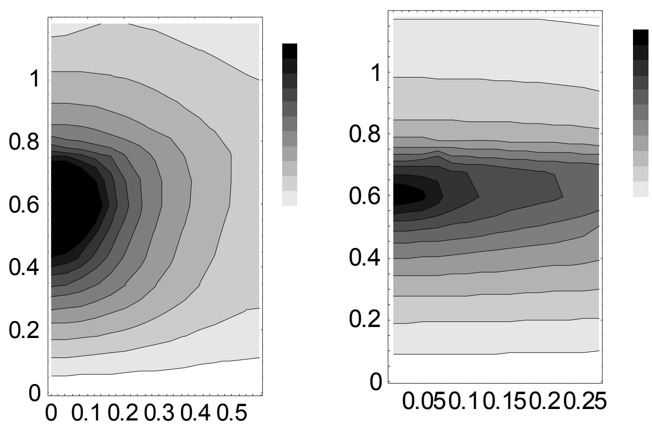

lst183

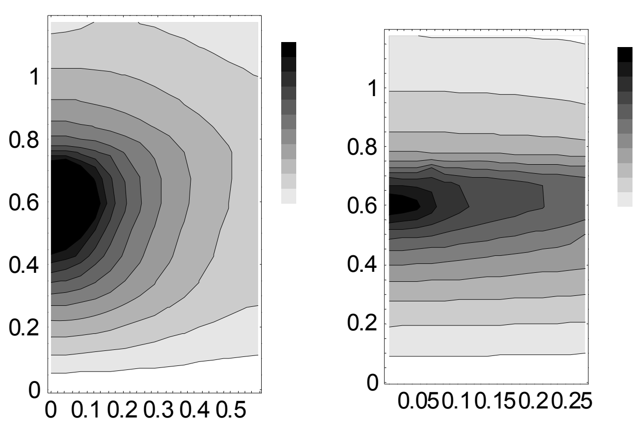

lst184

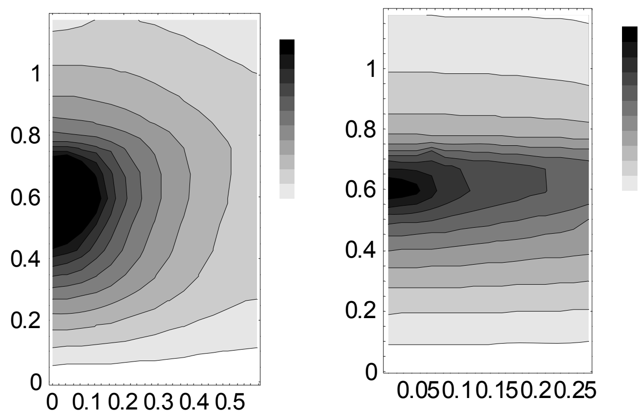

lst185

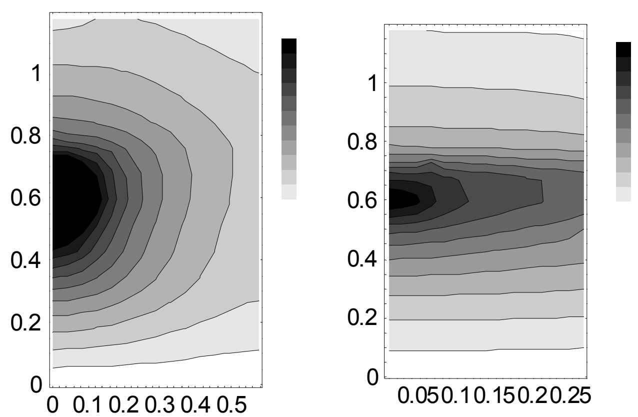

lst187

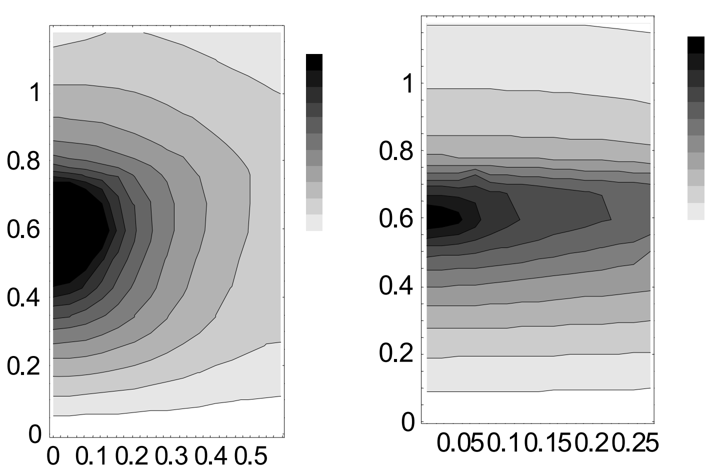

lst187

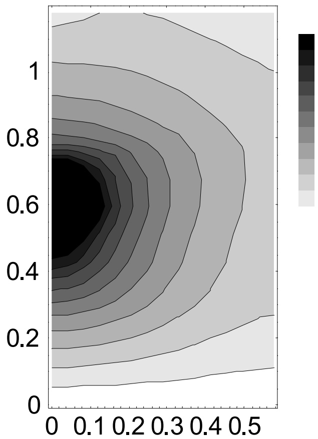

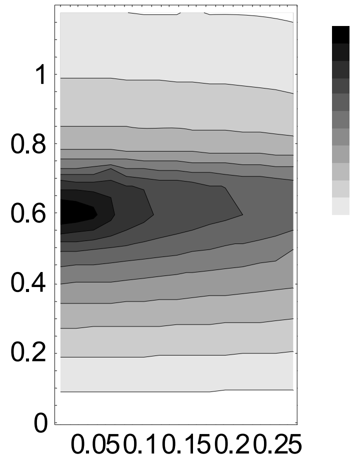

Fracture saturation

Saturations range for 0 (white) to the maximum (see Table 1 in this notebook). There are four slices taken from each simulation. Of the ten slices provided in each mathematica notebook, slices 1, 5, 9, and 10 are copied to this scientific notebook.

lst173

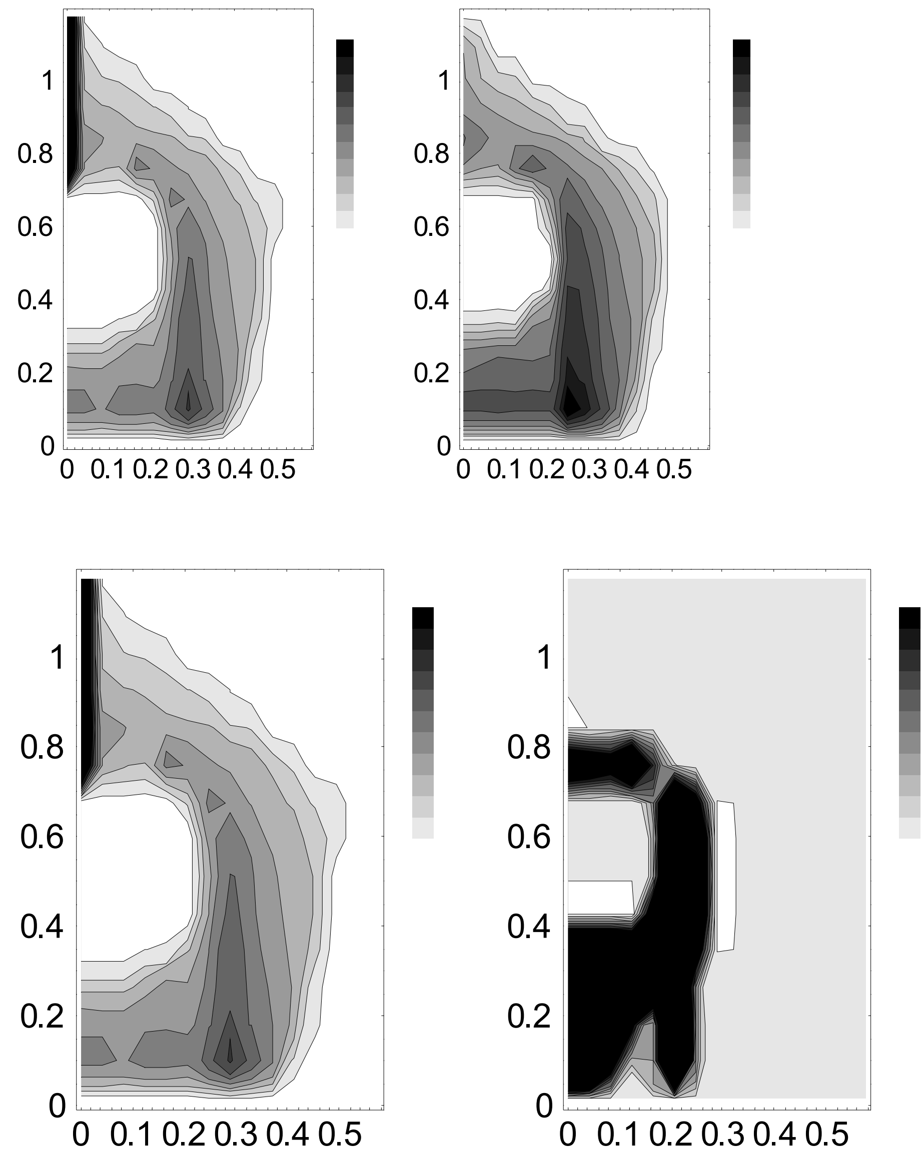

lst174

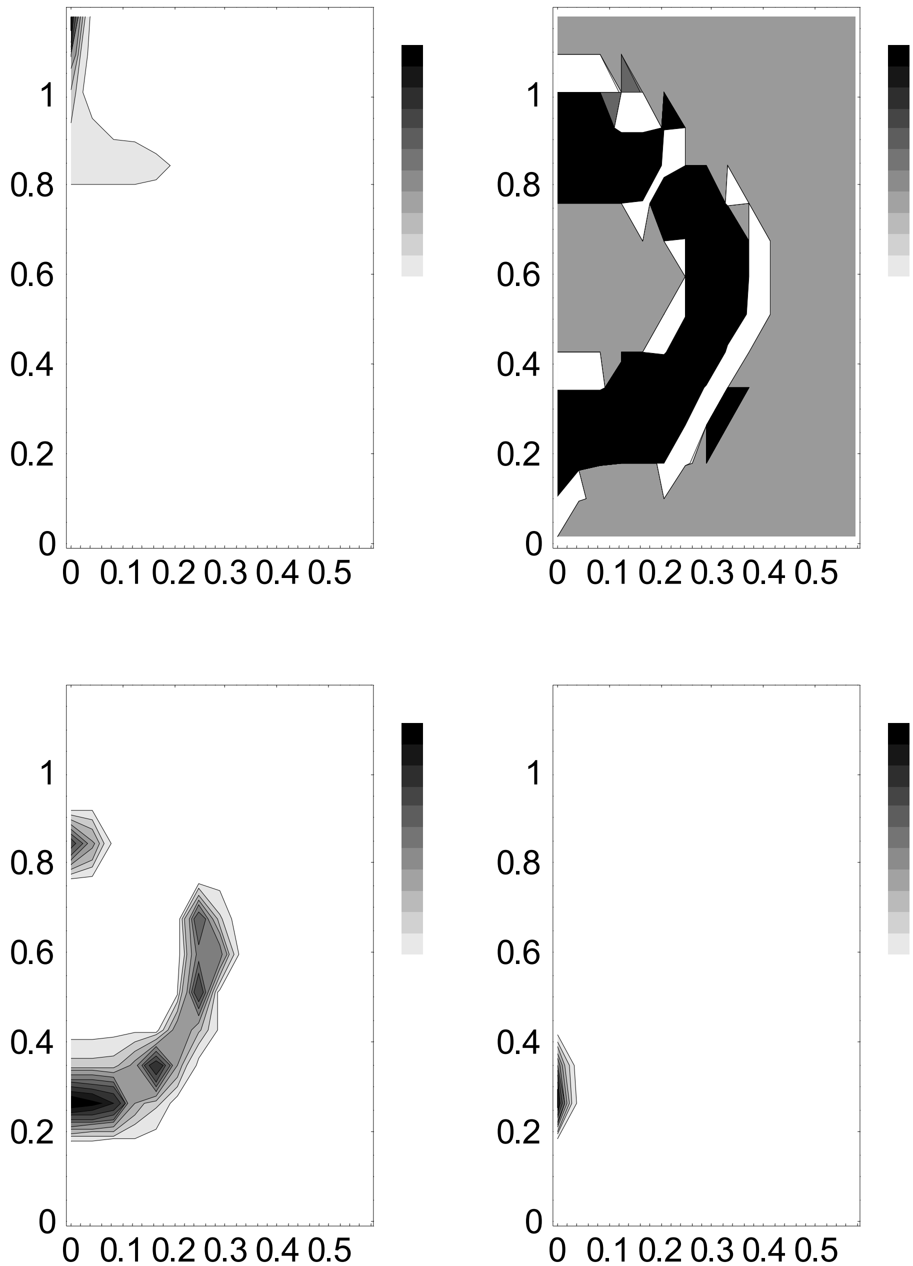
1
0.8
0.6
0.4
0.2
0
0 0.1 0.2 0.3 0.4 0.5
1
0.8
0.6
0.4
0.2
0
0 0.1 0.2 0.3 0.4 0.5
1
0.8
0.6
0.4
0.2
0
0 0.1 0.2 0.3 0.4 0.5
1
0.8
0.6
0.4
0.2
0
0 0.1 0.2 0.3 0.4 0.5

lst175

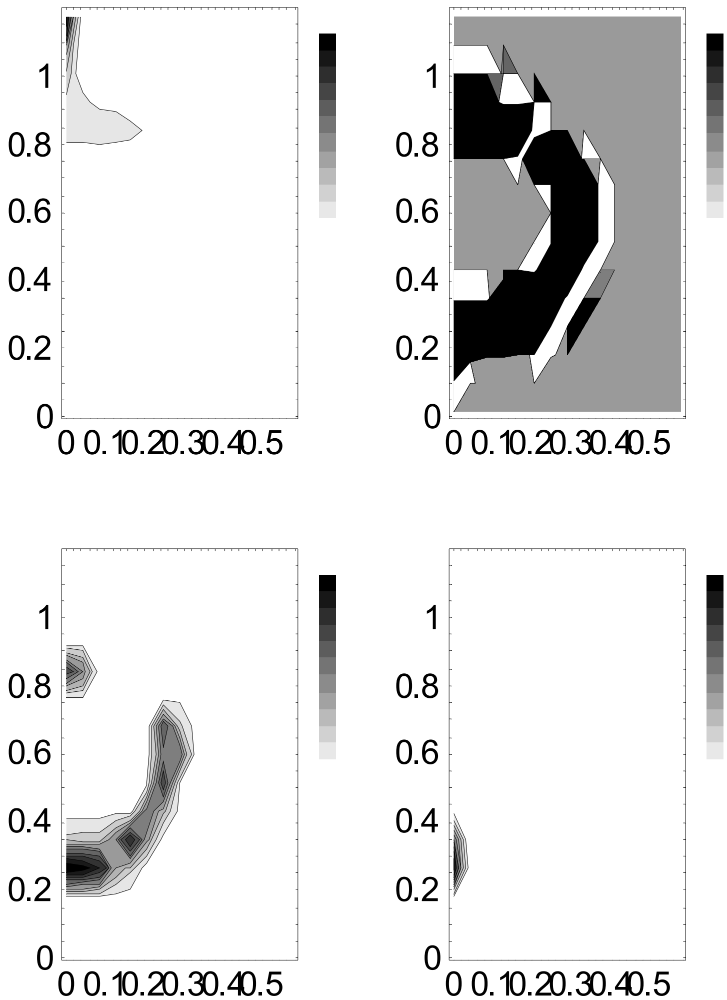

lst176

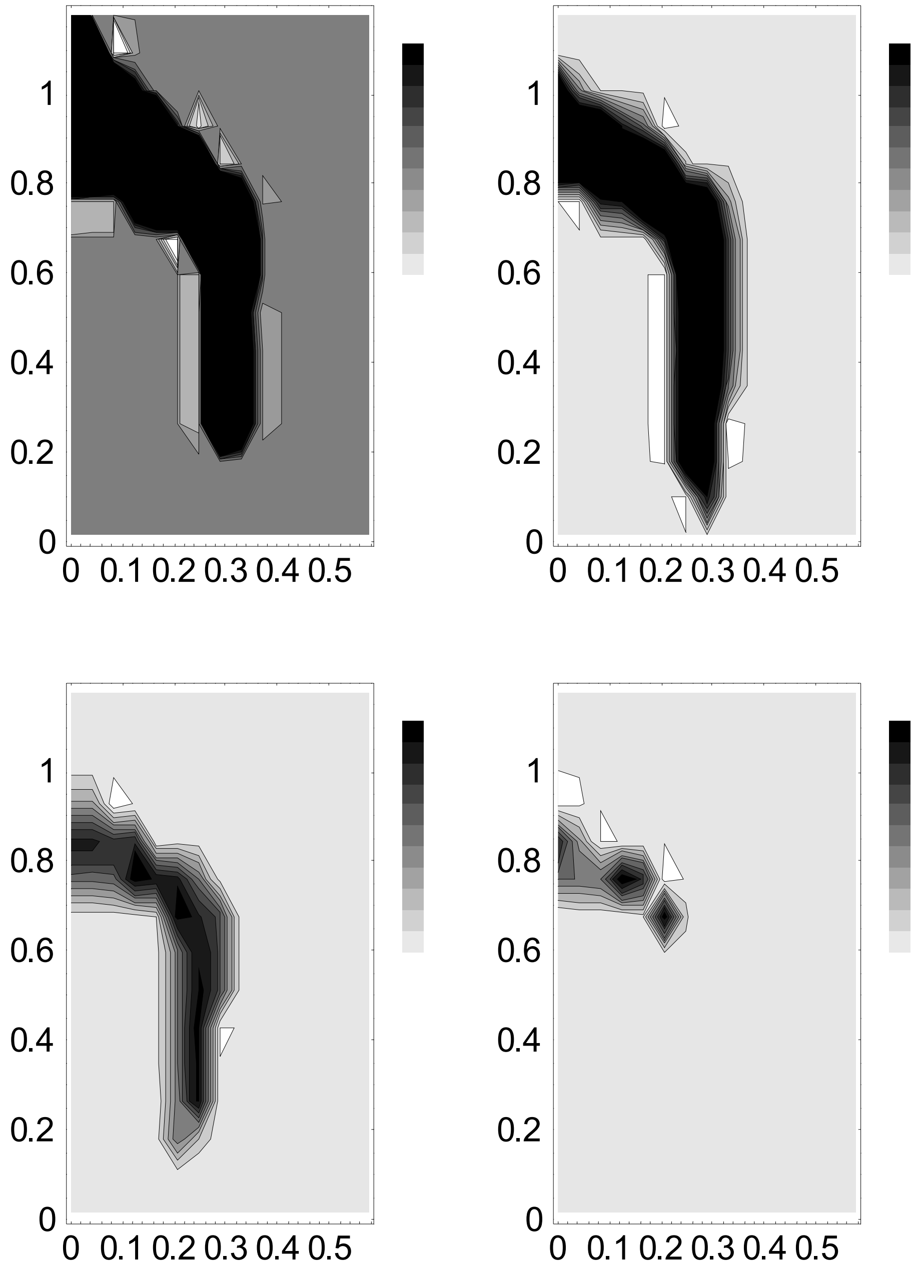

lst177

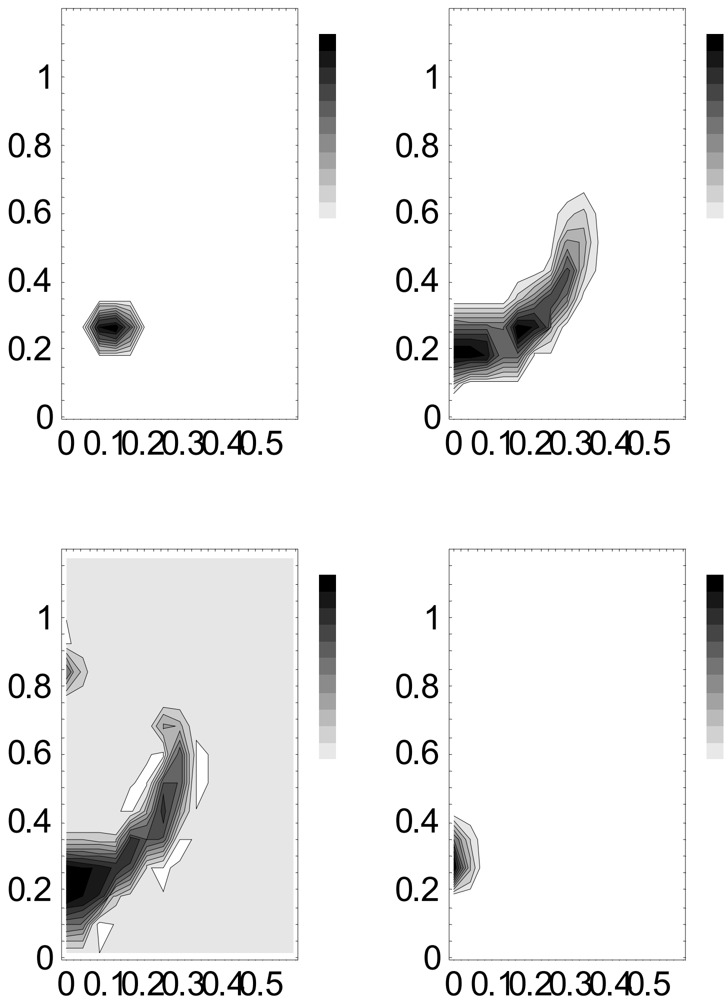

lst178

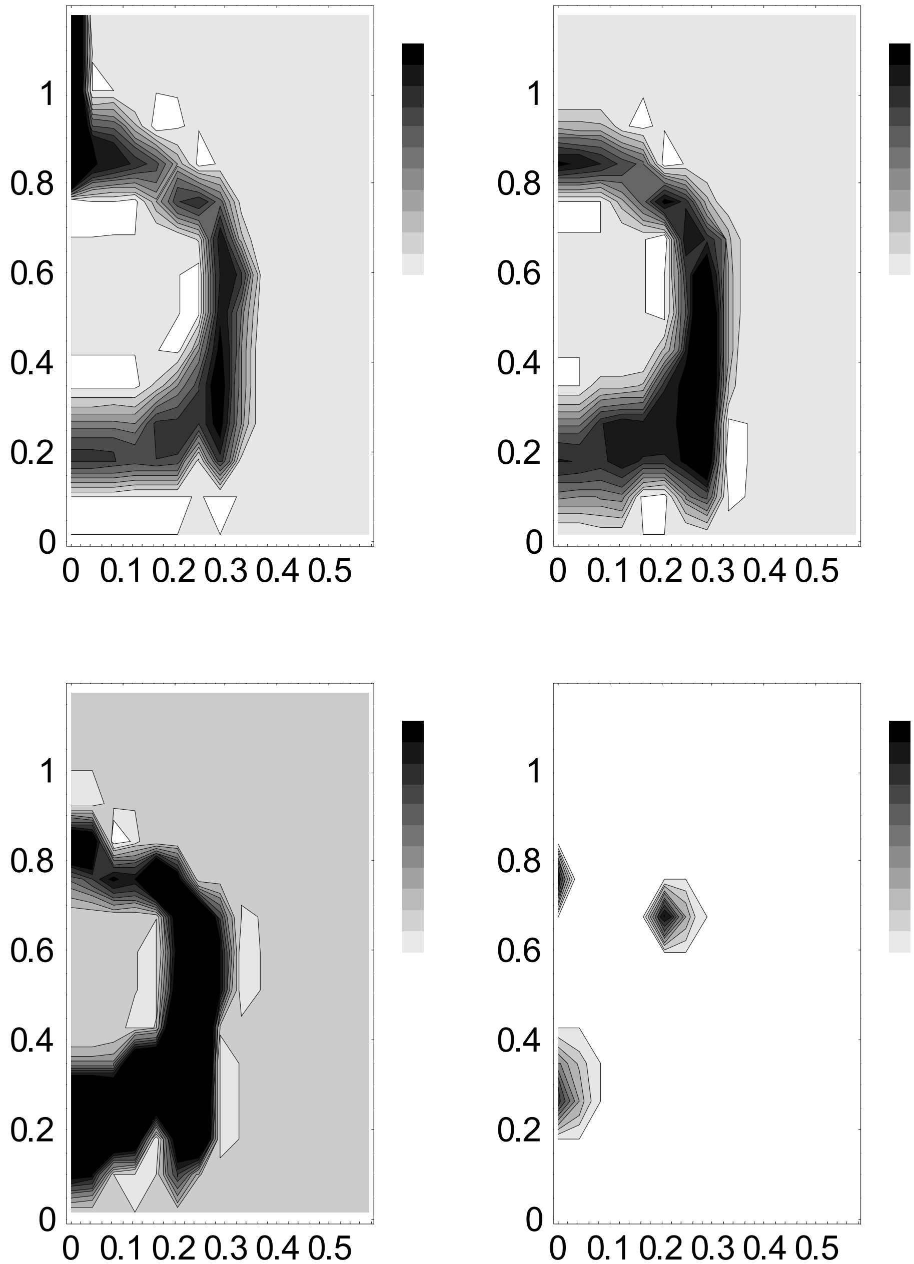

lst179

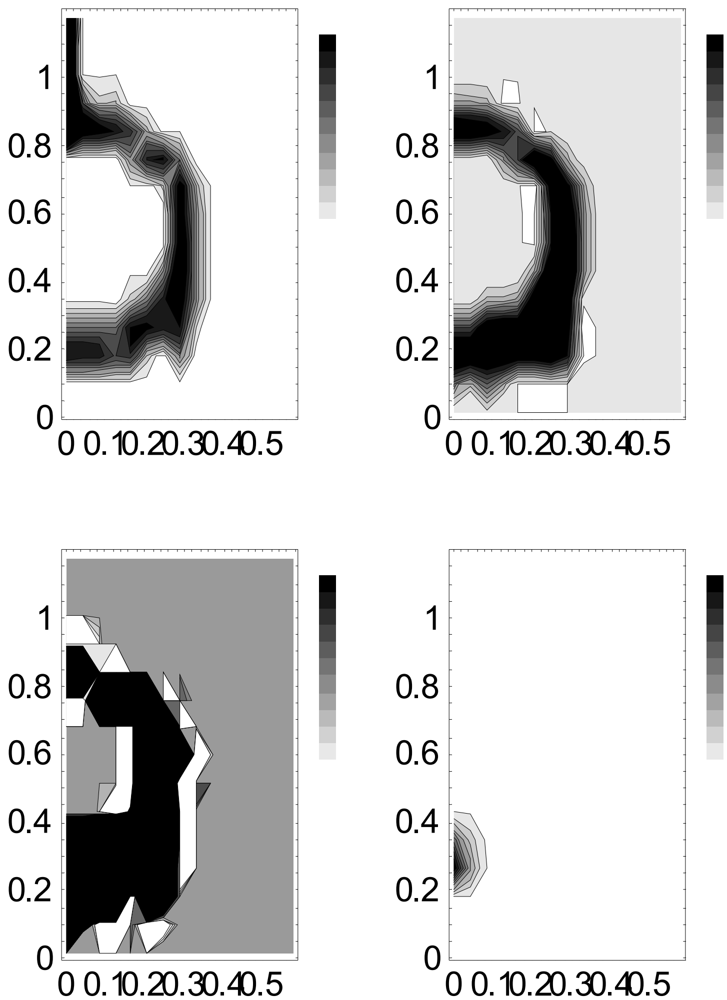

lst180

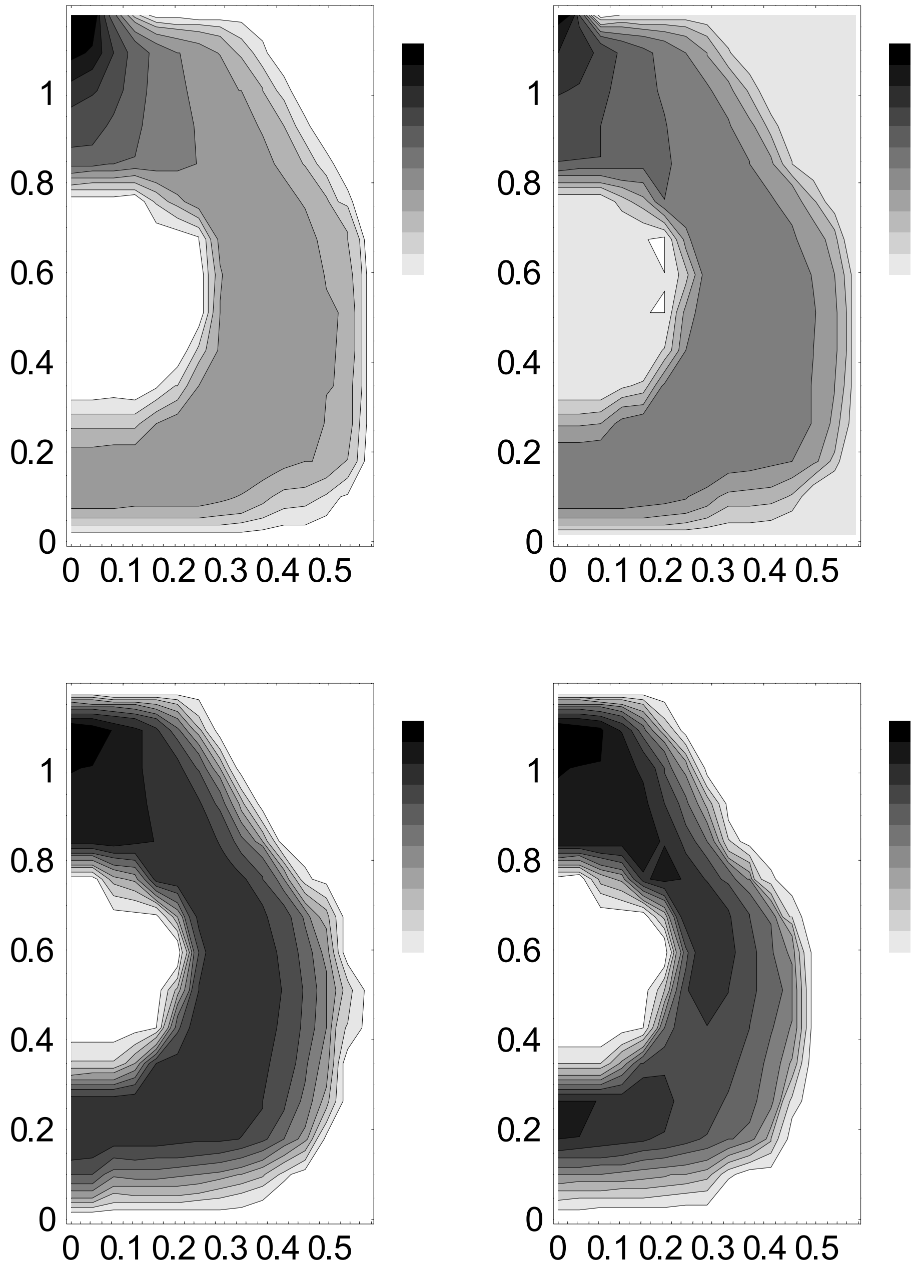

lst181

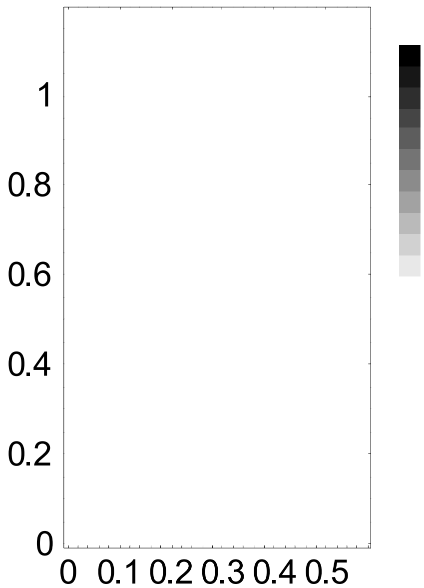

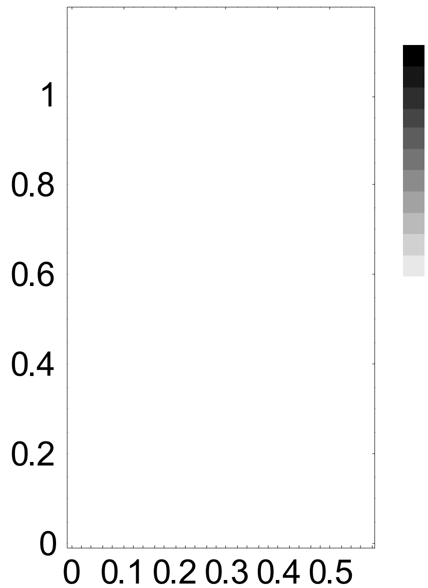

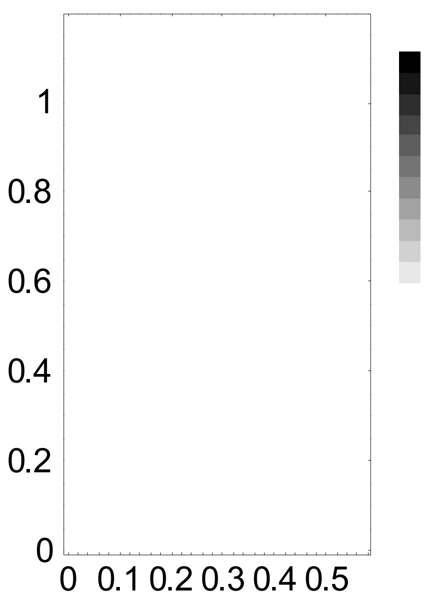

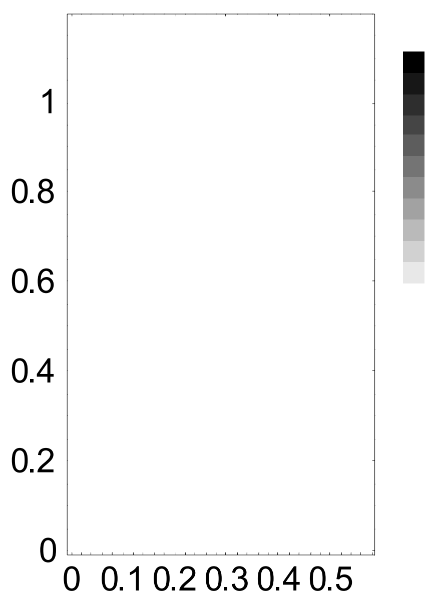

lst182

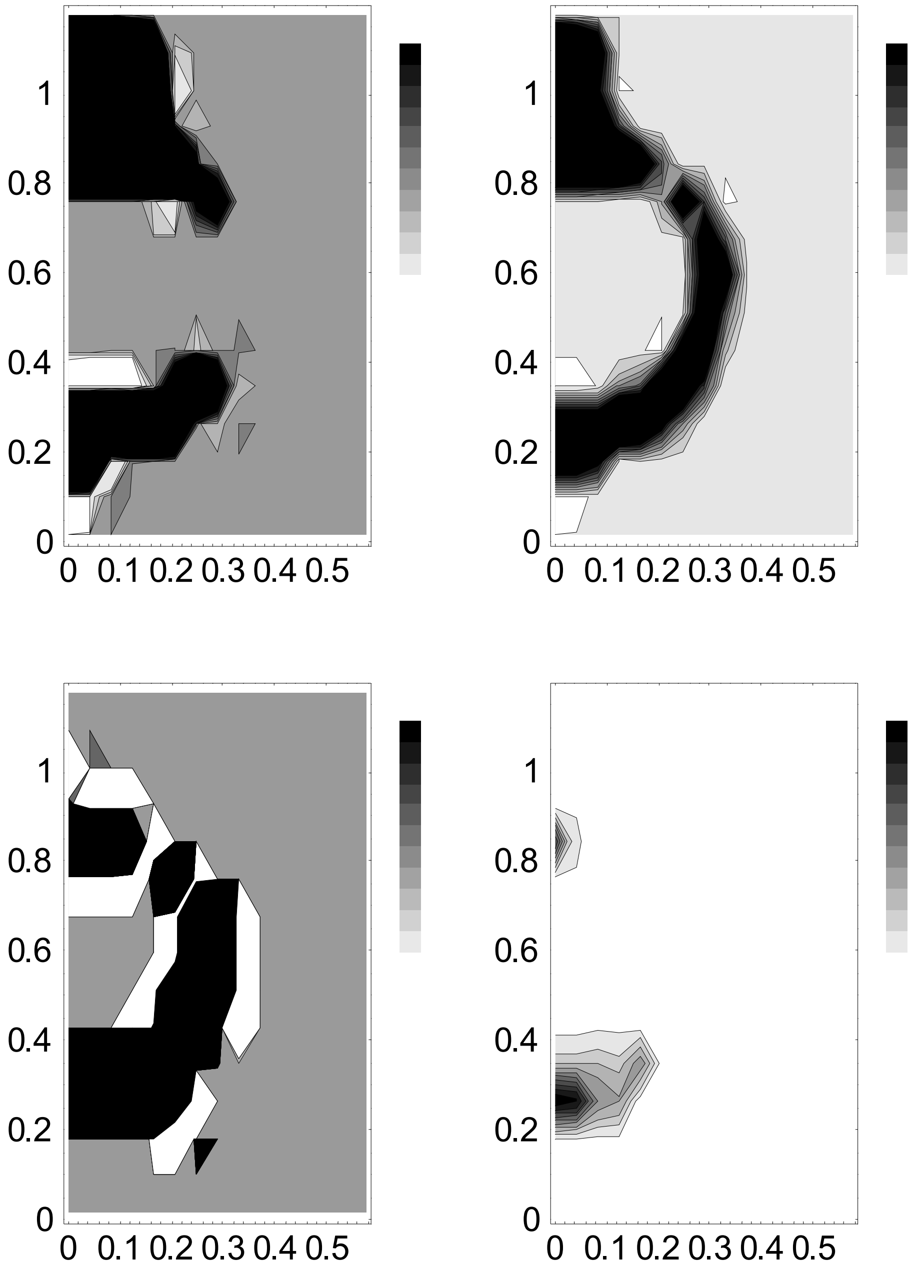

lst183

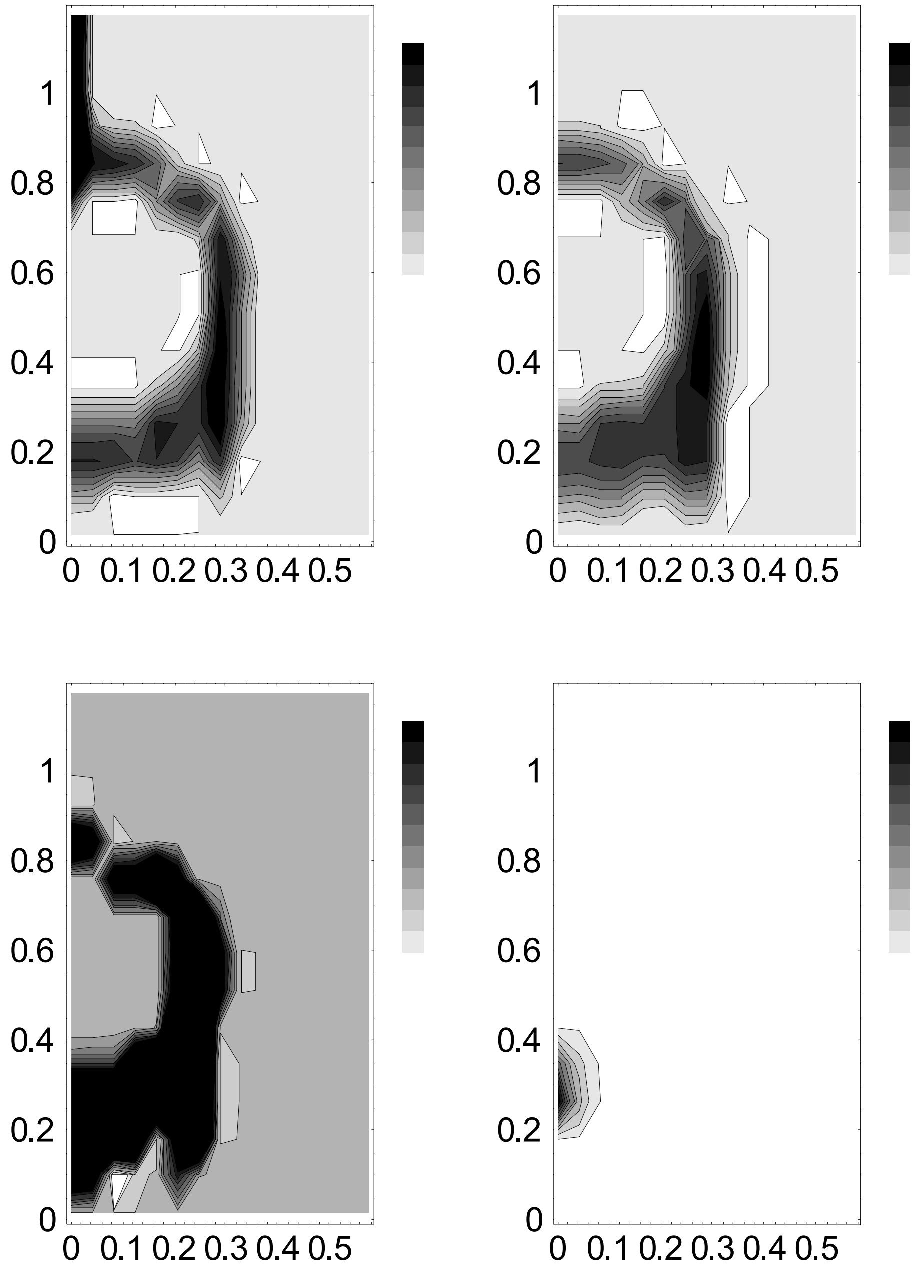

lst184

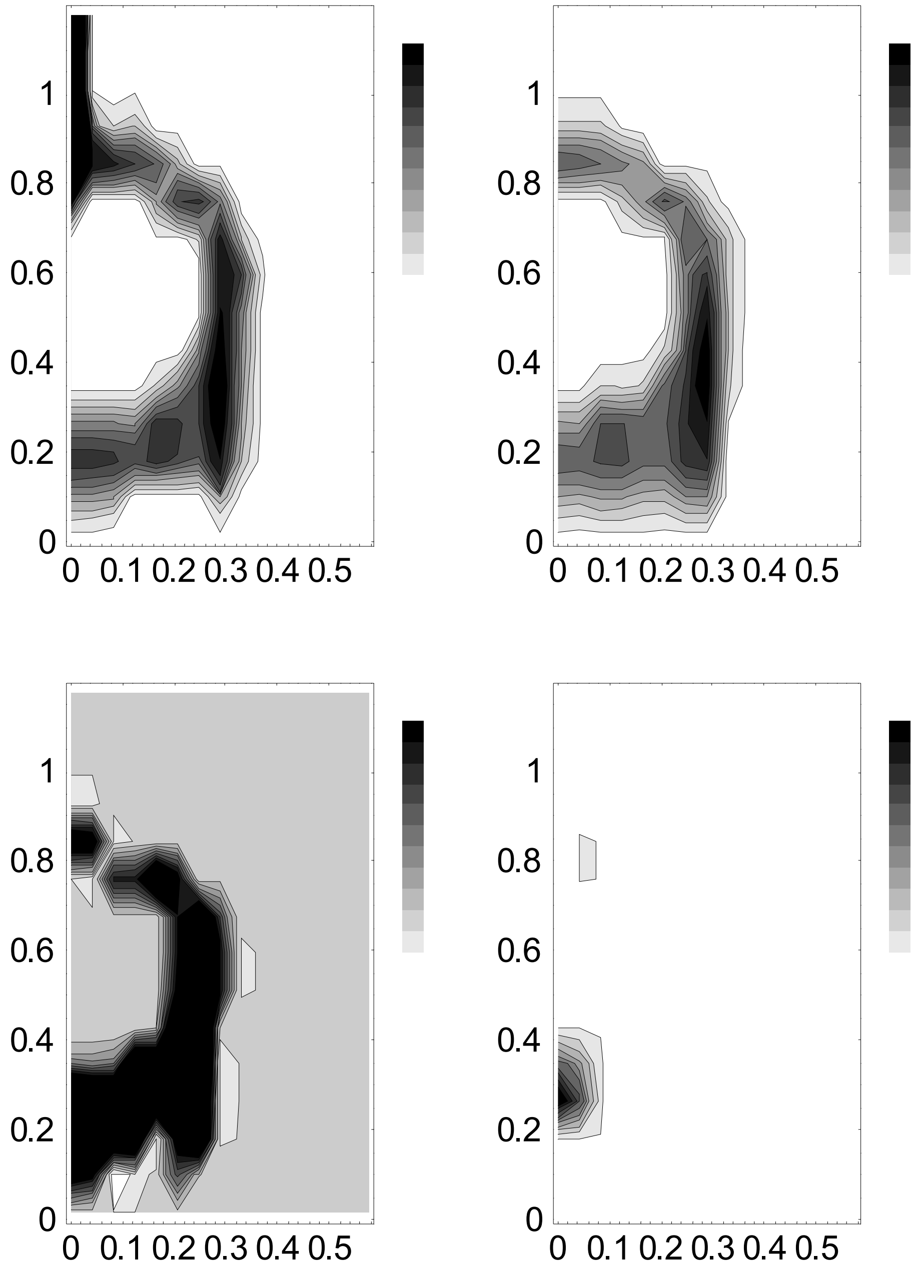

lst185

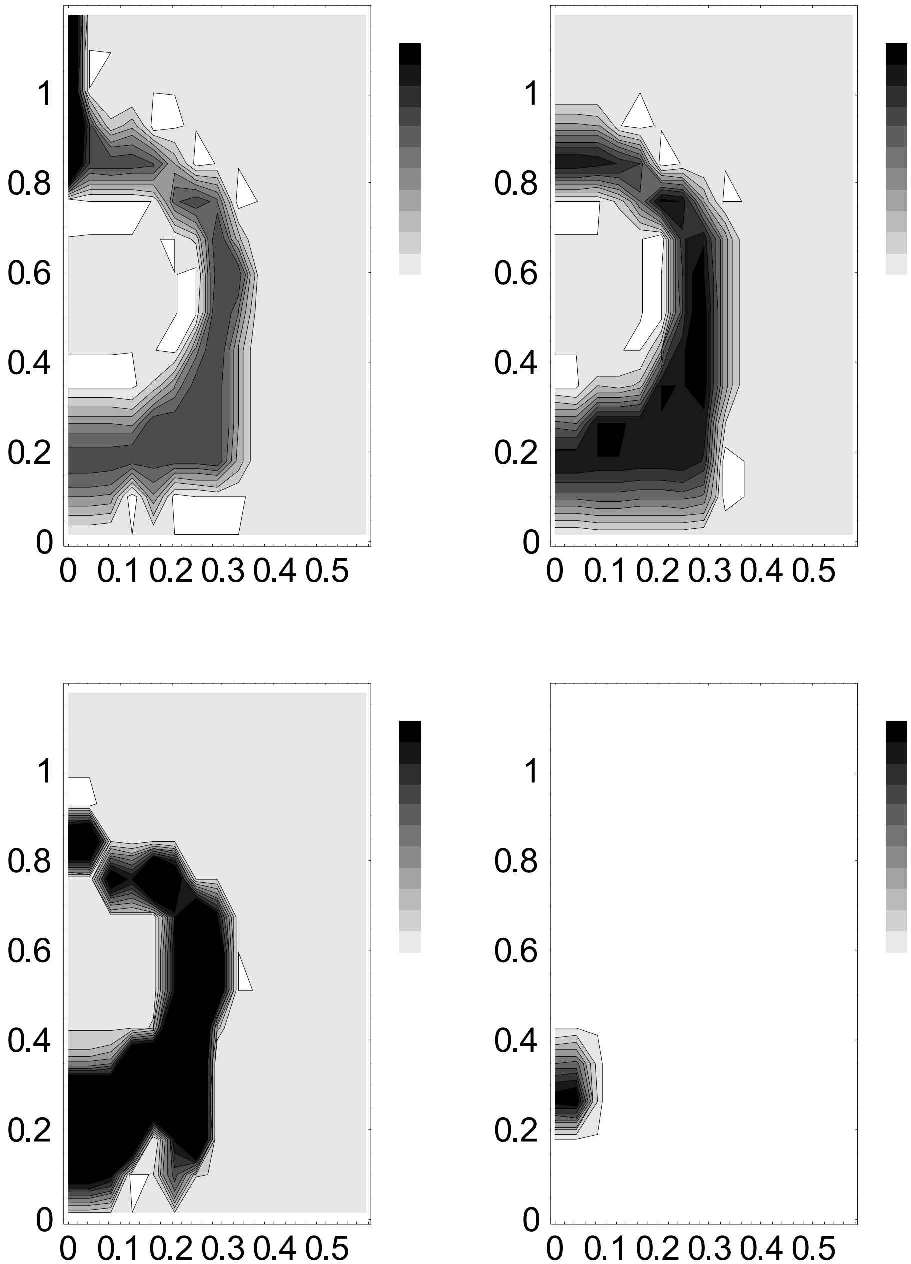

lst187

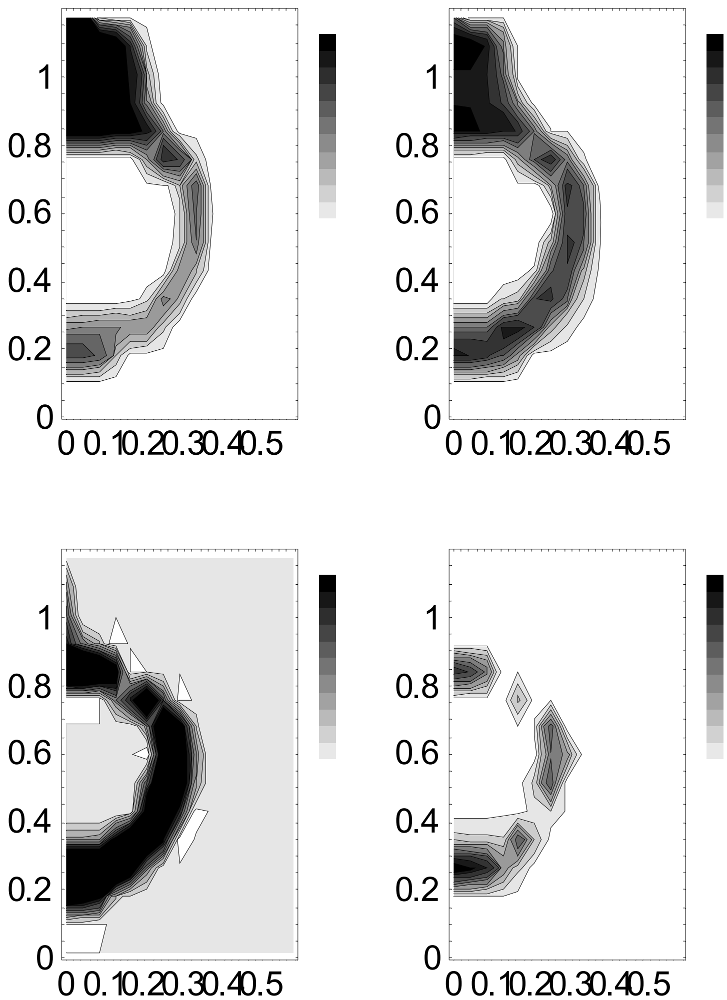

lst188

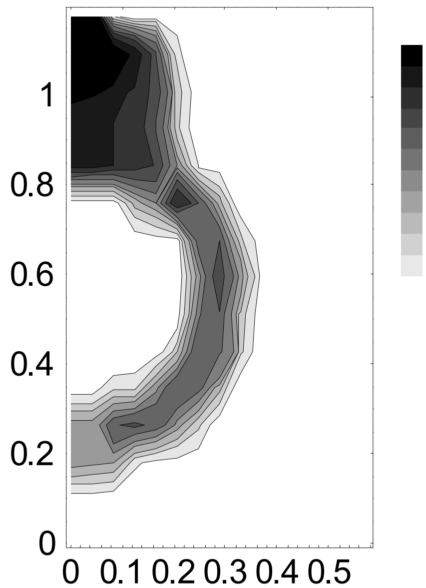

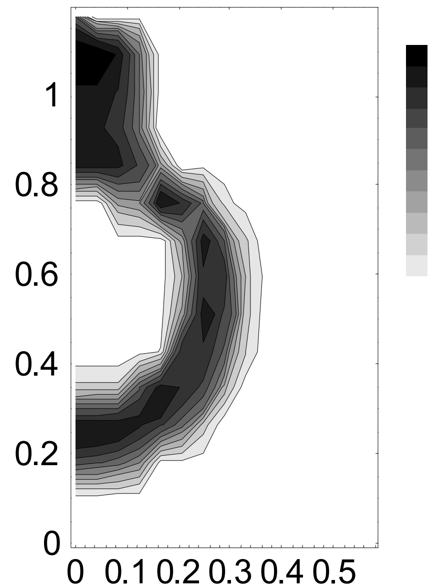

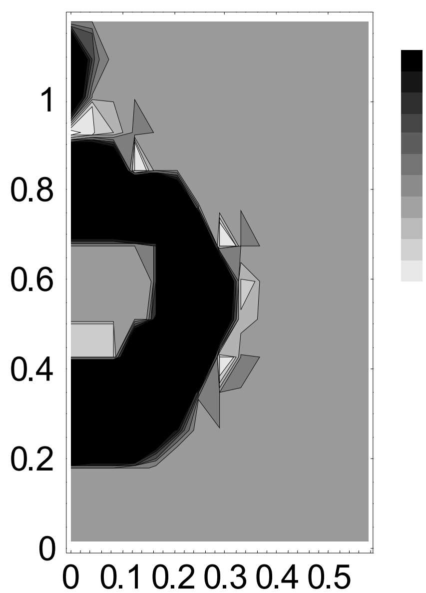

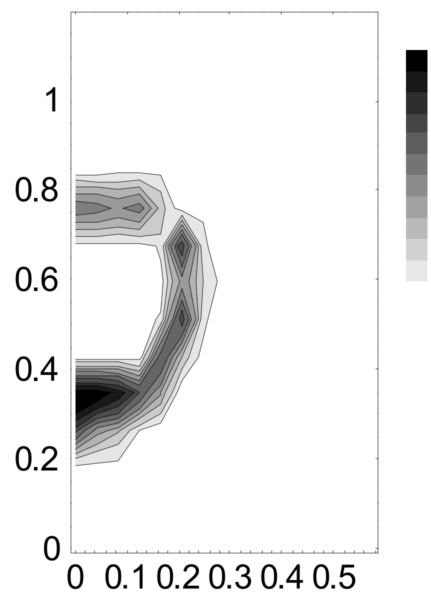

Listing of relative permeability values

A series of mathematica notebooks are used to generate tables of fracture-to-fracture and fracture-to-matrix relative permeability values. The notebook was initially developed by S. Painter and later modified by R. Green. Tables entries are generated by the notebook and written to a file. The file is in dos and needs to be converted to unix using dos2unix. Values vary with changes in the van Genuchten α and the AFM γ.

Following is a plot of log relative permeability versus liquid saturation for different values of γ in the AFM. γ = 0.0 (solid), 0.2 (dotted), 0.4 (small dash), 0.6 (medium dash), and 0.8 (long dash).

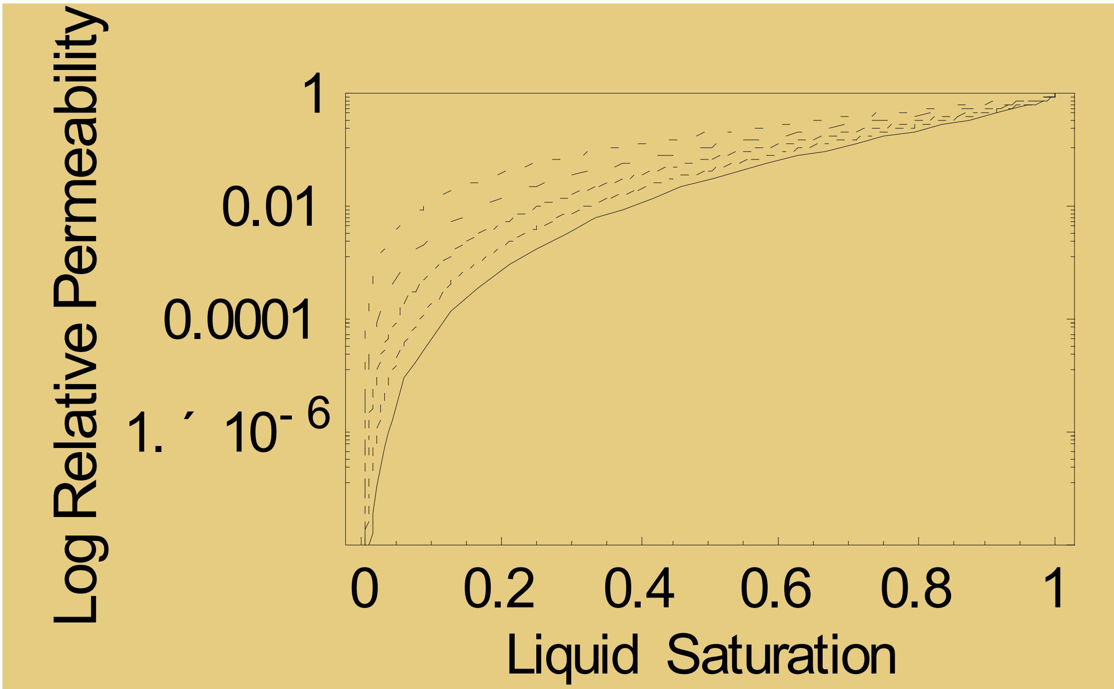

Table entries for relative permeability in Active Fracture Model

Table 5. Fracture to fracture relative permeability

Input file	Mathematica nb	Dos output	Unix output	γ	α
Lst180.dat	AFM_lst_180	lst_ff180.dat	ff180.dat	0.4	1e-3
Lst181.dat	AFM_lst_180	lst_ff180.dat	ff180.dat	0.4	1e-3
Lst182.dat	AFM_lst_180	lst_ff180.dat	ff180.dat	0.4	1e-3
Lst183.dat	AFM_lst_183	lst_ff183.dat	ff183.dat	0.4	1e-5
Lst184.dat	AFM_lst_184	lst _ff184.dat	ff184.dat	0.6	1e-4
Lst185.dat	AFM_lst_185	lst _ff185.dat	ff185.dat	0.8	1e-4
Lst187.dat	AFM_lst_180	lst _ff180.dat	ff180.dat	0.4	1e-3

Table 6. Fracture to matrix relative permeability

Input file	Mathematica nb	Dos output	Unix output	γ	α
Lst180.dat	AFM_lst_180	lst _fm180.dat	fm180.dat	0.4	1e-3
Lst181.dat	AFM_lst_180	lst _fm180.dat	fm180.dat	0.4	1e-3
Lst182.dat	AFM_lst_180	lst _fm180.dat	fm180.dat	0.4	1e-3
Lst183.dat	AFM_lst_183	lst_fm183.dat	fm183.dat	0.4	1e-5
Lst184.dat	AFM_lst_184	lst _fm184.dat	fm184.dat	0.6	1e-4
Lst185.dat	AFM_lst_185	lst _fm185.dat	fm185.dat	0.8	1e-4
Lst187.dat	AFM_lst_180	lst _fm180.dat	fm180.dat	0.4	1e-3

This notebook was completed on September 5, 2003

SCIENTIFIC NOTEBOOK
E590
Volume 2

by

Ronald Green

Southwest Research Institute
Center for Nuclear Waste Regulatory Analyses
San Antonio, Texas

September 9, 2003

Table of Contents

INITIAL ENTRIES

Scientific notebook: #590E Vol. 2
Issued to: R.T. Green
Issue Date: 21-May-2003, Continued on September 9, 2003 as Volume 2

A series of MULTIFLO simulations are performed to examine data collected during the two lab-scale heater tests described in Scientific Notebook 209. Additional analyses are documented in e-Notebook 590 Vol 1. This notebook contains continued documentation of those analyses.

All simulations were performed with MULTIFLO Version 1.5.2 August 2002.

LST THERMAL BOUNDARY CONDITIONS ANALYSES

The first task documented in this notebook is to re-evlaute the thermal boundary conditions assigned to the lab-scale heater test. Following is a summary of theses simulation analyses performed using MULTIFLO.

These simulation results will be compared with measured temperatures from Test 1 and Test 2 laboratory scale tests. Following are the measured temperatures at days 5, 50, and 110 during Test 1. These results were plotted using Surfer Version 8.03.

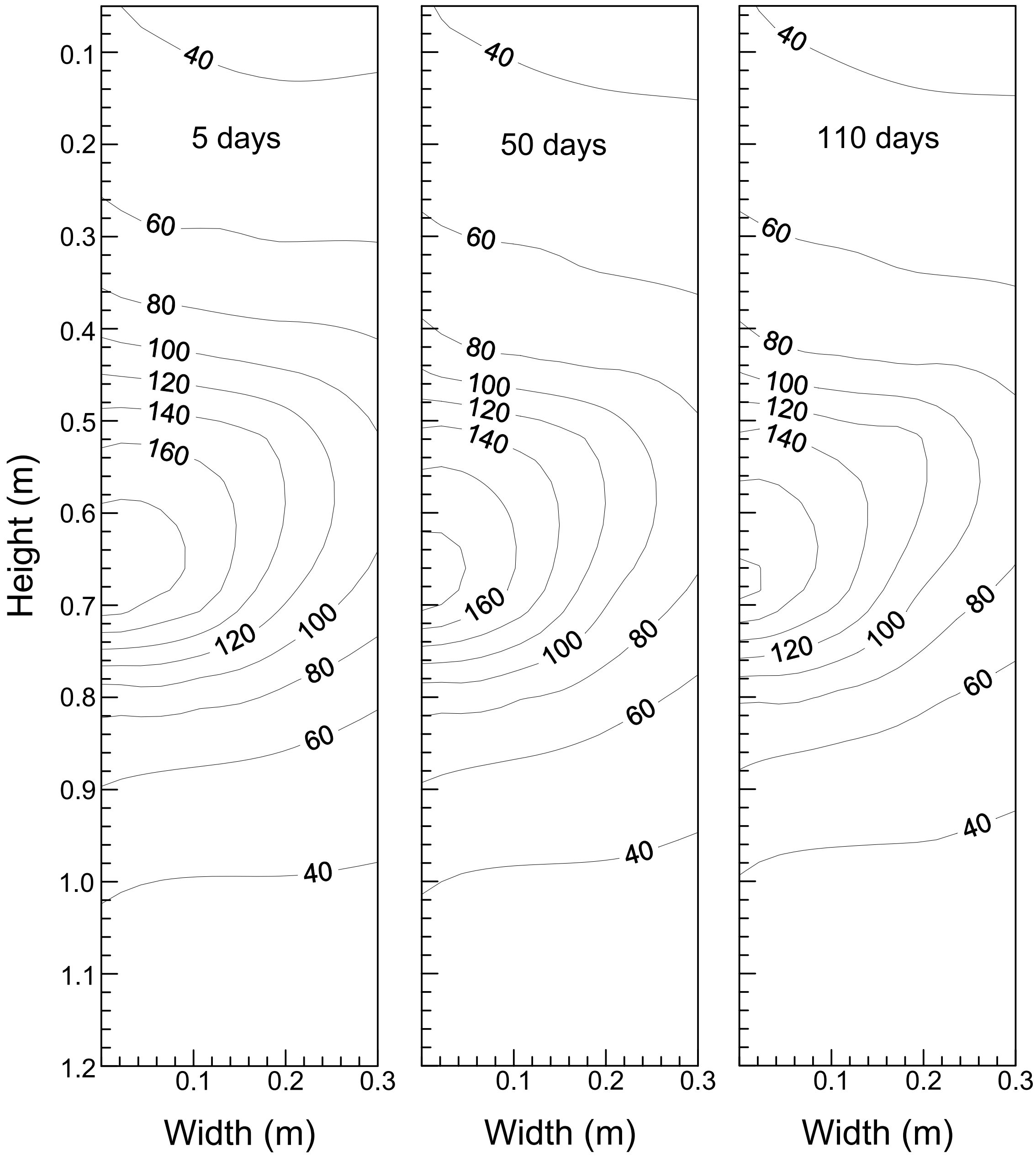

Test 1 data are in sideplotdata.xls in D:\Personal\text\kti\papers\wrr\.
Above are measured temperatures at days 5, 50, and 110 of Test 1. Maximum temperature is 201.5 C at day 5, 195.6 C at day 50, and 187.8 C at day 110.

Following are measured temperatures at days 10, 50, and 175 of Test 2. Maximum temperature was 245.6 C at day 10, 243.6 C at day 50, and 185.2 C at day 175. The highest temperature at each time was attributed to touching the cartridge heater and omitted. These data are found in isotherm_side_m.xls in D:\Personal\text\kti\papers\wrr\. There are 68 thermocouples in this plan according to the *xls file.

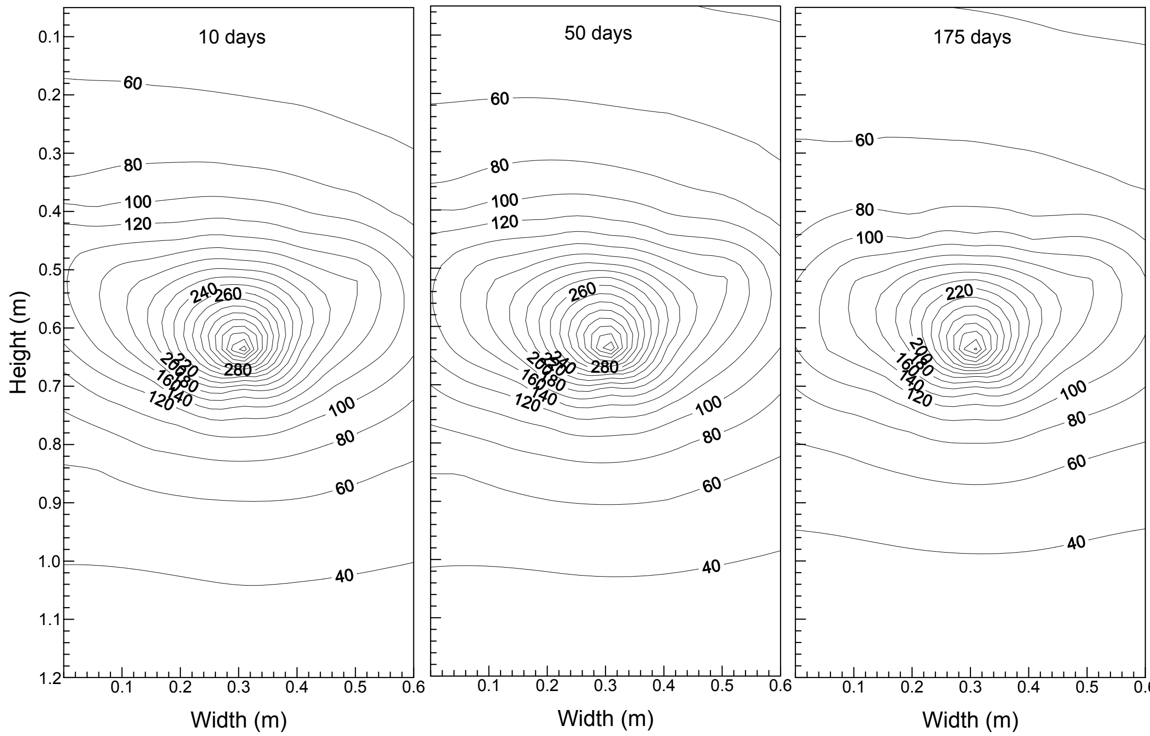

Table 1. Summary of experimental results

Test	Day	Measured temperature	
		maximum	minimum
Test 1	10	201.5	31.0
Test 1	50	195.6	30.4
Test 1	110	187.8	30.0
Test 2	10	220.76	33.19
Test 2	50	205.15	30.98
Test 2	175	197.49	27.73

These simulation results are located in /net/spock/home/rgreen/multi/lst/ross-lst/boundary/*. Following are descriptions of the simulations. All were run as variants to the assigned basecase in lst155.dat.

Table 2. Description of simulations for lst thermal boundary conditions analyses

Filename	Simulation descritpion	Result
Lst189	Dec volume of boundary elements	No heat loss through boundary
Lst190	Inc volume of boundary elements	Extreme heat loss thru boundary
Lst191	Set bc vol between lst155 and lst189	
Lst192	bc vol to default, inc bc heat cap at e4, e5	Did not converge
Lst193	bc vol to default, inc bc heat cap to 1e7	
Lst194	bc vol to default, inc bc heat cap to 5e5	
Lst195	bc vol to default, inc bc heat cap to 1e4	Did not converge
Lst196	bc vol to default, inc bc heat cap to 1e5	Did not converge

Basecase lst155 PhiK was assigned:

```
PhiK
: i1 i2 j1 j2 k1 k2 ist ithrm vb  porf permxf permyf permzf pormm permm  istm ithrmm
  1  24  1 14  1  30 4   7   0.0  1.00 1.e-10 1.e-10 1.e-10 0.50  2.e-17 1    1 ! matrix
:
: skip
: following are new bc with more mass to have lower edge temps
  1  24 14 14   1 30 4   7 1.0e-2 1.00 1.e-10 1.e-10 1.e-10 0.12  2.e-17 1    3 ! front
 24  24  1 14   1 30 4   7 1.0e-2 1.00 1.e-10 1.e-10 1.e-10 0.12  2.e-17 1    3 ! side
  1   4 14 14  14 19 4   7 1.0e-2 1.00 1.e-10 1.e-10 1.e-10 0.12  2.e-17 1   6 !front at heater
  1  24  1 14   1  1   4   7 1.0e-2 1.00 1.e-10 1.e-10 1.e-10 0.12  2.e-17 1    5 ! top
  1  24  1 14  30 30 4   7 5.0e-0 1.00 1.e-10 1.e-10 1.e-10 0.50  2.e-17 1    4 ! bottom
```

Bascase lst155 Thermal-prop was assigned:

```
Thermal-prop
: no rho       cpr    ckdry  cksat    crp  crt   tau  cdiff   cexp  enbd
  1  1.600e+03 840.0   0.50   1.00     0     0    .5  2.13e-5  1.8  0. 0 !matrix
  2  1.600e+03 840.0   10.0   10.0     0     0    .5  2.13e-5  1.8  0. 0 !drift
skip
  3  1.600e+03 5.0e+7  0.50   1.00     0     0    .5  2.13e-5  1.8  0. 0 !side boundaries
  4  1.600e+03 1.0e+9  0.50   1.00     0     0    .5  2.13e-5  1.8  0. 0 !bottom boundary
  5  1.600e+03 5.0e+7  0.50   1.00     0     0    .5  2.13e-5  1.8  0. 0 !top boundary
  6  1.600e+03 5.0e+8  1.50   2.00     0     0    .5  2.13e-5  1.8  0. 0 !front bc near heater
: noskip
  3  1.600e+03 840.0   0.50   1.00     0     0    .5  2.13e-5  1.8  0. 0 !side boundaries
  4  1.600e+03 840.0   0.50   1.00     0     0    .5  2.13e-5  1.8  0. 0 !bottom boundary
  5  1.600e+03 840.0   0.50   1.00     0     0    .5  2.13e-5  1.8  0. 0 !top boundary
  6  1.600e+03 840.0   0.50   1.00     0     0    .5  2.13e-5  1.8  0. 0 !front bc near heater
noskip
: skip
  3  1.600e+03 1.0e3   0.50   1.00     0     0    .5  2.13e-5  1.8  0. 0 !side boundaries
  4  1.600e+03 1.0e3   0.50   1.00     0     0    .5  2.13e-5  1.8  0. 0 !bottom boundary
  5  1.600e+03 1.0e3   0.50   1.00     0     0    .5  2.13e-5  1.8  0. 0 !top boundary
  6  1.600e+03 1.0e3   0.50   1.00     0     0    .5  2.13e-5  1.8  0. 0 !front bc near heater
  7  1.600e+03 1.0e3   0.50   1.00     0     0    .5  2.13e-5  1.8  0. 0 !fractures
: noskip
0
```

PhiK was modified in lst189 to:

```
PhiK
: i1 i2 j1 j2 k1 k2 ist ithrm vb  porf permxf permyf permzf pormm permm  istm ithrmm
  1  24  1 14  1  30 4   7   0.0  1.00 1.e-10 1.e-10 1.e-10 0.50  2.e-17 1    1 ! matrix
:
```

```
: skip
: following are new bc with more mass to have lower edge temps
  1  24 14 14   1 30 4   7 1.0e-4 1.00 1.e-10 1.e-10 1.e-10 0.12  2.e-17 1    3 ! front
 24  24  1 14   1 30 4   7 1.0e-4 1.00 1.e-10 1.e-10 1.e-10 0.12  2.e-17 1    3 ! side
  1   4 14 14  14 19 4   7 1.0e-4 1.00 1.e-10 1.e-10 1.e-10 0.12  2.e-17 1   6 ! front atheater
  1  24  1 14   1  1   4   7 1.0e-4 1.00 1.e-10 1.e-10 1.e-10 0.12  2.e-17 1    5 ! top
  1  24  1 14  30 30 4   7 5.0e-2 1.00 1.e-10 1.e-10 1.e-10 0.50  2.e-17 1    4 ! bottom
```

PhiK modified in lst190 to:

```
PhiK
: i1 i2 j1 j2 k1 k2 ist ithrm vb  porf permxf permyf permzf pormm permm  istm ithrmm
  1  24  1 14  1  30 4   7   0.0  1.00 1.e-10 1.e-10 1.e-10 0.50  2.e-17 1    1 ! matrix
:
: skip
: following are new bc with more mass to have lower edge temps
  1  24 14 14   1 30 4   7 1.0e-0 1.00 1.e-10 1.e-10 1.e-10 0.12  2.e-17 1    3 ! front
 24  24  1 14   1 30 4   7 1.0e-0 1.00 1.e-10 1.e-10 1.e-10 0.12  2.e-17 1    3 ! side
  1   4 14 14  14 19 4   7 1.0e-0 1.00 1.e-10 1.e-10 1.e-10 0.12  2.e-17 1   6 ! front atheater
  1  24  1 14   1  1   4   7 1.0e-0 1.00 1.e-10 1.e-10 1.e-10 0.12  2.e-17 1    5 ! top
  1  24  1 14  30 30 4   7 5.0e-1 1.00 1.e-10 1.e-10 1.e-10 0.50  2.e-17 1    4 ! bottom
```

PhiK modified in lst191 to:

```
PhiK
: i1 i2 j1 j2 k1 k2 ist ithrm vb  porf permxf permyf permzf pormm permm  istm ithrmm
  1  24  1 14  1  30 4   7   0.0  1.00 1.e-10 1.e-10 1.e-10 0.50  2.e-17 1    1 ! matrix
:
: skip
: following are new bc with more mass to have lower edge temps
  1  24 14 14   1 30 4   7 1.0e-3 1.00 1.e-10 1.e-10 1.e-10 0.12  2.e-17 1    3 ! front
 24  24  1 14   1 30 4   7 1.0e-3 1.00 1.e-10 1.e-10 1.e-10 0.12  2.e-17 1    3 ! side
  1   4 14 14  14 19 4   7 1.0e-3 1.00 1.e-10 1.e-10 1.e-10 0.12  2.e-17 1   6 ! front atheater
  1  24  1 14   1  1   4   7 1.0e-3 1.00 1.e-10 1.e-10 1.e-10 0.12  2.e-17 1    5 ! top
  1  24  1 14  30 30 4   7 5.0e-2 1.00 1.e-10 1.e-10 1.e-10 0.50  2.e-17 1    4 ! bottom
```

PhiK modified in lst192 to:

```
PhiK
: i1 i2 j1 j2 k1 k2 ist ithrm vb  porf permxf permyf permzf pormm permm  istm ithrmm
  1  24  1 14  1  30 4   7   0.0  1.00 1.e-10 1.e-10 1.e-10 0.50  2.e-17 1    1 ! matrix
:
: skip
: following are new bc with more mass to have lower edge temps
  1  24 14 14   1 30 4   7     0. 1.00 1.e-10 1.e-10 1.e-10 0.12  2.e-17 1    3 ! front
 24  24  1 14   1 30 4   7     0. 1.00 1.e-10 1.e-10 1.e-10 0.12  2.e-17 1    3 ! side
```

```
 1   4 14 14  14 19 4   7    0. 1.00 1.e-10 1.e-10 1.e-10 0.12  2.e-17 1    6 ! front at heater
 1  24  1 14   1  1  4  7    0. 1.00 1.e-10 1.e-10 1.e-10 0.12  2.e-17 1    5 ! top
 1  24  1 14  30 30 4   7    0. 1.00 1.e-10 1.e-10 1.e-10 0.50  2.e-17 1    4 ! bottom
```

and Therm-prop was modified in lst192 to:

```
Thermal-prop
: no rho      cpr    ckdry  cksat    crp  crt   tau  cdiff   cexp  enbd
  1  1.600e+03 840.0   0.50   1.00     0     0    .5  2.13e-5  1.8  0. 0 !matrix
  2  1.600e+03 840.0   10.0   10.0     0     0    .5  2.13e-5  1.8  0. 0 !drift
: skip
  3  1.600e+03 5.0e+3  0.50   1.00     0     0    .5  2.13e-5  1.8  0. 0 !side boundaries
  4  1.600e+03 1.0e+4  0.50   1.00     0     0    .5  2.13e-5  1.8  0. 0 !bottom boundary
  5  1.600e+03 5.0e+3  0.50   1.00     0     0    .5  2.13e-5  1.8  0. 0 !top boundary
  6  1.600e+03 5.0e+3  1.50   2.00     0     0    .5  2.13e-5  1.8  0. 0 !front bc near heater
noskip
skip
  3  1.600e+03 840.0   0.50   1.00     0     0    .5  2.13e-5  1.8  0. 0 !side boundaries
  4  1.600e+03 840.0   0.50   1.00     0     0    .5  2.13e-5  1.8  0. 0 !bottom boundary
  5  1.600e+03 840.0   0.50   1.00     0     0    .5  2.13e-5  1.8  0. 0 !top boundary
  6  1.600e+03 840.0   0.50   1.00     0     0    .5  2.13e-5  1.8  0. 0 !front bc near heater
: noskip
: skip
  3  1.600e+03 1.0e3   0.50   1.00     0     0    .5  2.13e-5  1.8  0. 0 !side boundaries
  4  1.600e+03 1.0e3   0.50   1.00     0     0    .5  2.13e-5  1.8  0. 0 !bottom boundary
  5  1.600e+03 1.0e3   0.50   1.00     0     0    .5  2.13e-5  1.8  0. 0 !top boundary
  6  1.600e+03 1.0e3   0.50   1.00     0     0    .5  2.13e-5  1.8  0. 0 !front bc near heater
noskip
  7  1.600e+03 1.0e3   0.50   1.00     0     0    .5  2.13e-5  1.8  0. 0 !fractures
: noskip
0
```

Therm-prop was modified in lst193 to: (lst193 PhiK same as lst192)

```
Thermal-prop
: no rho      cpr    ckdry  cksat    crp  crt   tau  cdiff   cexp  enbd
  1  1.600e+03 840.0   0.50   1.00     0     0    .5  2.13e-5  1.8  0. 0 !matrix
  2  1.600e+03 840.0   10.0   10.0     0     0    .5  2.13e-5  1.8  0. 0 !drift
: skip
  3  1.600e+03 5.0e+7  0.50   1.00     0     0    .5  2.13e-5  1.8  0. 0 !side boundaries
  4  1.600e+03 5.0e+7  0.50   1.00     0     0    .5  2.13e-5  1.8  0. 0 !bottom boundary
  5  1.600e+03 5.0e+7  0.50   1.00     0     0    .5  2.13e-5  1.8  0. 0 !top boundary
  6  1.600e+03 5.0e+7  0.50   1.00     0     0    .5  2.13e-5  1.8  0. 0 !front bc near heater
noskip
skip
  3  1.600e+03 840.0   0.50   1.00     0     0    .5  2.13e-5  1.8  0. 0 !side boundaries
```

```
  4  1.600e+03 840.0   0.50   1.00     0     0    .5  2.13e-5  1.8  0. 0 !bottom boundary
  5  1.600e+03 840.0   0.50   1.00     0     0    .5  2.13e-5  1.8  0. 0 !top boundary
  6  1.600e+03 840.0   0.50   1.00     0     0    .5  2.13e-5  1.8  0. 0 !front bc near heater
: noskip
: skip
  3  1.600e+03 1.0e3   0.50   1.00     0     0    .5  2.13e-5  1.8  0. 0 !side boundaries
  4  1.600e+03 1.0e3   0.50   1.00     0     0    .5  2.13e-5  1.8  0. 0 !bottom boundary
  5  1.600e+03 1.0e3   0.50   1.00     0     0    .5  2.13e-5  1.8  0. 0 !top boundary
  6  1.600e+03 1.0e3   0.50   1.00     0     0    .5  2.13e-5  1.8  0. 0 !front bc near heater
noskip
  7  1.600e+03 1.0e3   0.50   1.00     0     0    .5  2.13e-5  1.8  0. 0 !fractures
: noskip
0
```

Therm-prop was modified in lst194 to: (lst194 PhiK same as lst192)

```
Thermal-prop
: no rho       cpr    ckdry  cksat    crp  crt   tau  cdiff   cexp  enbd
  1  1.600e+03 840.0   0.50   1.00     0     0    .5  2.13e-5  1.8  0. 0 !matrix
  2  1.600e+03 840.0   10.0   10.0     0     0    .5  2.13e-5  1.8  0. 0 !drift
: skip
  3  1.600e+03 5.0e+5  0.50   1.00     0     0    .5  2.13e-5  1.8  0. 0 !side boundaries
  4  1.600e+03 5.0e+5  0.50   1.00     0     0    .5  2.13e-5  1.8  0. 0 !bottom boundary
  5  1.600e+03 5.0e+5  0.50   1.00     0     0    .5  2.13e-5  1.8  0. 0 !top boundary
  6  1.600e+03 5.0e+5  0.50   1.00     0     0    .5  2.13e-5  1.8  0. 0 !front bc near heater
noskip
skip
  3  1.600e+03 840.0   0.50   1.00     0     0    .5  2.13e-5  1.8  0. 0 !side boundaries
  4  1.600e+03 840.0   0.50   1.00     0     0    .5  2.13e-5  1.8  0. 0 !bottom boundary
  5  1.600e+03 840.0   0.50   1.00     0     0    .5  2.13e-5  1.8  0. 0 !top boundary
  6  1.600e+03 840.0   0.50   1.00     0     0    .5  2.13e-5  1.8  0. 0 !front bc near heater
: noskip
: skip
  3  1.600e+03 1.0e3   0.50   1.00     0     0    .5  2.13e-5  1.8  0. 0 !side boundaries
  4  1.600e+03 1.0e3   0.50   1.00     0     0    .5  2.13e-5  1.8  0. 0 !bottom boundary
  5  1.600e+03 1.0e3   0.50   1.00     0     0    .5  2.13e-5  1.8  0. 0 !top boundary
  6  1.600e+03 1.0e3   0.50   1.00     0     0    .5  2.13e-5  1.8  0. 0 !front bc near heater
noskip
  7  1.600e+03 1.0e3   0.50   1.00     0     0    .5  2.13e-5  1.8  0. 0 !fractures
: noskip
0
```

Therm-prop was modified in lst195 to: (lst195 PhiK same as lst192)

```
Thermal-prop
: no rho       cpr    ckdry  cksat    crp  crt   tau  cdiff   cexp  enbd
  1  1.600e+03 840.0   0.50   1.00     0     0    .5  2.13e-5  1.8  0. 0 !matrix
  2  1.600e+03 840.0   10.0   10.0     0     0    .5  2.13e-5  1.8  0. 0 !drift
```

: skip
  3 1.600e+03 **5.0e+4** 0.50   1.00   0   0   .5 2.13e-5 1.8 0. 0 !side boundaries
  4 1.600e+03 **5.0e+4** 0.50   1.00   0   0   .5 2.13e-5 1.8 0. 0 !bottom boundary
  5 1.600e+03 **5.0e+4** 0.50   1.00   0   0   .5 2.13e-5 1.8 0. 0 !top boundary
  6 1.600e+03 **5.0e+4** 0.50   1.00   0   0   .5 2.13e-5 1.8 0. 0 !front bc near heater
noskip
skip

Therm-prop was modified in lst196 to: (lst196 PhiK same as lst192
Thermal-prop
: no rho   cpr   ckdry cksat   crp crt   tau cdiff   cexp enbd
  1 1.600e+03 840.0   0.50   1.00   0   0   .5 2.13e-5 1.8 0. 0 !matrix
  2 1.600e+03 840.0   10.0   10.0   0   0   .5 2.13e-5 1.8 0. 0 !drift
: skip
  3 1.600e+03 **1.0e+5** 0.50   1.00   0   0   .5 2.13e-5 1.8 0. 0 !side boundaries
  4 1.600e+03 **1.0e+5** 0.50   1.00   0   0   .5 2.13e-5 1.8 0. 0 !bottom boundary
  5 1.600e+03 **1.0e+5** 0.50   1.00   0   0   .5 2.13e-5 1.8 0. 0 !top boundary
  6 1.600e+03 **1.0e+5** 0.50   1.00   0   0   .5 2.13e-5 1.8 0. 0 !front bc near heater
noskip
skip

Table 2. Summary of results for runs that converged

Filename	Matrix temp		Matrix sat		Fracture temp		Fracture sat	
	max	min	max	min	max	min	max	min
Lst155	185.1	20.01	0.9982	0.0	184.6	20.01	0.1792	0.0
Lst189	328.5	40.42	0.2203	0.0	328.0	40.42	0.0	0.0
Lst190	128.5	20.0	0.4179	0.0	127.9	20.0	0.0	0.0
Lst191	266.0	31.58	0.9359	0.0	265.4	31.58	0.0846	0.0
Lst193	120.4	20.0	1.0	0.0	119.9	20.0	0.7829	0.0
Lst194	194.5	48.11	0.999	0.0	193.9	48.12	0.7129	0.0

Simulated matrix temperature:

Basecase Lst155

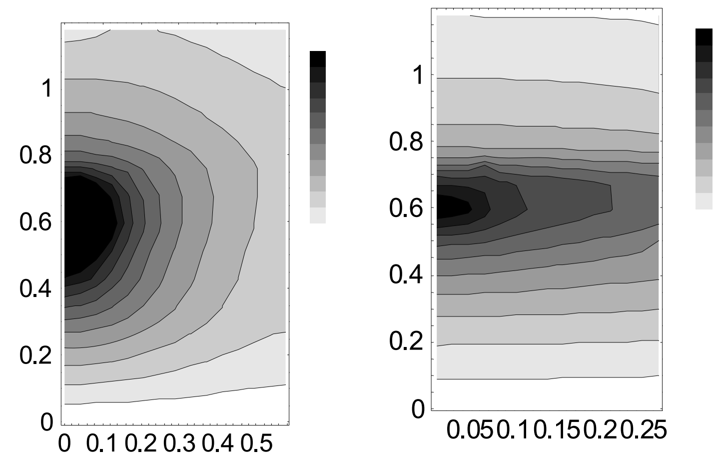

maximum matrix temp: 185.1

Lst189

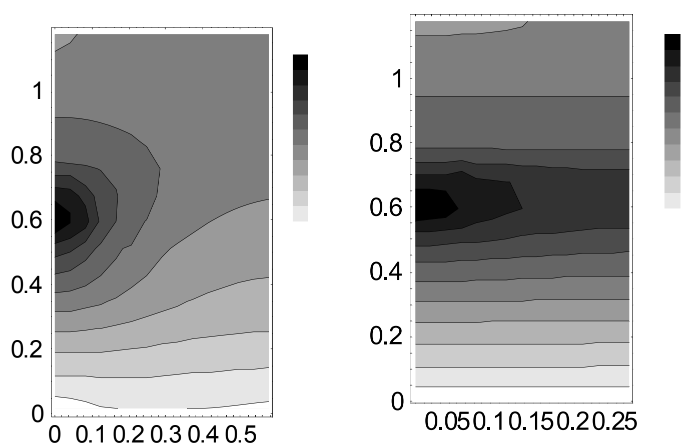

maximum matrix temp: 328.5

Lst190

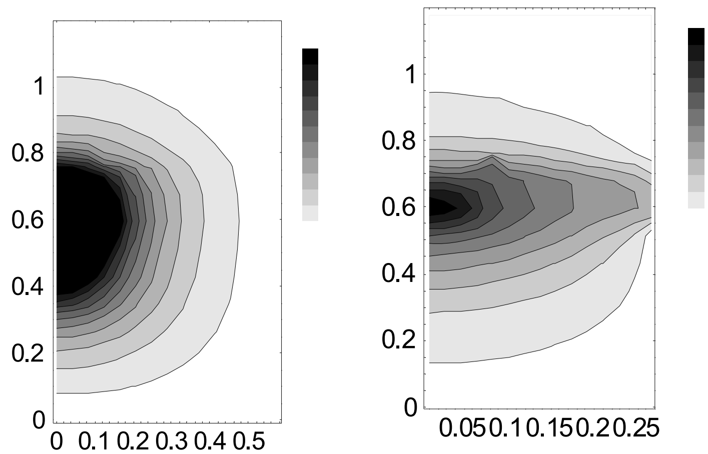

maximum matrix temp: 128.5

Lst191

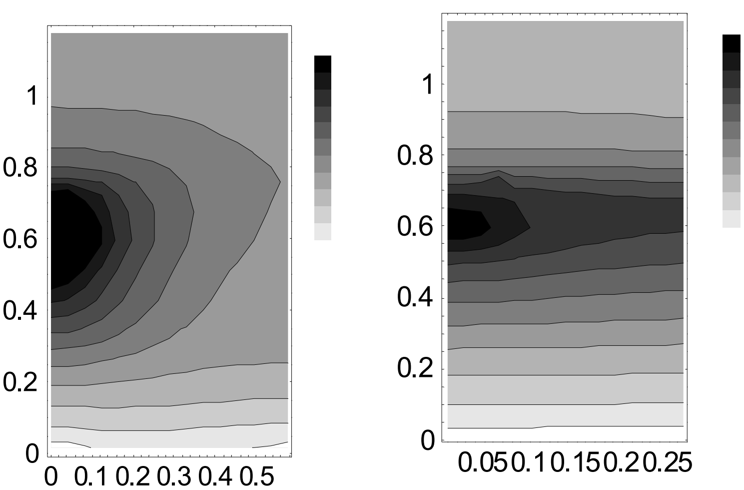

max matrix temp: 266.0

Lst193

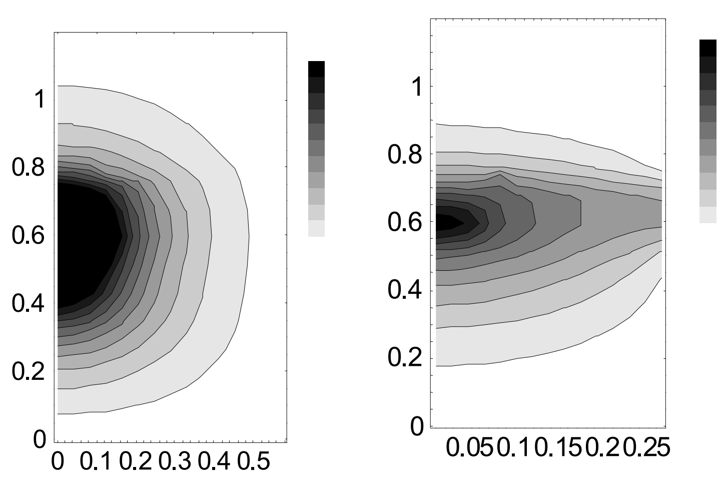

max matrix temp: 120.4

Lst194

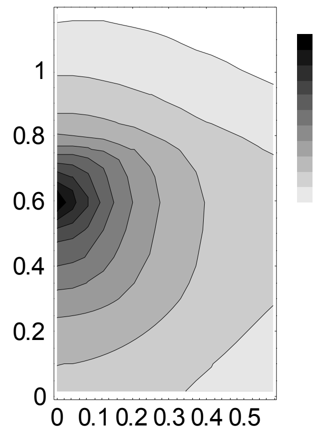

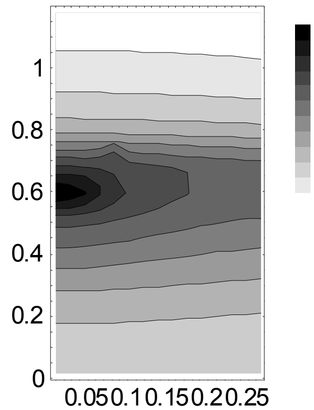

maximum matrix temp: 194.5

Matrix saturation
Measured matrix saturation

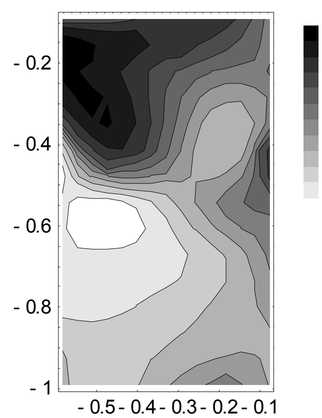

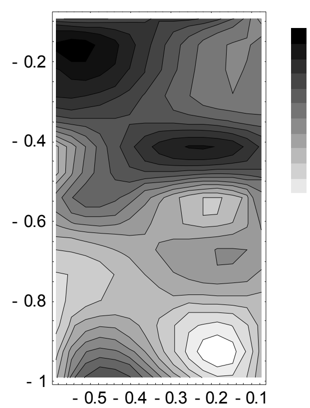

Basecase Lst155

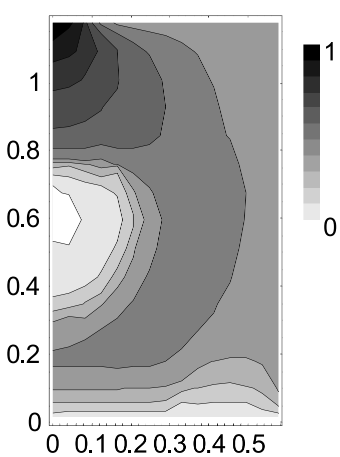

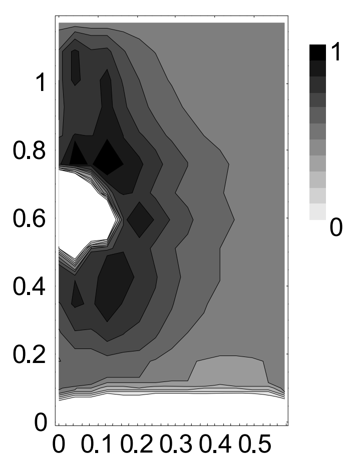

Lst189

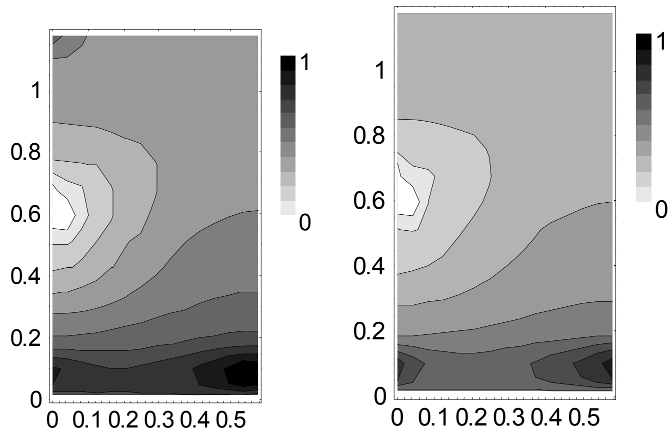

Lst190

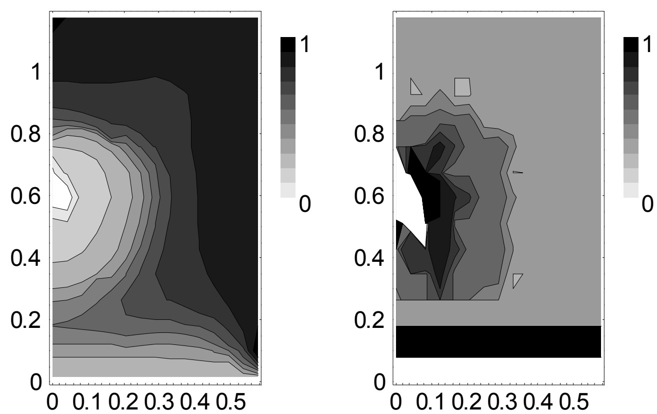

Lst191

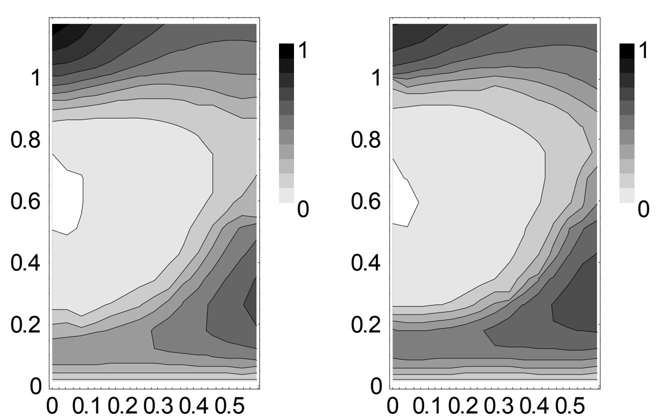

Lst193

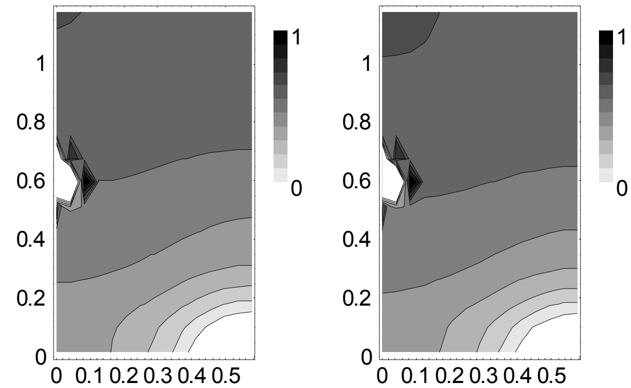

Lst194

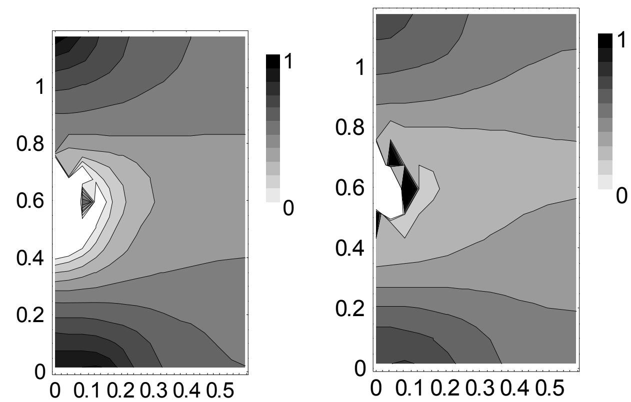

Fracture saturation

Basecase Lst155

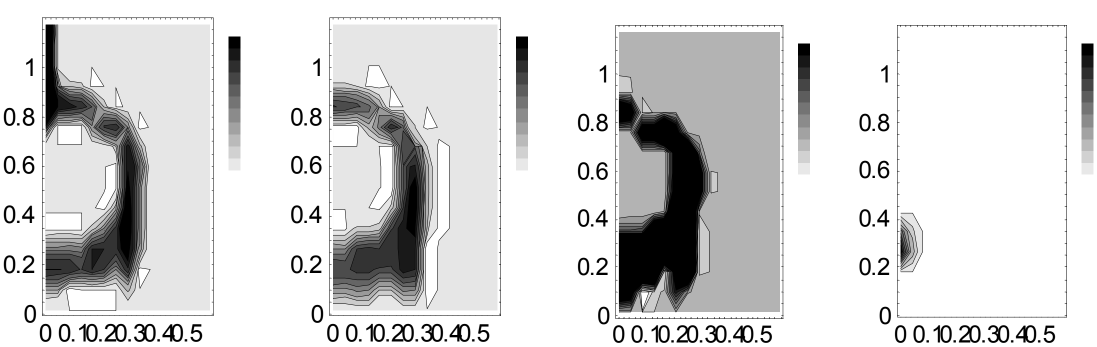

Lst189 (all fractures are at 0.0 saturation)

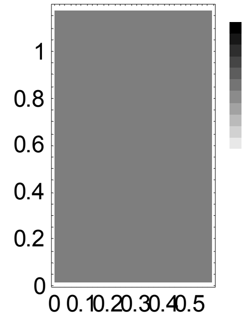

Lst190 (all fractures are at 0.0 saturation)

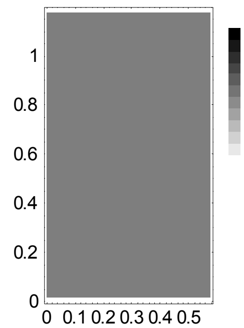

Lst191

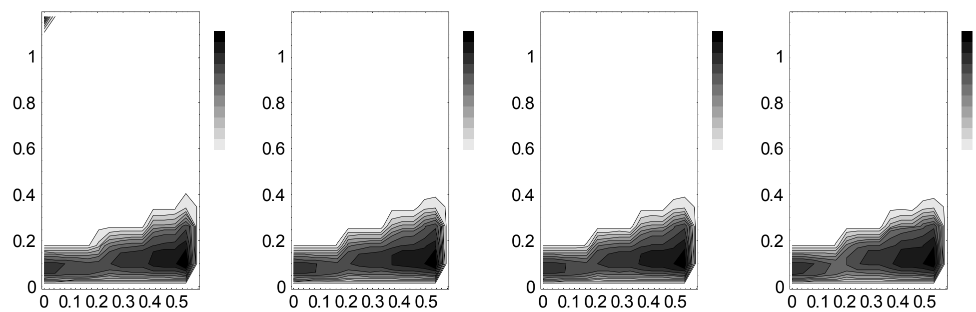

Lst193

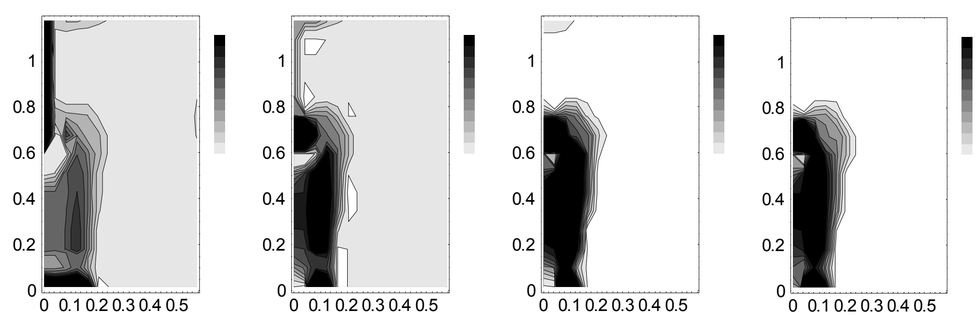

Based on these analyses, the basecase Lst155 has the best thermal boundary conditions.

Re-ran basecase with revised upper and lower boundary conditions. The lower is gravity drainage. The upper is at atmospheric pressure.

lst202, inc int temp to 30 from 20 C
lst204, inc source by scale = 1.4
lst205, inc by heat and mass in source by 1.4
lst206, inc mass in source by 1.7, heat inc by 1.4
lst207, inc mass in source by 2.0, heat inc by 1.4
lst208, dec matrix perm to 2e-18, same source as lst207
lst209, inc matrix perm to 2e-16, same source as lst207
lst210, set γ=0.8, α=1e-4, same source as lst207

Table x. Experimental and simulation results at 10 days

Filename	Matrix temp		Matrix sat		Fracture temp		Fracture sat	
	max	min	max	min	max	min	max	min
Test 1	201.5	31.0						
Test 2	220.76	33.19						
Lst155	130.9	20.00	0.4881	0.0	130.4	20.00	0.0536	0.0
Lst202	142.6	20.66	0.9931	0.0	142.0	20.66	0.0482	0.0
Lst204	190.6	20.71	0.9924	0.0	189.8	20.71	0.0543	0.0
Lst205	190.6	20.71	1.0	0.0	189.9	20.71	0.1090	0.0
Lst206	190.4	20.71	1.0	0.0	189.6	20.71	0.2450	0.0
Lst207	189.4	20.72	1.0	0.0	188.7	20.71	0.3066	0.0
Lst208	175.5	20.72	1.0	0.0	174.8	20.72	0.8500	0.0
Lst209	190.2	20.72	0.8471	0.0	189.4	20.71	0.0446	0.0
Lst210	176.7	20.67	1.0	0.0	176.0	20.66	0.3104	0.0

Table x. Experimental and simulation results at 50 days

Filename	Matrix temp		Matrix sat		Fracture temp		Fracture sat	
	max	min	max	min	max	min	max	min
Test 1	195.6	30.4						
Test 2	240.04	31.5						
Lst155	154.1	20.00	0.9470	0.0	154.3	20.00	0.0330	0.0
Lst202	164.6	20.62	0.9942	0.0	164.0	20.61	0.0480	0.0
Lst204	221.3	20.69	0.9932	0.0	220.5	20.68	0.0476	0.0
Lst205	221.1	20.68	1.0	0.0	220.3	20.68	0.1178	0.0
Lst206	219.6	20.69	1.0	0.0	218.9	20.69	0.2452	0.0
Lst207	216.6	20.69	1.0	0.0	215.9	20.69	0.3049	0.0
Lst208	192.4	20.70	1.0	0.0	191.7	20.70	0.5976	0.0
Lst209	219.4	20.69	0.8458	0.0	218.7	20.69	0.0444	0.0
Lst210	196.4	20.63	1.0	0.0	195.7	20.63	0.1366	0.0

Table x. Experimental and simulation results at 110 days

Filename	Matrix temp		Matrix sat		Fracture temp		Fracture sat	
	max	min	max	min	max	min	max	min
Test 1	187.8	30.0						
Test 2	205.15	30.98						
Lst155	171.1	20.00	1.0	0.0	171.1	20.00	0.3641	0.0

Lst202	179.5	20.63	0.9934	0.0	179.0	20.63	0.0510	0.0
Lst204	242.2	20.77	0.9916	0.0	241.6	20.77	0.0734	0.0
Lst205	242.0	20.77	0.9999	0.0	241.2	20.77	0.0769	0.0
Lst206	240.5	20.77	1.0	0.0	239.8	20.77	0.2282	0.0
Lst207	237.5	20.78	1.0	0.0	236.7	20.78	0.2927	0.0
Lst208	211.4	20.8	1.0	0.0	210.6	20.8	0.4045	0.0
Lst209	240.8	20.77	0.8414	0.0	240.0	20.77	0.0440	0.0
Lst210	213.4	20.68	1.000	0.0	212.6	20.68	0.1300	0.0

Table x. Experimental and simulation results at 175 days

Filename	Matrix temp		Matrix sat		Fracture temp		Fracture sat	
	max	min	max	min	max	min	max	min
Test 2	197.49	27.73						
Lst155	178.4	20.10	1.0	0.0	177.9	20.10	0.4189	0.0
Lst202	187.7	20.80	0.9926	0.0	187.2	20.80	0.0548	0.0
Lst204	255.1	21.05	0.9904	0.0	254.3	21.05	0.0768	0.0
Lst205	254.7	21.05	0.9998	0.0	253.9	21.05	0.0791	0.0
Lst206	242.0	20.77	0.9999	0.0	241.2	20.77	0.0769	0.0
Lst207	250.4	21.06	1.0	0.0	249.7	21.06	0.2835	0.0
Lst208	222.6	21.60	1.0	0.0	221.9	21.10	0.4007	0.0
Lst209	253.6	21.06	0.8384	0.0	252.9	21.06	0.0438	0.0
Lst210	223.1	20.92	1.0	0.0	222.3	20.92	0.1245	0.0

These results suggest that decreasing matrix permeability (as in lst208) results in lower temperature and slightly higher fracture saturations. Increasing matrix permeability (as in lst209) results in slightly higher temperatures, slightly lower matrix saturations, and much lower fracture saturations. The fracture saturations predicted for the lower matrix permeability (lst209) are too low to be possible. A matrix permeability of 2e-18 m^2 is therefore ruled out.

Temperature for lst202 is as follows

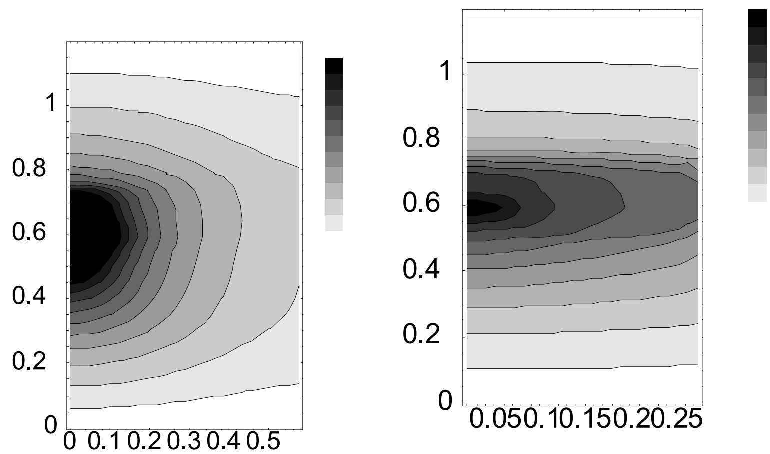

Temperature for lst204 at 172 days is as follows

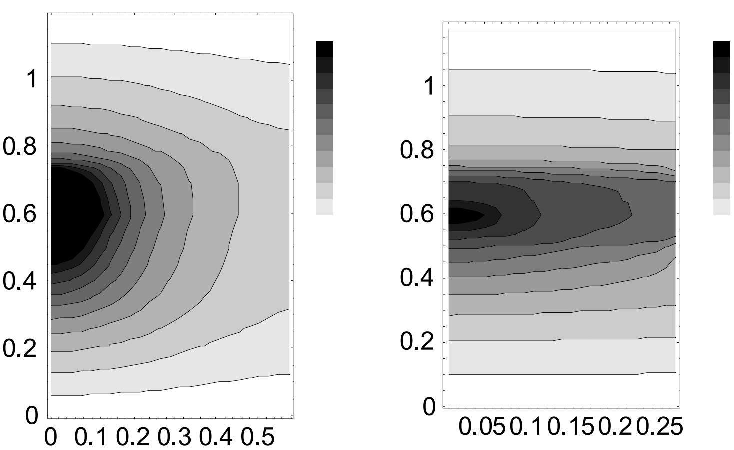

Matrix saturation for lst202 at day 172 is as follows

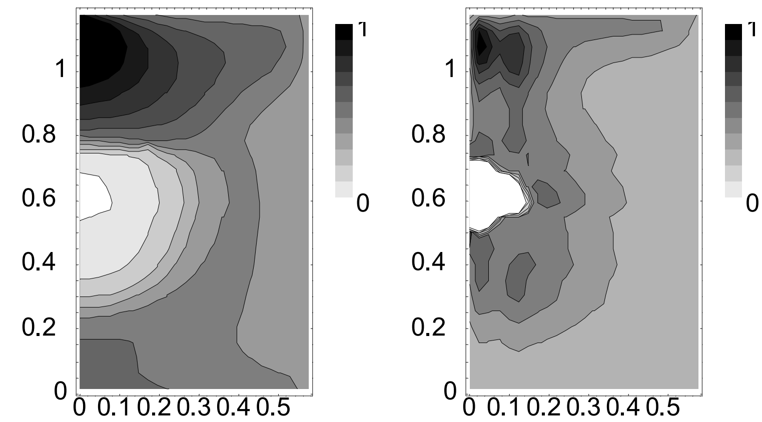

Matrix saturation for lst204 at day 172 is as follows

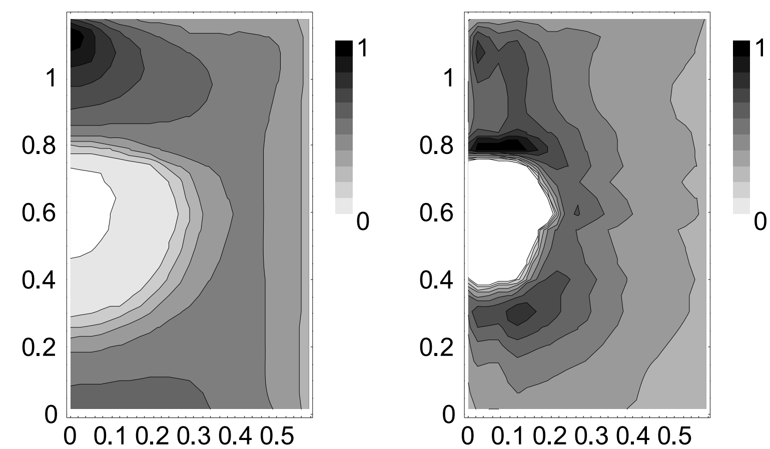

Saturations range for 0 (white) to the maximum (see Table 1 in this notebook). There are four slices taken from each simulation. Of the ten slices provided in each mathematica notebook, slices 1, 5, 9, and 10 are copied to this scientific notebook.

Fracture saturation for lst202 at day 172 is as follows [new basecase for new BC]

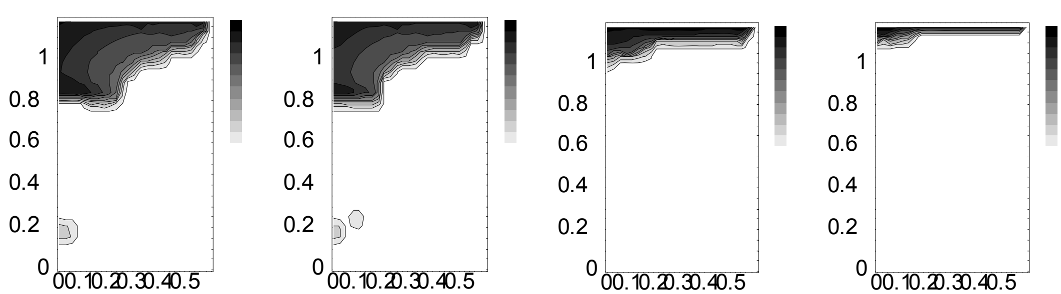

Fracture saturation for lst204 at day 172 is as follows [0nly diff from lst202 is inc heat by 1.4]

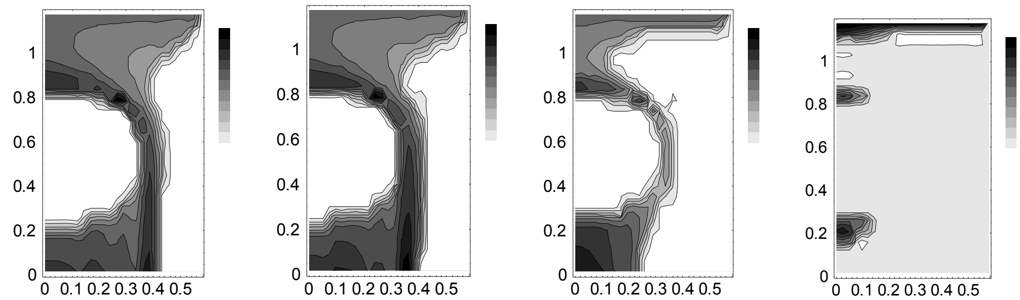

Fracture saturation for lst207 at day 172 is as follows

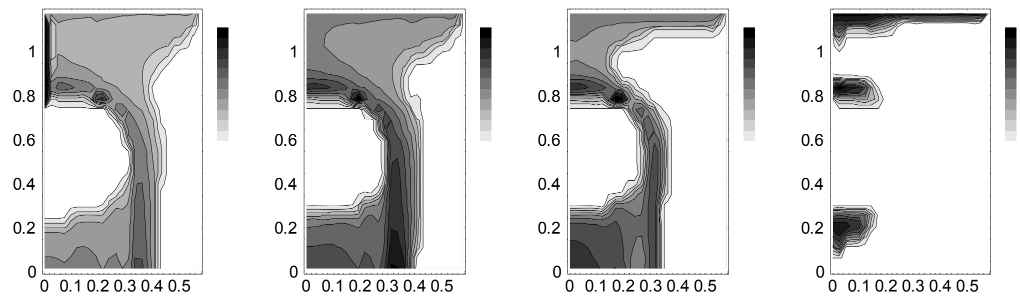

Fracture saturation for lst208 at day 172 is as follows

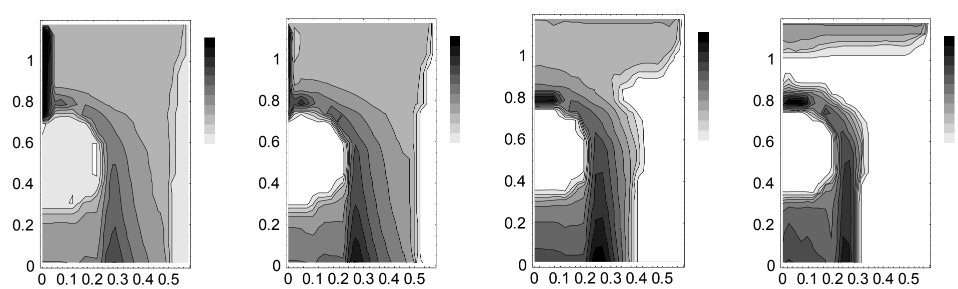

Fracture saturation for lst209 at day 172 is as follows

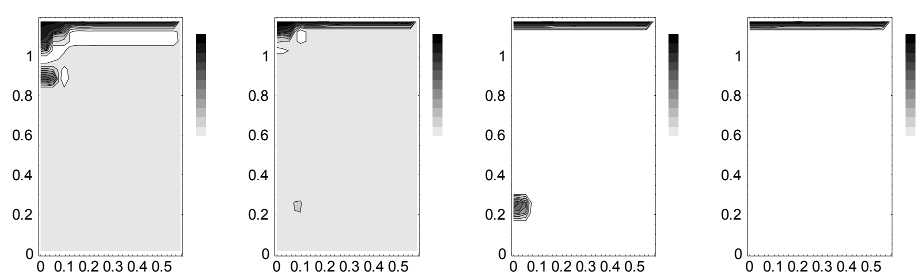

Fracture saturation for lst210 at day 172 is as follows

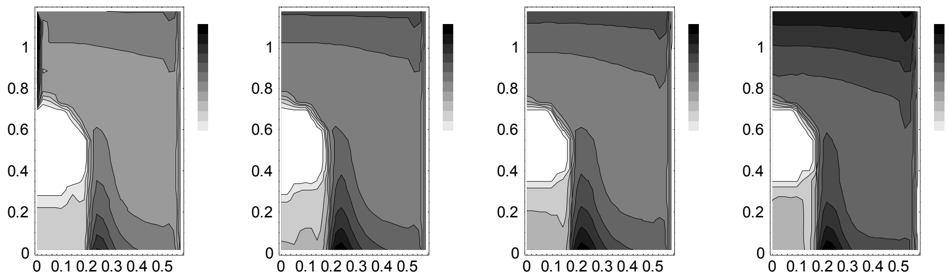

This notebook was completed on October 4, 2004.

SCIENTIFIC NOTEBOOK
E590
Volume 3

by

Ronald Green

Southwest Research Institute
Center for Nuclear Waste Regulatory Analyses
San Antonio, Texas

January 3, 2005

Table of Contents

INITIAL ENTRIES

Scientific notebook: #590E Vol. 3
Issued to: R.T. Green
Issue Date: 21-May-2003, Continued on January 3, 2005 as Volume 3

This notebook contains a continuation of the analyses of heat transfer through Tptpll. The body of the text will be converted into a paper or report. Calculations were consolidated into a excel spreadsheet:

Thermal_k_final_b.xls

and one mathematica notebook:

rayleigh.nb

This notebook is copied and included as Appendix A for convenience.

The original lab data are documented in Scientific Notebook 212. Although the data were collected in 2000, the data were not analyzed at that time because the DOE decided to not consider engineered backfill as a design option. The data were recently analyzed in light of the possibility for early drift collapse and rockfall in the Tptpll. This prospect highlighted the need to understand the mechanisms and properties of heat flow through rubble. The analyses associated with this study are being summarized into a paper that will be submitted to a journal.

The draft text and figures for the paper or report are attached on January 3, 2005 are attached as Appendix A as a wordperfect file: th-k-tptpll_d.txt

Information in rayleigh.nb includes

1. Calculation of the Rayleigh number for porous media with a width-to-height aspect ratio of unity.
2. Calculation of the Rayleigh number for porous media with a width-to-height aspect ratios of 1.,.9,.8,.7,.6,.5,.4,.3, .2,.15,.125, .1, 1/30.
3. Calculation of the Rayleigh number for an actual drift with collapse, at a variety of aspect ratios.

These values are plotted in excel spreadsheet Thermal_k_final_b.xls.

The abstract for a proposed journal article is as follows:

Thermally induced rock stresses at the potential high-level nuclear waste (HLW) repository at Yucca Mountain, Nevada, can degrade the drifts, possibly causing rubble to fall onto the dripshield overlying the emplaced waste packages. Thermal-hydrological processes will be altered by changes in thermal conductivity, ventilation, radiation, and convection resulting from such rockfalls. The purpose of this investigation is to measure heat transfer through crushed rock samples of the Topopah Spring lower lithophysal unit at Yucca Mountain as an analog of the rubble and to identify the important heat and mass transfer mechanisms for the expected range of conditions. A laboratory apparatus was used to measure heat transfer through the crushed tuff for temperatures as high as 173ºC and thermal gradients as large as 995ºC/m. A thermal conductivity value of 0.4 W/m-K was derived from measurements made at low temperatures, low

thermal gradients, and low saturation. Heat transfer by radiation was determined to be negligible, even at elevated temperatures, using empirical relations developed for granular packed bed media. Convection was determined to be that portion of heat transfer not attributed to conduction and radiation. Convection was observed in the laboratory apparatus at temperature gradients in excess of 600ºC/m. Heat transfer by convection through a rubble pile in a HLW emplacement drift, however, are calculated to occur at the much lower temperature gradients expected at the proposed Yucca Mountain geologic repository using a Rayleigh number analysis predicated on rubble properties calculated during these experiments.

The draft paper's introduction and background are as follows:

Thermally induced stress at emplacement drifts at the potential high-level nuclear waste (HLW) repository at Yucca Mountain has been shown to lead to drift degradation (Gute et al., 2003; Ofoegbu et al., 2004). Drift degradation will be manifested as rockfall into the drift, possibly onto the dripshield overlying the emplaced waste packages. The transfer of heat through the zone near the degraded emplacement drifts will be altered by changes in thermal conductivity, ventilation, radiation, and convection resulting from the rockfall. In particular, the rubble pile will alter the thermal-hydrological processes by acting as a thermal insulator in the zone between the heat source (i.e., HLW canister) and the intact host rock and will affect the movement of liquid as vapor or liquid by altering the gas and liquid permeability for this region. Determining the impact of rubble on the design of a geologic repository is made difficult because heat and mass transfer through the engineered barrier and a rubble pile is a complex and coupled process. Complicating this transfer process is a high level of uncertainty in assigning property values to the highly heterogeneous structure of a rubble pile.

A significant portion of the potential repository at Yucca Mountain as currently designed is predominately placed in the lower lithophysal unit of the Topopah Springs (Tptpll). Recent laboratory testing of the Tptpll by Brodsky et al. (2003a) provided relevant thermal conductivity measurements of intact samples of the rock matrix. Similarly, Brodsky et al. (2003b) has initiated field-scale thermal conductivity measurements of the Tptpll at the Enhanced Characterization of the Repository Block (ECRB) Cross Drift at Yucca Mountain Exploratory Studies Facility (ESF) to account for volume-average thermal conductivity of the rock including lithophysae. These two studies provide valuable end points in the continuum of possible rock textures that could comprise emplacement drift rock collapse. This does not imply that these texture end points also represent extreme values of thermal conductivity. In fact, actual rockfall thermal conductivity values could vary outside the range of values bracketed by the laboratory- (Brodsky et al., 2003a) and field- (Brodsky et al., 2003b) scale measurements.

Transient and steady-state methods are available for measuring thermophysical properties. Both classes of methods have strengths and weaknesses. Transient methods permit calculation of thermal diffusivity and require shorter heating periods than steady-state methods of thermophysical properties (Singh and Chaudhary, 1992). Conversely, steady-state methods allow unambiguous determination of thermal conductivity as compared to transient methods which usually require an independent determination or estimation of heat capacity in order to determine thermal conductivity from thermal diffusivity measurements. Because the heat transfer processes at a geologic repository are expected to vary slowly, transient thermal effects are assumed to be of secondary importance compared to identification of the specific mechanisms active in the transfer of heat through rockfall. Therefore, thermal conductivity (or effective thermal conductivity), and not heat capacity or thermal diffusivity, is the primary focus of this investigation.

The purpose of this investigation is the assessment of the thermophysical properties of an analog rubble pile and identification of the important heat and mass transfer mechanisms anticipated to be active under quasi-steady-state conditions in rubble collapsed around HLW canisters for conditions expected at a potential geologic HLW repository. To accomplish this objective, a steady-state laboratory apparatus was used to directly measure bulk thermal conductivity of crushed rock for a range of temperatures. The laboratory method used in these experiments closely paralleled the methodology developed by Green et al. (1997). Laboratory experiments and analyses were conducted to investigate the various heat transfer mechanisms that might be active in a rubble pile expected in emplacement drifts (Gute et al., 2003; Ofoegbu et al., 2004). Analyses were conducted to identify the range of thermal-physical conditions over which the various heat transfer mechanisms would be active. This information is used to analyze the effects of a rubble pile in emplacement drifts at the potential repository that experience rockfall.

Background

Conduction, convection, and radiation can potentially contribute to the transfer of heat from HLW canisters emplaced in a geologic repository. The complexity of the heat and mass transfer system near the heat-generating canister is compounded because the mechanisms that transfer heat through the drift space can vary in both space and time. These mechanisms could remain constant under stable drift conditions or they could be significantly altered in the event that rockfall occurs causing the dripshield overlying the canisters to be buried in a rubble pile. Heat transfer mechanisms would change due to the rubble pile acting as an insulator and the alteration of the free air space available for heat transfer by radiation and convection.

The individual contributions by conduction, convection, and radiation to total heat transfer through the rockfall can be determined if sufficient information is available. At relatively low temperatures, heat transfer through intact rock at the potential repository will probably occur by conduction only. Heat transfer mechanism such as convection and radiation are expected to contribute to the total heat flow only at high temperatures or high thermal gradients. For circumstances with limited information, an effective thermal conductivity value which represents all active heat transfer mechanisms can be assigned to the medium for a specified range of conditions (Kaviany, 1995). This approach, however, may violate Fourier's law of heat conduction which assumes a linear relationship between heat flux and temperature gradient. Nonetheless, assuming an effective thermal conductivity is oftentimes expedient and, in reality, the only viable option available.

Heat transfer through rockfall at higher temperatures may be complicated if a heat pipe is encountered. Heat pipes are a highly efficient heat transfer mechanism in which coupled evaporation, condensation, latent-heat transfer, and capillary-driven return flow of liquid remove heat at higher rates than normally experienced by conduction and convection (Mills, 1995). A heat-transfer mechanism similar to a heat pipe may form in the fractured, porous media near a heat-generating HLW canister. In this mechanism, which is commonly referred to as counter current, the return flow of water is driven by gravity, rather than by capillary forces active in a heat pipe.

The rock unit under consideration is the Tptpll. The texture and strength of the Tptpll will affect drift integrity and how the rock breaks after failure. For example, heat transfer through large pieces of brittle rock will differ from heat transfer through crushed rock with lithophysae and a large portion of powder and fine-grained material. Therefore, evaluation of heat transfer through rockfall that may occur at the potential HLW repository at Yucca Mountain is performed on the actual host rock, that is, the Tptpll.

Actual heat transfer through a rubble pile will depend on the physical properties of the native rock (i.e., fragment size distribution and packing) and thermal-hydrological conditions (i.e., temperature, temperature gradient, and saturation) encountered. The fragment size distribution and packing expected in the rubble pile are expected to be comparable to the sample tested in this analysis because the test specimen is the from the Tptpll unit although some rubble pile fragments may be larger. The assumption of low saturations used in this analysis is considered appropriate because the rubble pile will likely have a low saturation due to long durations (i.e., 100’s to 1,000’s of years) of heating expected for the repository as currently designed (DOE, 2004). The low saturation of the specimen will also diminish the potential importance of heat transfer by a heat pipe.

Appendix A: Draft of the paper is at thermalK_journal_3.doc

Calculation of time required for steady state to be attained during heating.

Following is the equation used to calculate the time needed to raise the initial cell temperature to the final steady state temperature.

$$t_{steadystate} = \frac{A}{q}\left[\frac{\left(T_{bottom}^{final} - T_{top}^{final}\right)}{2} + \frac{\left(T_{bottom}^{initial} - T_{top}^{initial}\right)}{2}\right] C_p \; M_{rock}$$

where:

A is the cross-sectional area of the test cell, 0.81 m^2,

C_p is specific heat, 840 J/kg-K,

M_{rock} is the mass of the test medium, 165 kg, and

q is the heat flux measured at the bottom boundary, 186.6 W/m^2.

This calculation assumes that all heat flux entering the test volume measured at the bottom heat flux sensors remained in the test specimen. The actual times needed to attain steady state in the tests were somewhat greater than this estimate mostly due to the fact that heat was removed from the system at the upper boundary heat sink before the entire test specimen attained the final desired temperature distribution. Nonetheless, this estimate provided a first-order approximation of the time required to make a valid measurement.

To calculate the time required to approximate steady-state conditions, a specific heat of 840 J/kg-K was assigned to the crushed Tptpll. The mass of the test medium was determined to be 165 kg. Although initial temperatures in the experiments were dependent on the final temperature of the preceding experiment, the maximum increase in temperature from one test to the next was no greater than the 55ºC difference observed between Tests 9 and 10. The heat flux at the bottom boundary was measured 186.6 W/m^2 at during Test 10. The time for steady-state temperatures to be achieved was estimated to be about 9 hours (actually 9.2 hrs). During conduct of the tests, a minimum of 48 hours was allowed for each test to attain steady-state temperatures. In addition, all experiments were continued until both the lower and upper heat flux measurements became steady, a condition that was realized in all twelve tests. Therefore, the assumption of steady-state heat flux conditions was justified for all tests.

March 25, 2005

Calculations for the convection fitting parameter

The convection fitting parameter was calculated using equation (8) from a draft of the thermal conductivity paper:

$$q_{conv} = -c^*_{conv}\left(\nabla T^{\frac{5}{4}} - \nabla T^{\frac{5}{4}}{}_{critical}\right)$$

This was modified to solve for c^*_{conv}.

$$-c^*_{conv} = q_{conv} \;/ \left(\nabla T^{\frac{5}{4}} - \nabla T^{\frac{5}{4}}{}_{critical}\right)$$

The critical temperature gradient is set at 2800. Plotting of the data are included in sheet 4 of the excel spreadsheet thermal_k_final_b. The convection fitting parameter has a value of -0.346 for Test 1. This outlier was removed from the consensus plot. Test 5 is slightly anomalously high at 0.0759.

Test No.	**Q_{conv}**	**$\nabla T^{5/4}$**	**c^*_{conv} -2500**	**c^*_{conv} -2550**	**c^*_{conv} -2600**	**c^*_{conv} -2650**	**c^*_{conv} -2700**	**c^*_{conv} -2750**
1			0.2295	0.3174	**0.5147**	1.3593	-2.1198	-0.5955
2	0.8	1378.2	-0.0007	-0.0007	**-0.0007**	-0.0006	-0.0006	-0.0006
3	-6.1	829.7	0.0037	0.0036	**0.0035**	0.0034	0.0033	0.0032
4	-3.5	2095.3	0.0087	0.0078	**0.0070**	0.0064	0.0059	0.0054
5	7.3	2895.9	0.0184	0.0211	**0.0246**	0.0296	0.0372	0.0499
6	29.9	4024.6	0.0196	0.0203	**0.0210**	0.0217	0.0225	0.0234
7	62.2	5112.3	0.0238	0.0243	**0.0247**	0.0253	0.0258	0.0263
8	-3.9	1243.3	0.0031	0.0030	**0.0029**	0.0028	0.0027	0.0026
9	-7.6	556.0	0.0039	0.0038	**0.0037**	0.0036	0.0035	0.0035
10	2.3	2275.2	-0.0101	-0.0083	**-0.0070**	-0.0061	-0.0054	-0.0048
11	23.2	3696.4	0.0194	0.0202	**0.0212**	0.0222	0.0233	0.0245
12	71.4	5590.2	0.0231	0.0235	**0.0239**	0.0243	0.0247	0.0251

Tests 2, 3, 4, 8, 9, and 10 are sufficiently close to 0 (i.e., ±0.007). Tests 5, 6, 7, 11, and 12 are all 0.021 to 0.025 for a critical threshold of 2600. The plot for this table is (not plotting for 2750 and omitting Test 1):

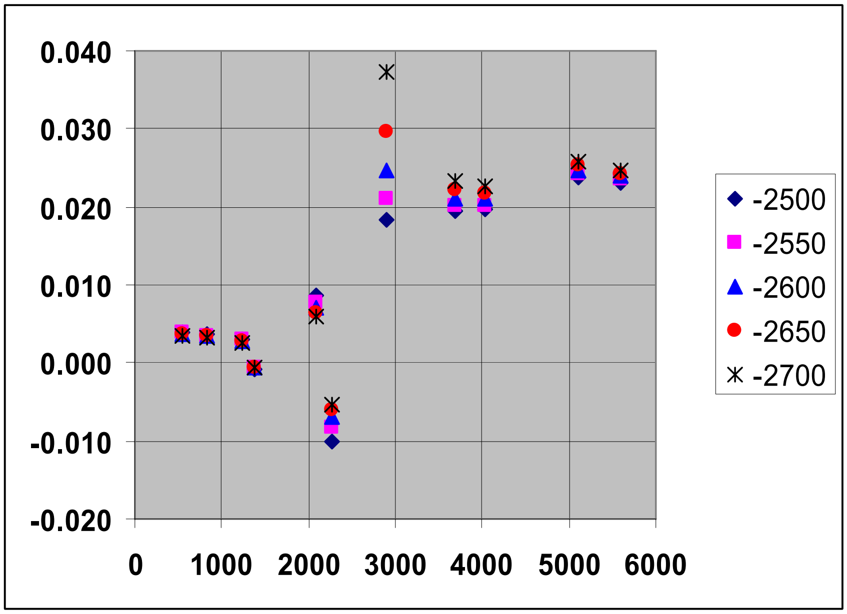

The critical threshold was selected from this graph. Values for the convection fitting parameter near the onset of convection are sensitive to the choice of the critical threshold. Values for the fitting parameter above and below the transition zone, however, are not sensitive to this selection.

Data for a critical threshold of 2600 only are plotted on the following graph. Test 1 is an outlier and has been omitted.

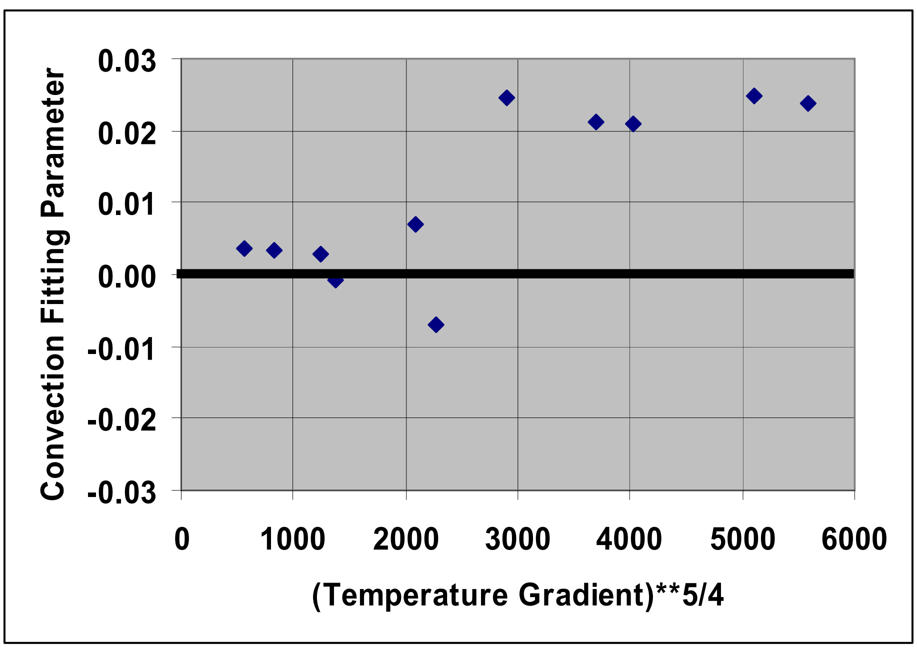

This plot illustrates the onset of convection occurs at a temperature gradient**5/4 of about 2500-2700.

March 30, 2005

Slightly modified version of figure illustrating the convection fitting parameter as a function of (temperature gradient)**(5/4).

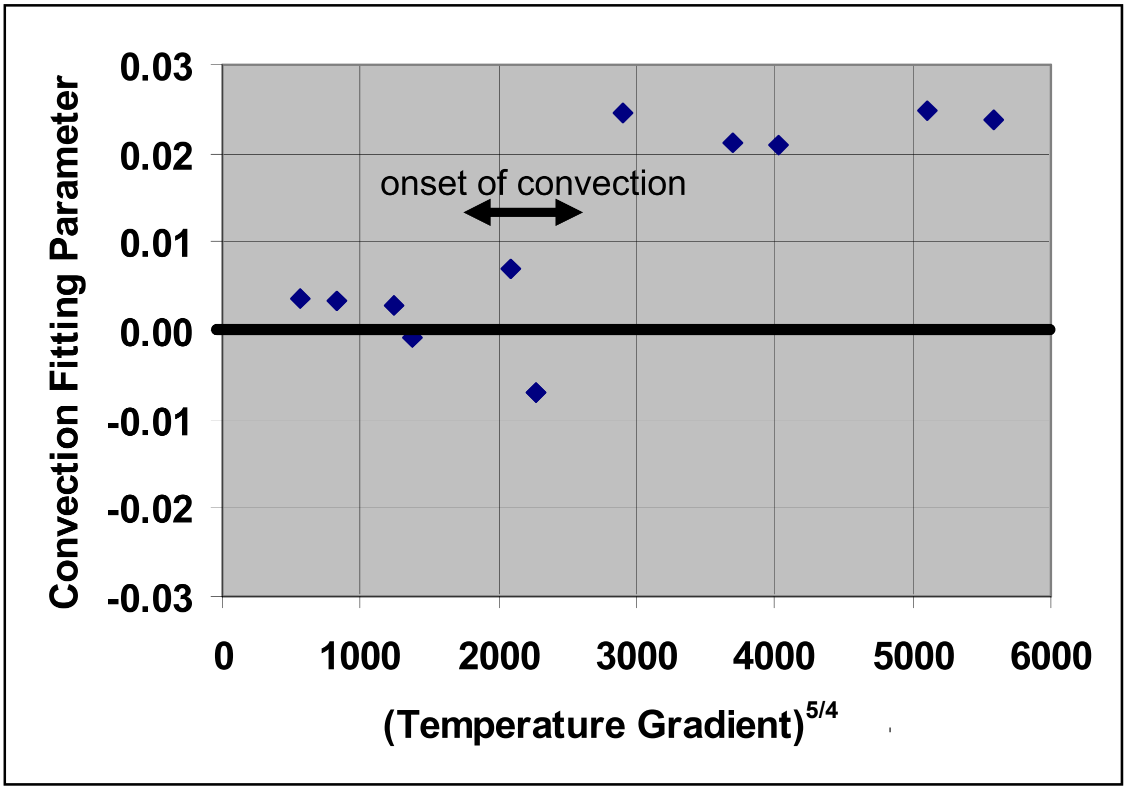

This version of the plot illustrates the onset of convection occurs at a slightly different temperature gradient**5/4 of about 1800-2600.

April 22, 2005

This entry concludes SN 590E Vol 3, with the exception of the two page Appendix A, a printout of a mathematica notebook.

Appendix A: Printout of mathematica notebook rayleigh.nb

Rayleigh Number Calculation (Ron Green 12/29/04)

```
$Version
 5.0 for Microsoft Windows (June 11, 2003)
 $DefaultFont={"Helvetica-Bold",18}
big = {"Helvetica-Bold",18}
Needs["Graphics`Graphics`"]
Needs["Graphics`Colors`"]
Off[General::spell1]
 {Helvetica-Bold,18}
 {Helvetica-Bold,18}
 AllColors;
```

Critical Rayleigh number for width/height aspect ratio of unity

```
perm = 1 10.^-3 cm^2;
rho = 0.0012 g/cm^3;
grav = 980.0 cm/sec^2;
beta = 3. 10^-3 1/c;
delt = 50. c;
cv = 0.9 J/{g c};
dist = 15.0 cm;
mu = 2. 10^-4 g/{cm sec};
xi = 0.4 10^-3 J/{cm c sec};

ra = perm*rho^2*grav*beta*delt*cv*dist/(mu*xi)

 {35.721}
```

Critical Rayleigh number for width/height aspect ratio of less than unity (s=aspect ratio) from Donaldson (1970)

```
s={1.,.9,.8,.7,.6,.5,.4,.3, .2,.15,.125, .1, 1/30.};
s={0.5,0.33333,0.25,.2,0.166666667,0.142857143,0.125};
factor = 1+(-1/2 + (1/2) (1 + 4 s^2)^(1/2))
m = IntegerPart [factor]
m=1;
ra = Pi^2 (m^2 + s^2)^2/(m^2 s^2)

 {1.20711,1.10092,1.05902,1.03852,1.02705,1.02001,1.01539}
 {1,1,1,1,1,1,1}
 {61.685,109.664,178.27,266.874,375.319,503.551,651.548}
```

Calculate Rayleigh number for collapsed drift

```
perm=1 10.^-3 cm^2;
rho=0.0012 g/cm^3;
grav=980.0 cm/sec^2;
beta=3. 10^-3 1/c;
delt=50. c;
cv=0.9 J/{g c};
dist={ 3500. } cm;
mu=2. 10^-4 g/{cm sec};
xi=0.4 10^-3 J/{cm c sec};
```

```
ra=perm*rho^2*grav*beta*delt*cv*dist/(mu*xi)
 Calculate collapsed drift for number Rayleigh
 {8334.9}
```

SCIENTIFIC NOTEBOOK
E590
Volume 4

by

Ronald Green

Southwest Research Institute
Center for Nuclear Waste Regulatory Analyses
San Antonio, Texas

January 23, 2006

Table of Contents

INITIAL ENTRIES

Scientific notebook: #590E Vol. 4
Issued to: R.T. Green
Issue Date: 21-May-2003, Continued on January 23, 2006 as Volume 4

This notebook contains a continuation of the analyses of heat transfer through Tptpll.

The title of the experiment and associated analyses is evaluation of heat flow through crushed Tptpll.

Ron Green is the principal investigator and is responsible for data analysis. Jim Prikryl was responsible for the execution of the laboratory experiment.

The experiment entailed the measurement of heat flow through a container filled with crushed Tptpll under different temperatures and different temperature gradients. Analyses are performed to determine what modes of heat transfer contributed to heat flow through the Tptpll sample, either by conduction, convection, or radiation.

The mathematica notebook in SN #590E volume 3 contained the following:

```
perm = 1 10.^-7 m^2;
rho = 1.2 kg/m^3;
grav = 9.80 m/sec^2;
beta = 3. 10^-3 1/C;
delt = 50. C;
cv = 900.0 J/{kg C};
dist = 0.15 m;
mu = 2. 10^-5 kg/{m sec};
xi = 0.4 10^-1 J/{m C sec};

ra = perm*rho^2*grav*beta*delt*cv*dist/(mu*xi)
```

The critical value of Ra is $4\pi^2$ or 39.478.

The permeability of coarse gravel is 1 x 10^{-7} m^2 per Freeze and Cherry.

Density of moist air is 1.225 kg/m^3

Gravity is 9.80 m/sec^2

Beta is the coefficient of volumetric expansion 3.67 x 10^{-3} C^{-1} for air.

Delta temperature is 50 C this value is approximate for the experiments, actual values ranged from 23.6 to 149.3 C.

Cv is the specific heat at constant volume in J/kg C, this is 661 J/kg C for oxygen and 741 J/kg C for nitrogen at 25 C. For air, specific heat at constant volume: .715 Joules per gram per degree Kelvin or .17 BTU's per pound per degree Rankine. Taken from nasa website: http://www.grc.nasa.gov/WWW/Wright/airplane/airprop508.html

Distance is 0.15 m from the experiment

mu is (absolute or dynamic) viscosity of air 2 x 10^{-5} kg/m sec, from Fox and McDonald

xi is effective thermal conductivity, measured at 0.4 J/(m C sec) or 0.4 W/(m C)

Based on this summary, the value for thermal conductivity in the table above was low by a factor of 10. It should be 0.4 W/m K, not 0.04 W/m K. The value of Ra is decreased from 35.721 to 3.572.

If the delta temperature is changed from 50 C to 149.3 C (as in test 12), then the Ra is 10.666.

Dynamic viscosity at 150 C and standard pressure is approximately 2.38 10^{-5} kg/m sec, then Ra is 12.693. From chart taken from internet.

If the density of air is changed from 1.2 to 1.225 kg/m^3, then Ra is 12.957. This is still a factor of 3 below the critical Ra.

It can be argued that coarse gravels have permeabilites as large as 10^{-6} m^2. If so, this would push Ra above the critical value. Reference: Characterization of Hydraulic Properties of Potentially Fractured Industrial D Landfill Sites, and A Study of Heterogeneity Effects on Fate and Transport in Groundwater. US EPA National Risk Management Research Laboratory. Subsurface Protections and Remediations division. Ada, OK. 74820. March 1998.
http://www.epa.gov/epaoswer/hazwaste/id/hwirwste/pdf/risk/reports/s0548.pdf
also: API, 1989. Hydrogeologic Database for Groundwater Modeling. API Publication No. 4476, American Petroleum Institute. Or Newell, C.J., L.P. Hopkins, and P.B. Bedient. 1989. *Hydrogeologic Database for Ground Water Modeling.* API Publication No. 4476. American Petroleum Institute, Washington, DC.

April 3, 2006

Another issue to resolve in the peer review of the Nuclear Technology journal article submittal is measurement error. An additional section was added. This section reads as follows:

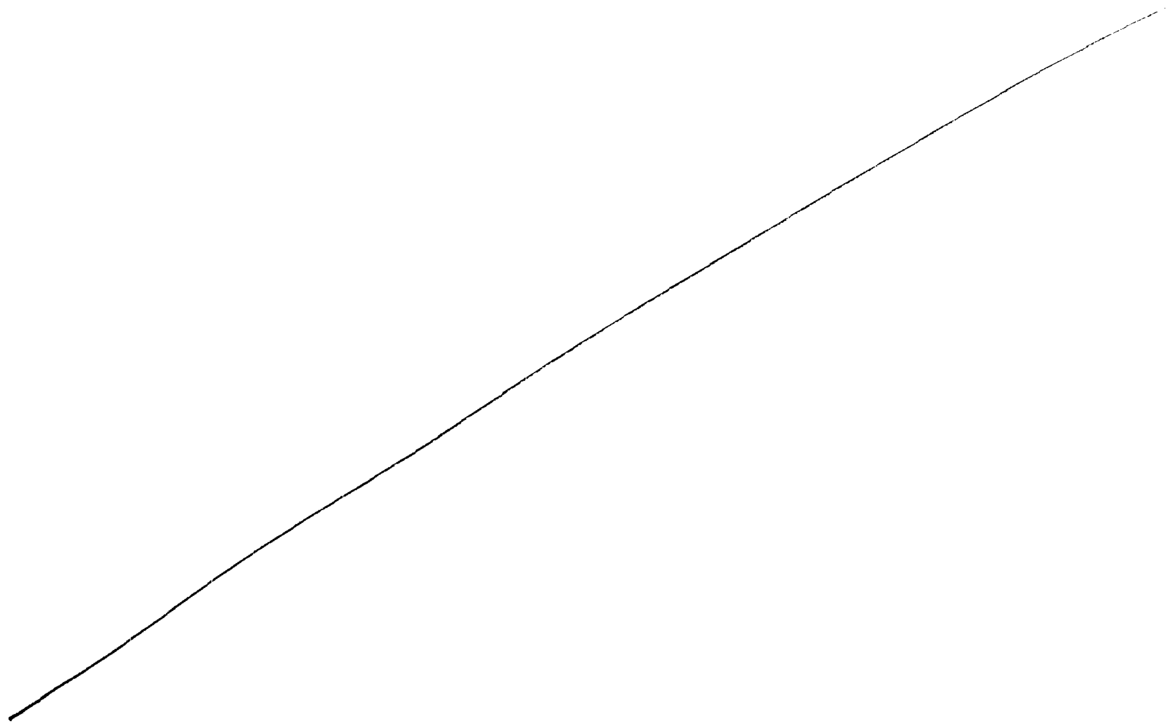

The standard deviations of heat flux measurements, as illustrated by the outer error bars in Figure 4, are sufficiently large that they could conceivably account for the entire departure of measured heat flux from the pure conduction straight line in Figure 4. The standard deviation included in Figure 4 is interpreted to include instrument uncertainty and experiment variability. Instrument accuracy can be quantified using published absolute calibration accuracy values of 3-5% for the Micro-Foil^{TM} heat flux sensors (RdF Corporation, 2006). An inner set of error bars, based on 5%, are included in Figure 4.

The difference between the 5% measurement error bars and the larger observed standard deviation is attributed to experimental variability resulting mostly from non-uniform thermal contact between the metal heat exchangers and the irregularly sized and shaped rock fragments. The variability in heat flow measurement at the four heat flux sensors in the top and in the bottom are indicative of variability of heat flux measured at places where the thermal contact between the rock fragments and the heat exchanger was high, hence high heat flux, and places where the thermal contact between the rock fragments and the heat exchanger was low, hence low heat flux. Minimizing this variability was achieved, in part, by placing crumpled tin foil between the top of the rock and the top heat exchanger. This procedure was not used at the bottom where better thermal contact was believed to have been achieved during packing of the rock fragments in the test cell.

This assessment of experimental variability is supported by the fact that variability among heat sensor measurements exhibited clear trends: (i) variability was larger at higher temperatures and higher temperature gradients and (ii) the same heat flux sensors in the top and bottom consistently had the highest, and lowest, measured heat flux in all tests. The relative consistency of these measurements supports the premise that the experiment variation was due to differences in thermal contact between the heat flux sensors and the rock fragments and was not due to either significant non-linear heat flow through the rock fragments or random measurement error. Based on this reasoning, the average values for heat flux are believed to be valid and calculation of the non-conductivity component of heat flux from the departure from the linear segment of the curve is also believed to be valid.